The role of Polo-like kinase 1 interacting checkpoint helicase (PICH) interaction with SUMOylated proteins on genome stability

By

Victoria Hassebroek

Submitted to the graduate degree program in Molecular Biosciences and the Graduate Faculty of the University of Kansas in partial fulfillment of the requirement for the degree of Doctor of Philosophy.

Chairperson: Yoshiaki Azuma, Ph.D.

Kristi Neufeld, Ph.D.

Berl Oakley, Ph.D.

Erik Lundquist, Ph.D.

Justin Blumenstiel, Ph.D.

Date defended: May 12, 2020

The Dissertation Committee for Victoria Hassebroek certifies that this is the approved version of the following dissertation:

The role of Polo-like kinase 1 interacting checkpoint helicase (PICH) interaction with SUMOylated proteins on genome stability

_____

Chairperson: Yoshiaki Azuma, Ph. D

Date Approved: May 12, 2020

Abstract

SUMOylation is a post-translational modification that is important for mitosis, specifically chromosome segregation. SUMOylation occurs when a SUMO paralog (SUMO-1, SUMO-2, or SUMO-3) is transferred to a substrate at a lysine residue. SUMOylation can cause differential protein targeting, regulate enzymatic activity, target a protein for degradation, and important for my work, cause complex assembly. This occurs between a SUMOylated protein and a protein which has SUMO-interacting motifs (SIMs). This dissertation will focus on a protein with three SIMs called Polo-like kinase interacting checkpoint helicase (PICH). PICH is an ATP-dependent DNA translocase that moves along doubled stranded DNA. PICH has been shown to be important in chromosome structure, organization, and segregation in mitosis. PICH utilizes its SIMs to localize to centromere regions and resolve chromosome bridges. PICH translocase activity has also been shown to be important for chromosome bridge resolution. This indicates that PICH interaction with a SUMOylated protein via SIMs and translocation activities are cooperative for proper chromosome segregation. A candidate for that PICH function is Topoisomerase IIα (TopoIIα). TopoIIα is an appropriate interaction candidate because it is a known SUMOylated substrate that is important in chromosome segregation. More support for TopoIIα as the interaction partner of PICH is found in PICH knockout studies which show that *PICH*$^{-/-}$ cells are hypersensitive to a TopoII inhibitor called ICRF-193. This inhibitor blocks TopoIIα in a closed clamp conformation with both strands of decatenated DNA bound within it. ICRF-193 treatment has also been shown to increase SUMOylation of TopoIIα which could make it a primary target of PICH SIMs in ICRF-193 treatment. By implementing a novel auxin inducible degron (AID) and Tet-inducible mutant add back system I found that when PICH is depleted in DLD-1 cells, SUMOylated chromosomal protein levels, including SUMOylated TopoIIα, increase and replacement with translocase deficient PICH shows strong SUMO foci with which PICH colocalized. This indicates that SUMOylated chromosomal proteins are the

target of PICH and PICH can remodel these proteins by using its DNA translocase activity. Intriguingly, when cells are treated with ICRF-193, which increases SUMOylated TopoIIα, PICH foci on chromosomes are increased. Alternatively, when TopoIIα was depleted with the AID system, the increased PICH foci observed in ICRF-193 treatment is lost. This suggests that PICH specifically targets SUMOylated TopoIIα when TopoIIα function is perturbed by ICRF-193. Previous work from our lab has shown that TopoIIα SUMOylation is important in activating the TopoII-dependent checkpoint. This checkpoint functions through Aurora B kinase and is independent of the spindle assembly checkpoint (SAC). To study the biological relevance of PICH/SUMOylated TopoIIα interaction, ΔPICH cells were imaged using live-cell microscopy and scored for the mitotic duration. ΔPICH cells were observed to have a longer than average duration of mitosis, and this phenotype was rescued by PICH WT replacement. When ΔPICH was replaced with a non-SUMO interacting mutant (d3SIM) or the translocase deficient mutant (K128A), they were observed to have a longer than average mitosis. This indicates that both SUMO binding ability and translocase activity are necessary for PICH function in controlling the progression of mitosis, presumably by regulating the TopoII-dependent checkpoint by regulating stalled SUMOylated TopoIIα. Collectively, I demonstrate PICH's novel and essential function in mitosis as a SUMOylated chromosomal protein remodeler. This function towards SUMOylated TopoIIα is biologically relevant and reveals a novel role for PICH in the progression of mitosis.

Acknowledgements

I want to begin by thanking the KU faculty whom I interacted with on a weekly basis and my committee members. Thank you for cultivating a place in which to grow as a scientist. Next, I would love to thank all of my lab mates both current and past, you all have been so patient with my constant chatter and I truly appreciate always having the ability to pop over to your desk and ask a question or just to chat. Nootan, you were so missed for the last 9 months! Sanjana, keep knitting between experiments, Yoshi will understand. Lastly, Hyewon…where to begin! You have the patience of a saint and I appreciate all of the times you had to re-explain the same concept to me until I finally understood. Your patience and teaching are what made me the scientist I am today and for that, I will be forever thankful. Thank you for trying to instill an eye for meticulous detail in me. You are an incredibly loyal friend and you will be dearly missed in my next lab. To all of you friends who helped me get through graduate school, I will forever be indebted to you. I am so thankful to everyone at KU for being there to laugh and chat at lunch and to study and complain before our comps or GoD presentations! Friends outside of KU, know that graduate school is never easy, and your constant encouragement was so needed and so appreciated, thank you so much. Lastly, I want to thank you Taybor, for your ability to talk me off of every ledge when anxiety was ruining my ability to see the world clearly. For your ability to take complex scientific ideas and explain them to me in an understandable way. For your constant cheer and laughter during our lunches together. For being the best friend, a person could ask for, you have no idea how much this friendship has meant to me over the years. I truly hope we can keep in touch and continue to shred on the slopes! Dearest Yoshi, this may be the hardest thank you of all, how can you thank someone for being so incredibly good at their job? You are the most supportive, positive-thinking, intelligent mentor a person could ask for. Your ability to adapt to each student and mentor them in the style they need is incredible. I will never forget our long chats about everything and nothing, they are memories I will cherish until the day

I die. In addition, your leadership skills in the lab are ones that I will hope to utilize in my future positions. Your ability to ask complex IMPORTANT scientific questions is something that I can only hope I have learned from you. Thank you from the bottom of my heart for everything. I am who I am today because of you and I am happy to say that I am proud to have been your student. I would also like to thank my family; without your constant support, I would not have been able to make it through these long five years. Mom, the commute to Lawrence every day went from something I hated to something I looked forward to because of our daily phone conversations. Thank you for always being someone I can lean on and complain to. Dad, thank you for cultivating a love of science in me from day one. Your encouragement and guidance throughout my life is why I became a scientist; I am so proud to be your daughter. Micah, Katie, and Annaka thank you all for your hilarity during all of my visits home. You three never cease to make me laugh and I love you all for that. Micah, thank you for being my sidekick on all fishing/exploring adventures, those are memories I cherish. Katie, thank you for literally ALWAYS knowing how to make me laugh, even on my darkest days. Annaka, thank you for sharing my love for science and investigation, our conversations are so interesting and fun. Last but never least, thank you to my dear husband. Trevor, I don't even know where to begin. You have been on this journey with me since day one when if I remember correctly, your answer to me saying I want to go to graduate school was "why?!" Although I know it has been so hard being married to a graduate student your constant love and support have helped push me to get through this. Every time I came home late to find a dinner plate saved for me was another reminder of your love and commitment to me. Thank you for always listening to my practice seminar talks with only a few eye rolls. Thank you to everyone who has helped and encouraged me along the way, I truly owe it all to you.

Table of Contents

List of figures

List of Tables

List of abbreviations

PICH – Polo-like kinase 1 interacting checkpoint helicase

SUMO – Small ubiquitin-like modifier

SIM – SUMO-interacting motif

SENP – SUMO-proteases

TopoIIα – Topoisomerase IIα

PARP1 – Poly (ADP-ribose) polymerase I

BLM – Bloom's syndrome helicase

CENP-A – Centromeric protein A

CENP-E – Centromeric protein E

UFB – ultra-fine DNA bridges

XEE – *Xenopus laevis* egg extract

Chapter 1 Introduction

Biological question leading to this project

During each cell cycle the entirety of the genome must be accurately replicated and concisely divided between two daughter cells. Replicated sister chromatid segregation during mitosis is a highly dynamic process which relies on many proteins to cooperate for faithful cell division. One major part of this regulatory process is timing. A cell must not only sense that chromosomes are properly condensed, held together by cohesin, and each sister chromatid is attached to spindles of opposing centrioles, but also that they are all fully decatenated before division (Piskadlo and Oliveira, 2016). The presence of catenation between sister chromatids was observed and indicated to play a critical role in sister chromatid cohesion in addition to that mediated by cohesin (Wang et al., 2010). If these checks are not in place, dysregulation of this process can lead to genomic instability, in turn leading to cancer and other diseases. Although studies about sensing decatenation and mitotic timing have been underway for decades, this process is not well understood and therefore the long-term goal of this research is to better understand the cooperation between proteins which lead to faithful chromosome segregation and accurate mitosis.

Mechanism for timing and chromosome structure

Arguably the most critical timing during mitosis is the metaphase-to-anaphase transition. This transition is the point of no return, once the duplicated chromosomes begin to divide, if there is a mistake can be deleterious to either or both progeny cells (Farr and Cohen-Fix, 1999). Post-translational modifications have well established roles

in the regulation of chromosome segregation. An example of such is phosphorylation. There are many active kinases during mitosis, a major example being Aurora B kinase. Aurora B kinase functions to regulate two major regulatory steps that occur during mitosis, error correction (EC), and the spindle assembly checkpoint (SAC) (Krenn and Musacchio, 2015). Aurora B phosphorylation is necessary for proper localization to kinetochore regions in prometaphase cells (Petsalaki et al., 2011). These modifications are necessary to ensure that all of the chromosomes have been replicated and condensed. Once all of the chromosomes have been attached properly to microtubules this leads to activation, controlled by phosphorylation of the anaphase promoting complex/cyclosome (APC/C). This leads to the ubiquitylation and subsequent degradation of securin, an inhibitor of the protease separase. Separase then cleaves the Scc1 subunit of cohesin, freeing sister chromatids from their topological constraints maintained by interaction with cohesin rings (Yamano, 2019). But, just activating cohesin cleavage is not enough to separate sister chromatids, the activity of TopoIIα is also necessary for complete sister centromere segregation. This was shown by Wang et al. in 2009 where depletion of Shugoshin (Sgo1) the anchor to which cohesin subunits attach, caused loss of cohesion between sisters. They found that cells treated with the TopoIIα inhibitor, ICRF-193, maintained sister chromatid cohesion, even in the absence of cohesin. This indicated that DNA catenations also occur between sisters and play a role in cohesion and require TopoIIα activity to be resolved before anaphase. Intriguingly, previous work has shown that ICRF-193 causes increased SUMOylation of TopoIIα, emphasizing the potential role of SUMOylation of TopoIIα (Agostinho et al., 2008).

The idea that TopoIIα SUMOylation is biologically relevant was strengthened by a study performed by Azuma et. al. which indicated that TopoIIα is modified by SUMO-2/3 during mitosis and that SUMOylation is necessary for chromosome segregation. A more recent study in *Xenopus laevis* egg extract has shown that inactivation of PIASγ, a SUMO E3 ligase known to SUMOylate Topoisomerase IIα (discussed in the next section), interfered with chromatid segregation. In addition, loss of SUMOylation of Topoisomerase II leads to precocious separation of centromeres which indicates that a potential role of TopoII SUMOylation on the regulation of timing of sister chromatid separation (Bachant et al., 2002).

This implicated the role of SUMOylation on chromatid segregation leading to the hypothesis that DNA catenations between sisters, controlled by TopoIIα, play a role in keeping sister chromatids together until the onset of anaphase.

Post-translational modifications have been shown to be crucial for each step of mitotic progression but regulation of activity and protein/protein interactions by the modification SUMOylation is still not well understood. The work for this dissertation started with an aim to understand the functional interaction between a SUMO binding protein called PICH (explained later in this chapter), and the highly dynamic enzyme TopoIIα, which has been found to be SUMOylated during mitosis. By pioneering CRISPR/Cas9 editing in our lab, I found that PICH interacts with SUMOylated TopoIIα during mitosis and this interaction is necessary to mediate chromosome bridge resolution and mitotic progression.

Discovery of Small Ubiquitin-like Modified (SUMO) and its implications during mitosis

SUMO (Small Ubiquitin-like Modifier) was first discovered in *Saccharamyces cerevisiae* in a genetic screen to elucidate suppressors of MIF2. MIF2 is the yeast homolog of human CENP-C, a critical centromere protein which plays a central role in the assembly of kinetochore proteins (Meluh and Koshland, 1995). CENP-C has also been shown to be important for recruitment of CENP-A proteins to centromere regions and therefore is critical in the maintenance of the centromere (Wan et al., 2012). SUMO was first named for its yeast function as Suppressor of MIF2 3 (Smt3) (Meluh and Koshland, 1995). This was a critical finding because it implicated SUMO in centromere regulation and led to further study of this new centromere target. After the identification of SUMO, characterization of the SUMO protein was carried out by Shen et. al. which found that SUMO is a binding partner of the proteins RAD51, RAD52, FAS, and PML in a yeast two-hybrid assay (Shen et al., 1996). Then, SUMO was discovered to covalently attach to Ran GTPase-activating protein RanGAP1(Matunis et al., 1996; Pichler et al., 2002). These initial studies had two important findings: Post translational modification by SUMO, SUMOylation, exists in all eukaryotes, SUMOylation shares similarities with Ubiquitylation in terms of its reaction, and that SUMOylation of a substrate caused altered protein localization by changing protein interactions (Geiss-Friedlander and Melchior, 2007). A great example is the RanGAP1 protein, which natively localizes to the cytosol, but when SUMOylated localizes to the nuclear pore via interaction with nucleoporin RanBP2 (Mahajan et al., 1997). This led to an explosion in the field, where hundreds of SUMO targets have now been identified (McManus et al., 2018). This drove

the identification and definition of a consensus SUMOylation site (discussed below) and by mutating such a site, groups can work to elucidate how modification by SUMO effects their target or interest.

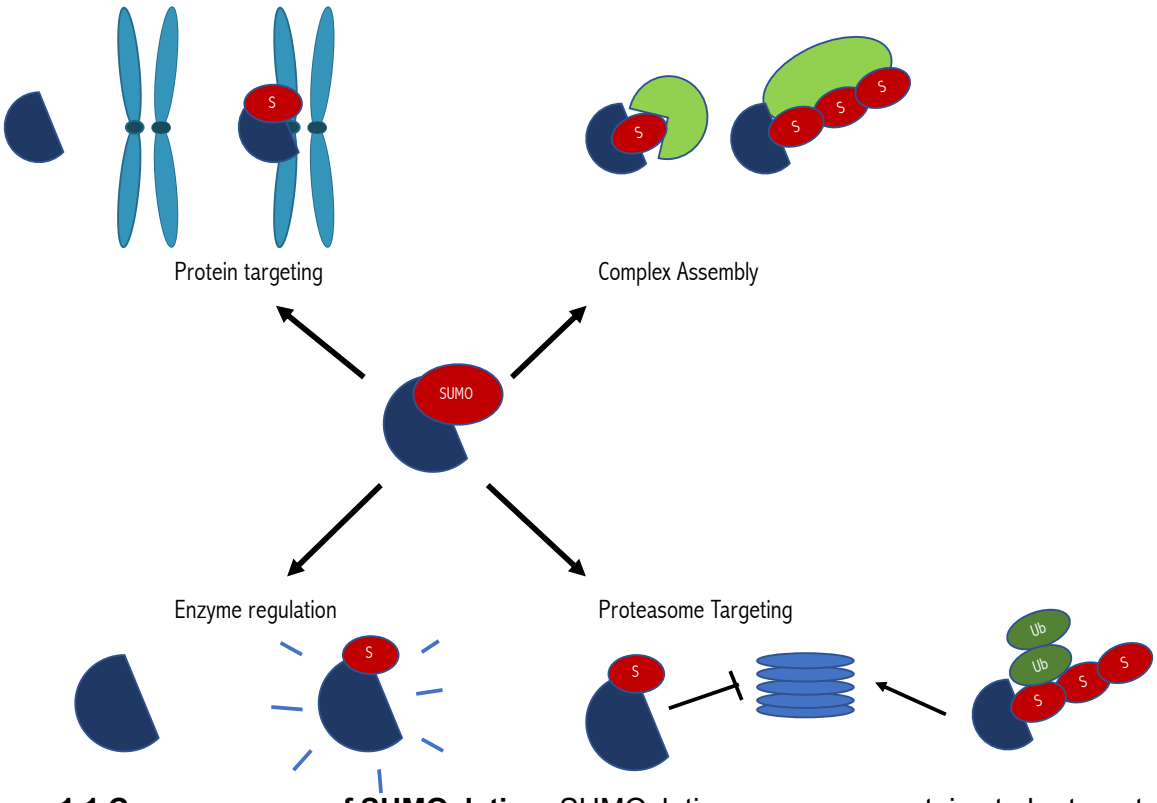

Figure 1.1 Consequences of SUMOylation. SUMOylation can cause proteins to be targeted to different cellular locations, regulate enzyme activity, mark a protein for degradation, and cause complex assembly between SUMOylated proteins and proteins that have SUMO-interacting motifs (SIMs).

Different SUMO isoforms have been discovered in a wide range of model organisms. Yeast, *C. elegans,* and *Drosophila melanogaster* have a single SUMO gene. But, species such as humans and mice have multiple genes that encode for SUMO. SUMOylation has been shown to be an essential process in *S. cerevisiae, C. elegans,*

Arabidopsis thaliana, and mice (Fraser et al., 2000; Johnson et al., 1997; Nacerddine et al., 2005; Saracco et al., 2007). Overall, SUMOylation has been shown to be essential in a wide variety of model organisms.

Modification by Small Ubiquitin-like MOdifier (SUMO)

Post-translational modification by SUMO can have different consequences such as; protein targeting, enzyme control, proteasomal degradation, and complex assembly (Figure 1.1) (Cubeñas-Potts et al., 2013). Complex assembly requires SUMO/SIM interaction and is the focus of my study. SIMs bind SUMO via their hydrophobic core defined by a V/I-X-V/I-V/I motif (Hecker et al., 2006; Song et al., 2004). SUMOylation has been shown to be a key process in many different pathways. The essential part of SUMO's role as a molecular switch is the reversibility of the modification, which is dictated by SUMO-specific enzymes which attach SUMO to its target substrates. SUMO begins as a pre-SUMO molecule which requires cleavage at the C-terminal by a SUMO-specific isopeptidase, exposing characteristic di-glysine residues. Now the first SUMO-specific enzyme called E1, which consists of an Aos1/Uba2 complex activates the SUMO molecule (Desterro et al., 1999; Gong et al., 1999; Johnson et al., 1997). This occurs at the SUMO C-terminus in a two-step ATP hydrolysis reaction. Next, the SUMO molecule is bound to the Aos1/Uba2 in a thioester bond and can go through the next step in the reaction. This step is controlled by the E2 conjugating enzyme, called Ubc9. The Ubc9 enzyme plays a critical role in the SUMOylation pathway, more than most ubiquitin E2 enzymes. This is due to the ability of Ubc9 to bind to specific SUMO substrates via a consensus sequence (Bernier-Villamor et al., 2002). Unlike the ubiquitin pathway, the SUMOylation pathway has only one E2. This enables substrate

specificity to be regulated by SUMO E3 ligases, or by deSUMOylation enzymes. SUMO E3 ligases have been shown to mediate or stabilize the interaction between the target substrate and the charged E2/SUMO molecules (Desterro et al., 1997; Johnson and Blobel, 1997, 1997; Lee et al., 1998). Two families of E3 enzymes exist; PIAS and RanBP2, the first of which we study in our lab. The PIAS family of SUMO E3 ligases is the largest E3 ligase family consisting of PIAS1, PIASχα, PIASχβ, PIAS3, and PIASγ (Kahyo et al., 2001; Nishida and Yasuda, 2002; Sachdev et al., 2001; Sapetschnig et al., 2002; Schmidt and Müller, 2002). SUMO is attached at a lysine residue and this modified lysine is typically part of a consensus sequence: ψKxE (where ψ is a hydrophobic amino acid, K is the modified lysine, x is any amino acid followed by E, glutamate) (Figure 1.2) (Muller et al., 2000).

SUMOylation is a reversible process which requires the deSUMOylation activity of SUMO proteases. To date, a surprisingly small number of SUMO isopeptidases have been identified. The sentrin-specific proteases (SENPs) were identified in mammals and consist of 7 isoforms (SENP1, -2, -3, -4, -5, -6, and -7). These SENPs have some target specificity and when knocked out in mice, show early embryonic lethality (Di Bacco et al., 2006; Gong and Yeh, 2006).

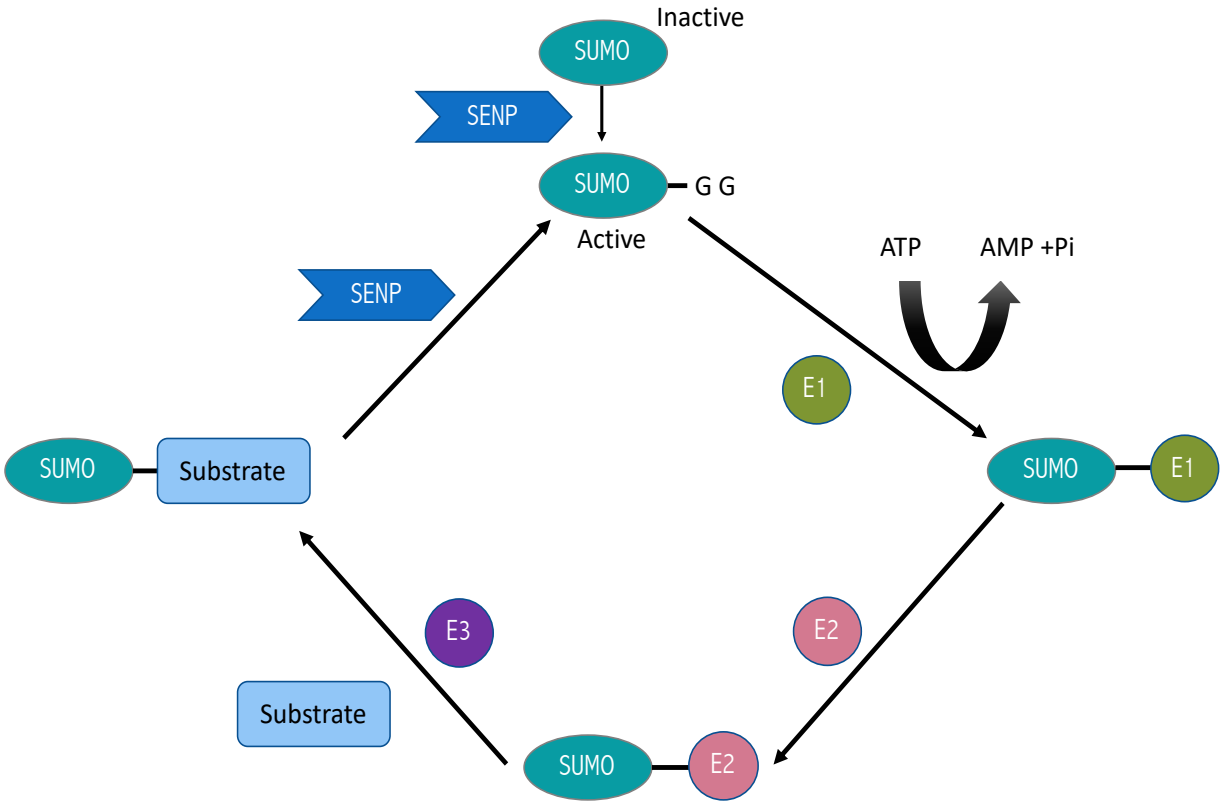

Figure 1.2 The mechanism of reversible SUMOylation. This schematic indicates the proteins involved in the SUMOylation pathway.

SUMOylation in cell division and chromosome segregation

When Seufert et al. showed that Ubc9 is required for M-phase cyclin degradation, the link between mitosis and SUMO was established (Seufert et al., 1995). This link was further shown in yeast when a screen for defective chromosome segregation identified SMT3 (SUMO) (Meluh and Koshland, 1995). A review written by Wan and Zhang showed SUMOylation's importance during chromosome segregation (Wan et al., 2012). Multiple genetic studies which inhibited different SUMO enzymes

both in yeast and mammalian cells have also indicated the role of SUMOylation in chromosome segregation (Cubeñas-Potts et al., 2013; Hari et al., 2001; Nacerddine et al., 2005; Seufert et al., 1995; Tanaka et al., 1999; Zhang et al., 2008). But, to understand what role SUMO plays during mitosis, it is critical to identify its targets as well as targets that have SUMO-binding ability. Several SUMOylated chromosomal proteins were identified for their potential role in chromosome segregation, for example; TopoIIα, CENP-A, CENP-E, FoxM1, and Orc2 (Bachant et al., 2002; Huang et al., 2016; Ohkuni et al., 2018; Schimmel et al., 2014; Zhang et al., 2008).

But, extensive study into how SUMOylation plays a role in regulating the function of these targets is lacking. Due to SUMO's ability to cause complex assembly, we wanted to identify different proteins which interacted with SUMOylated substrates. Our lab utilized Mass spectrometry to identify SUMOylation-dependent binding proteins for our identified SUMOylated targets, Poly (ADP-ribose) polymerase 1 (PARP1), and Topoisomerase IIα (TopoIIα). PARP1 was found to be SUMOylated, but its SUMOylation status did not affect enzymatic activity (Zilio et al., 2013). In contrast, TopoIIα SUMOylation at specific lysine residues decreased TopoIIα decatenation activity (Ryu et al., 2010). In addition, SUMOylation on other lysines does not affect its activity but is required for mitosis (Bachant et al., 2002). To understand the purpose of TopoIIα and PARP1 SUMOylation we utilized SUMO modified substrates, PARP1 and TopoIIα, as bait in a large-scale pull-down assay. Three important proteins for the work discussed in this dissertation were identified; Claspin, Haspin, and Polo-like kinase 1 interacting checkpoint helicase (PICH) (Ryu et al., 2015; Sridharan et al., 2015; Yoshida et al., 2016). The kinase Haspin is known to regulate the recruitment of the

Chromosome Passenger Complex (CPC) to centromere regions by phosphorylating histone H3 at threonine 3 (H3T3) (Jeyaprakash et al., 2011; Kelly et al., 2010). Claspin is a DNA damage checkpoint adaptor protein which binds to Chk1, a kinase described in previous sections which activates Aurora B (Kumagi A, 2003; Petsalaki et al., 2011; Ryu et al., 2015). Lastly, one protein around 250kDa was found to be prominently bind SUMOylated PARP1. We identified this protein using LC-MS/MS (Liquid chromatography-Mass spectrometry) as Polo-like kinase 1 interacting checkpoint helicase (PICH) (Sridharan et al., 2015).

Polo-like kinase 1 interacting checkpoint helicase (PICH)

PICH was first discovered as a Plk1 binding partner by utilizing a Far Western ligand binding assay with Plk1-PBD as bait. This assay revealed a protein with a catalytic domain, Walker A and B motifs, and HELICc domain in the N-terminus, which classified this protein as an SNF2 family ATPase. Although, PICH was later found to have no helicase activity. Tetratricopeptide repeats were found in both the N and C termini, suggesting that there are protein-protein interactions mediated at these sites (Baumann et al., 2007). Although PICH's name suggests that it is a checkpoint protein, this was found to be an siRNA off-target effect in which the siRNA used to target PICH also targeted Mad2 (Hübner et al., 2010). Thus, currently, the role of PICH on mitotic progression is unclear.

By performing immunohistochemistry using a PICH primary antibody, Baumann et al. found that PICH labeled an ultra-thin structure seen between dividing nuclei. These structures were DAPI negative and named Ultra-Fine Bridges (UFBs) (Figure 1.3) (Baumann et al., 2007). To identify what these structures were made of, the

Baumann group performed an siRNA experiment knocking down Mad1, BubR1, and Bub1 to examine the possible relationship between UFBs and lagging chromosomes. But, increasing the number of chromosome segregation errors did not increase the number of UFBs. To determine if UFBs represented stretched chromatin extending between sister kinetochores, they then depleted Sgo1 by siRNA. Depletion of Sgo1 increased the number of UFBs and showed that premature removal of cohesins enhanced UFB formation. UFBs were also found to be tension sensitive, and when microtubule dynamics were inhibited by paclitaxel the UFBs disappeared. The threads were then found to be DNase but not RNase sensitive reiterating that they are made of stretched DNA (Baumann et al., 2007). Prompted by a previous report which showed that the catalytic activity of Topoisomerase IIα (TopoIIα) (discussed later in this chapter) is required for sister chromatid segregation during anaphase Baumann et. al. asked if the resolution of PICH-positive threads requires TopoIIα and found that it does (Baumann et al., 2007). This indicates that PICH associates with catenated DNA that is under tension until its resolution by TopoIIα.

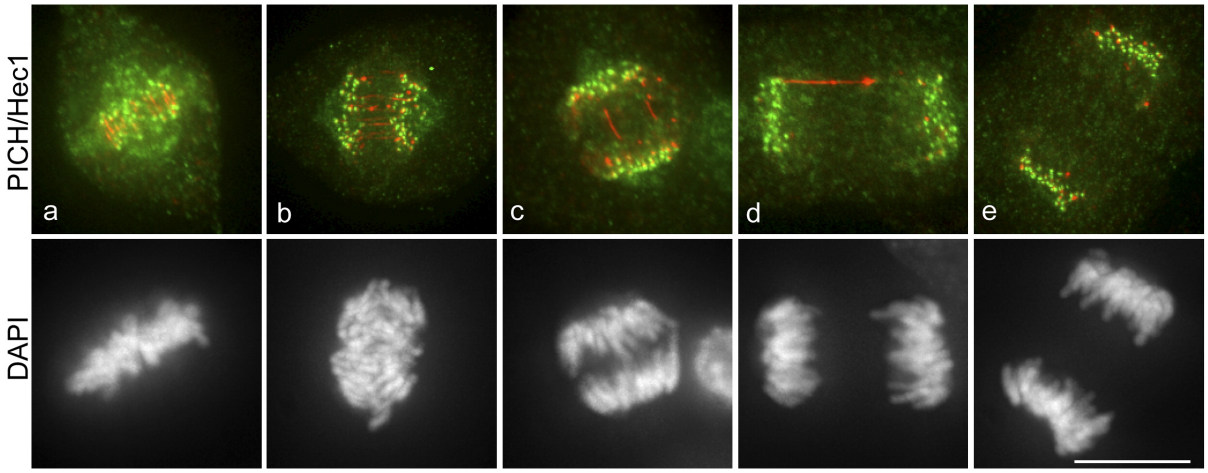

Figure 1.3. PICH coated ultra-fine bridges. Adapted from Baumann et al., 2007. The top row shows Hec1 kinetochore regions in green and PICH in red in a cell going through mitosis. The bottom row shows DNA labeled with DAPI.

PICH is a DNA-dependent ATPase which moves on double stranded DNA and has a functional domain structure similarity to SWI/SNF family proteins, thus it was proposed to be a nucleosome remodeling factor (Narlikar et al., 2013). Although PICH is classified as a putative nucleosome remodeler, PICH has never been shown to have robust remodeling activity for core histones (Ke et al., 2011). But PICH translocase activity has been shown to be important for proper chromosome segregation. This was shown by Sridharan et al., when the translocase activity was knocked out by mutating a lysine at position 128 to an alanine (K128A). K128A mutants could localize to mitotic centromeres but could not resolve chromosome bridges (Sridharan and Azuma, 2016). This suggests an important role for the translocase activity that is known to be important for chromosome segregation but whose actual target remains unknown.

PICH was first discovered in our lab as a SUMOylated PARP1 binding protein and further analysis showed that PICH binds SUMOylated proteins promiscuously

(Sridharan et al., 2015). Utilizing PICH truncations, the region of PICH needed to bind SUMOylated proteins was identified as the C-terminal portion, specifically amino acid numbers 616-1250. This region of PICH was put into a prediction software application and four SUMO-interacting motifs were identified, two of which overlapped, and these were named SIMs 1, 2, and 3. Utilizing its three SIMs PICH was found to bind both single SUMO moieties, as well as SUMO chains (Sridharan et al., 2015). PICH SIMs were further validated by mutations which changed all hydrophobic amino acids within SIMs to alanine (Table 1.1). Each SIM on PICH was mutated and found to be essential for the proper centromeric localization of PICH. PICH's role in chromosome segregation was shown utilizing HeLa cells transfected with either an EGFP-PICH WT, or EGFP-PICH d3SIM. Upon fluorescent analysis it was observed that d3SIM expressing cells showed no PICH foci at mitotic centromeres. To analyze which SIM is essential for PICH localization individual EGFP SIM mutants were made. SIM3 was found to be critical for the centromere localization of PICH, while both SIM1 and SIM2 showed normal centromeric localization (Sridharan and Azuma, 2016).

Depletion of PICH has been shown to cause chromosome segregation defects (Biebricher et al., 2013). By using the same methodology as described above for K128A and d3SIMs mutants, chromosome segregation was studied in SIM1, SIM2, and SIM3 expressing cells. It was found that SIM1/2 were both equally critical for proper chromosome segregation while SIM3 was dispensable. These data indicate that each SIM has a unique function in the regulation of PICH. SIM3 is important for the localization at mitotic centromeres, while SIM1/2 are required for the activity of PICH at centromeres for resolving chromosomes bridges (Table 1.1) (Sridharan and Azuma,

2016). This difference indicates that there are distinct interacting proteins, most likely SUMOylated on mitotic chromosomes, targeted by SIMs.

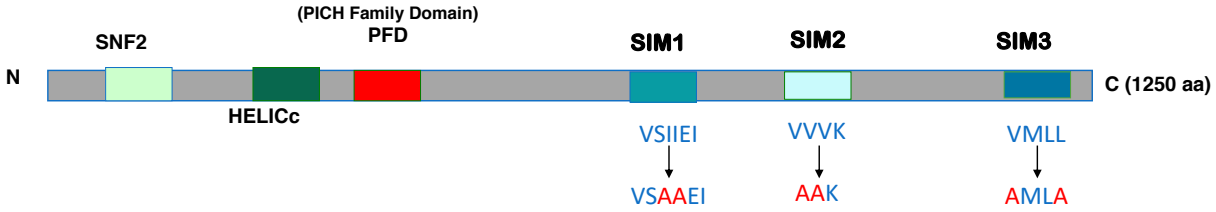

PICH CONSTRUCT	CENTROMERE LOCALIZATION	CHROMATIN BRIDGE	DNA translocase activity	UFB LOCALIZATION
WT	Yes	No	Yes	Yes
d3SIM	No	Yes	Yes	Yes
dSIM3	No	No	NE	Yes
dSIM1&2	Yes	Yes	NE	Yes
K128A (ATPase mutant)	Yes	Yes	No	Yes

Table 1.1. PICH activity on chromatin bridge resolution and UFB localization. Summary of PICH functional regions and their effect on chromosome bridge resolution. (NE: Not examined). Modified from Sridharan et. al., 2016.

A recent paper by Nielson et al., showed that chicken cells lacking PICH were hypersensitive to the TopoIIα inhibitor ICRF-193. In this report they showed that treating *PICH*$^{-/-}$ cells with a catalytic inhibitor of TopoIIα, ICRF-193, caused increased chromosome bridge formation, binucleation, and micronuclei formation. This phenotype was rescue by expression of WT PICH but not by the translocase deficient K128A mutant (Nielsen et al., 2015). This increased sensitivity to ICRF-193 indicates that there is cooperation between PICH and TopoIIα in resolution of chromosome bridges and other chromosome abnormalities. Interestingly, it has been shown that treatment with

ICRF-193 causes increased TopoIIα SUMOylation (Agostinho et al., 2008), indicating that PICH can recognize SUMOylated TopoIIα.

Topoisomerase IIα (TopoIIα) an ATP-dependent decatenase

Topoisomerase IIα (TopoIIα) is an ATP-dependent decatenase which functions during S-phase and mitosis to detangle DNA. TopoIIα does this through a Strand Passage Reaction (SPR). The TopoIIα SPR is a highly regulated enzymatic process which begins with the binding of one DNA molecule within the N-gate then, as a second DNA molecule is bound, the first is passed to the DNA-gate. Using ATP hydrolysis, a cut is made in the first DNA molecule and the second is passed through. Once the second is passed through, the first DNA molecule is re-ligated. Finally, both DNA molecules are released. By using its catalytic activity TopoIIα ensures that during S-phase replicated DNA does not become tangled. Also, this activity is essential during mitosis where it ensures that sister chromatids are not prematurely separated. TopoIIα enzyme activity can be inhibited using TopoII specific inhibitors, two used in the studies described below are Merbarone and ICRF-193. Merbarone blocks the cleavage step of TopoII. ICRF-193 blocks the release step of TopoII, blocking it in a closed clamp conformation with both strands of decatenated but not released DNA bound within it (Fortune and Osheroff, 1998). In addition, ICRF-193 has been shown to increase TopoIIα SUMOylation (discussed in Chapter three) (Figure 1.4) (Azuma, 2009; Pandey et al., 2020).

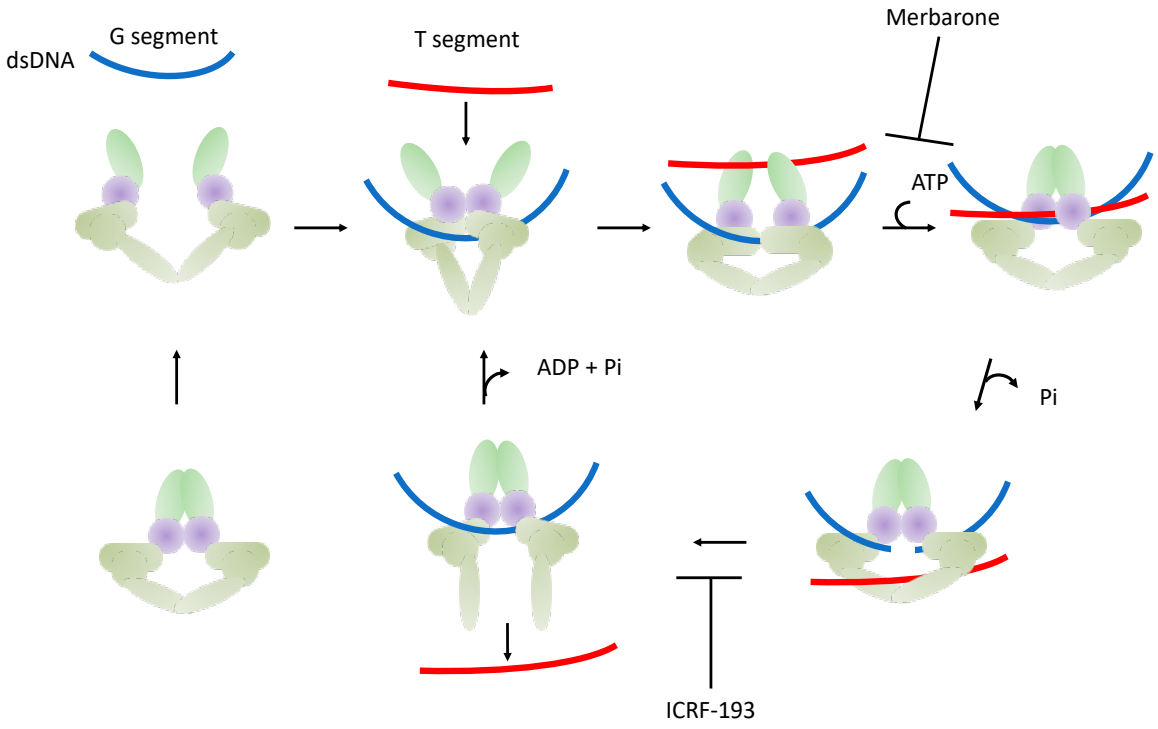

Figure 1.4 TopoIIα Strand Passage Reaction. TopoIIα acts as a homodimer which first binds the G-segment of DNA, then binds a second DNA strand called the T-segment. TopoIIα then cleaves the T-segment passing through the G-segment before re-ligating the T-segment then both decatenated segments are released. Merbarone acts to inhibit the ATPase dependent cleavage step in the SPR. ICRF-193 acts to block the release step in the SPR, maintaining TopoIIα in a closed clamp conformation.

It is known that TopoIIα can be upregulated in some cancers and due to its activity and importance in multiple cellular processes TopoIIα has been a long-standing target for chemotherapeutics (Nitiss, 2009). Thus, understanding the role of TopoIIα in chromosome segregation is incredibly important. The long-standing consensus in the field is that TopoIIα SPR is its major function, but why then, is the C-terminal domain necessary for cellular function? Recent studies have shown the importance of the C-terminal domain (CTD) in TopoIIα function (Clarke and Azuma, 2017). Although this

region is dispensable for the SPR, it is important for mitotic fidelity. This has been shown by discoveries which revealed that TopoIIα is a major component of mitotic chromosomes (Earnshaw et al., 1985). This led to the question of how TopoIIα associates with chromatin. We know that some TopoIIα molecules form a scaffold for chromosomes and help to maintain chromosomal structure, and without TopoIIα, chromosomes undergo condensation defects leading to misalignment and segregation defects (Clarke and Azuma, 2017). But we know that TopoIIα function is necessary for other cellular functions during mitosis, such as decatenation of sister chromatids and thus, cannot be solely secluded to chromosome scaffolds. Cytological analysis shows TopoIIα at the chromosome core, but live cell analysis found that TopoIIα highly dynamically spans across the entirety of chromosomes (Warburton and Earnshaw, 1997). How can TopoIIα have such a variable and dynamic localization? Likely, TopoIIα targeting to chromatid cores and to chromatin in general is not well understood. But recent evidence implicates the CTD as a molecular interface between TopoIIα and chromatin. What gives the CTD the ability to recognize and bind specific loci on the chromosomes? An important feature within the CTD is three verified SUMOylation sites (Figure 1.5).

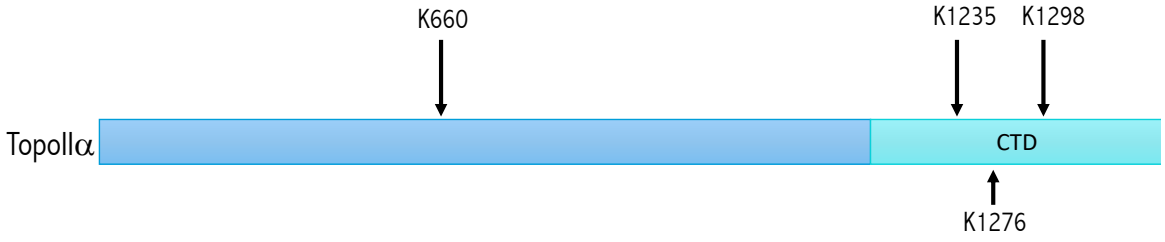

Figure 1.5. TopoIIα SUMOylation sites. Schematic illustrating the four verified TopoIIα SUMOylation sites.

How can TopoIIα CTD be important for cellular fidelity? The most likely answer to this lies within the SUMO/SIM interface. TopoIIα CTD SUMOylation is conserved from yeast to vertebrates. In mice, the SUMOylation of TopoIIα has been shown to be important for preventing chromosome segregation errors during mitosis, showing mice without TopoIIα SUMOylation having higher incidence of tumors (Nacerddine et al., 2005).

Role of TopoIIα C-Terminal Domain (CTD) SUMOylation

Although TopoIIα has been studied extensively, the role of CTD SUMOylation has not been well defined. A recent paper by Pandey et al., showed that cells possess a mechanism to delay the onset of anaphase when TopoIIα is perturbed. This delay is independent of the SAC checkpoint. This study indicated that TopoIIα SUMOylation is important in mobilizing Aurora B kinase from the inner centromere to the kinetochore proximal region of the centromere and the core of chromosome arms. This mobilization causes recruitment of Haspin kinase and is marked by histone H3 throenine-3 phosphorylation. Remarkably, this checkpoint requires both Aurora B and Haspin kinases. Mobilization of Aurora B was found to be TopoIIα CTD SUMOylation-specific through replacement with non-SUMOylatable TopoIIα which bypasses checkpoint activation. In all, the data show that SUMOylated TopoIIα recruits Aurora B, leading to a molecular cascade controlling the activation of the metaphase checkpoint when TopoIIα is catalytically inhibited (Pandey et al., 2020). This is critical in understanding how cells without PICH respond to treatment with ICRF-193. These cells show increased levels of TopoIIα SUMOylation, indicating increased checkpoint activation but without PICH seem unable to resolve trapped TopoIIα, indicating a role of PICH in the resolution of

TopoIIα (discussed in Chapter three) and in the TopoII-dependent checkpoint (discussed in Chapter four).

Summary

The work in this dissertation aimed to understand the role of SUMOylation on regulating mitosis. In Chapter two of this dissertation, I show how pioneering a CRISPR/Cas9 mediated system for endogenous protein degradation and exogenous mutant expression allowed us to observe cleaner phenotypic outcomes. Using novel molecular genetic approaches, in Chapter three of this dissertation, we show that PICH translocase activity is required for organization of SUMOylated proteins like SUMOylated TopoIIα on DLD-1 chromosomes. We also introduce a novel system for deSUMOylation on mitotic chromosomes to elucidate how this affects PICH and TopoIIα localization and interaction. Additionally, we saw that depletion of endogenous PICH caused accumulation of SUMOylated proteins on mitotic chromosomes and expression of translocase deficient mutant PICH caused an enrichment of SUMO2/3 signals on chromosomes. This led to the hypothesis that PICH uses its SIMs to bind SUMOylated substrates and causes redistribution of SUMOylated substrates using its translocase activity. This is a novel regulatory mechanism indicating that SUMOylation can be a targeting signal for protein remodeling. In Chapter four of this dissertation, we show that depletion of PICH causes a mitotic delay and this cannot be rescued by either translocase mutant or non-SUMO interacting mutant of PICH suggesting that both of these activities are required for normal mitotic progression. This is a novel function of PICH indicating a role in the resolution of tangled DNA during the decatenation checkpoint. Chapter five of this dissertation briefly summarizes the results presented

and looks to the future of PICH/SUMO research. Discoveries described in this dissertation have led to novel understandings of how protein interactions are regulated by SUMOylation, the role PICH plays on SUMOylated TopoIIα, and mitotic progression. Overall this work enhances the understanding of regulation of mitosis by SUMOylation.

References

Agostinho, M., Santos, V., Ferreira, F., Costa, R., Cardoso, J., Pinheiro, I., Rino, J., Jaffray, E., Hay, R.T., and Ferreira, J. (2008). Conjugation of human topoisomerase 2 alpha with small ubiquitin-like modifiers 2/3 in response to topoisomerase inhibitors: cell cycle stage and chromosome domain specificity. Cancer Res. *68*, 2409–2418.

Azuma, Y. (2009). Analysis of SUMOylation of topoisomerase IIalpha with Xenopus egg extracts. Methods Mol. Biol. Clifton NJ *582*, 221–231.

Bachant, J., Alcasabas, A., Blat, Y., Kleckner, N., and Elledge, S.J. (2002). The SUMO-1 isopeptidase Smt4 is linked to centromeric cohesion through SUMO-1 modification of DNA topoisomerase II. Mol. Cell *9*, 1169–1182.

Baumann, C., Körner, R., Hofmann, K., and Nigg, E.A. (2007). PICH, a centromere-associated SNF2 family ATPase, is regulated by Plk1 and required for the spindle checkpoint. Cell *128*, 101–114.

Bernier-Villamor, V., Sampson, D.A., Matunis, M.J., and Lima, C.D. (2002). Structural basis for E2-mediated SUMO conjugation revealed by a complex between ubiquitin-conjugating enzyme Ubc9 and RanGAP1. Cell *108*, 345–356.

Biebricher, A., Hirano, S., Enzlin, J.H., Wiechens, N., Streicher, W.W., Huttner, D., Wang, L.H.-C., Nigg, E.A., Owen-Hughes, T., Liu, Y., et al. (2013). PICH: a DNA translocase specially adapted for processing anaphase bridge DNA. Mol. Cell *51*, 691–701.

Clarke, D.J., and Azuma, Y. (2017). Non-Catalytic Roles of the Topoisomerase IIα C-Terminal Domain. Int. J. Mol. Sci. *18*.

Cubeñas-Potts, C., Goeres, J.D., and Matunis, M.J. (2013). SENP1 and SENP2 affect spatial and temporal control of sumoylation in mitosis. Mol. Biol. Cell *24*, 3483–3495.

Desterro, J.M., Thomson, J., and Hay, R.T. (1997). Ubch9 conjugates SUMO but not ubiquitin. FEBS Lett. *417*, 297–300.

Desterro, J.M., Rodriguez, M.S., Kemp, G.D., and Hay, R.T. (1999). Identification of the enzyme required for activation of the small ubiquitin-like protein SUMO-1. J. Biol. Chem. *274*, 10618–10624.

Di Bacco, A., Ouyang, J., Lee, H.-Y., Catic, A., Ploegh, H., and Gill, G. (2006). The SUMO-specific protease SENP5 is required for cell division. Mol. Cell. Biol. *26*, 4489–4498.

Earnshaw, W.C., Halligan, B., Cooke, C.A., Heck, M.M., and Liu, L.F. (1985). Topoisomerase II is a structural component of mitotic chromosome scaffolds. J. Cell Biol. *100*, 1706–1715.

Farr, K.A., and Cohen-Fix, O. (1999). The metaphase to anaphase transition: a case of productive destruction. Eur. J. Biochem. *263*, 14–19.

Fortune, J.M., and Osheroff, N. (1998). Merbarone inhibits the catalytic activity of human topoisomerase IIalpha by blocking DNA cleavage. J. Biol. Chem. *273*, 17643–17650.

Fraser, A.G., Kamath, R.S., Zipperlen, P., Martinez-Campos, M., Sohrmann, M., and Ahringer, J. (2000). Functional genomic analysis of C. elegans chromosome I by systematic RNA interference. Nature *408*, 325–330.

Geiss-Friedlander, R., and Melchior, F. (2007). Concepts in sumoylation: a decade on. Nat. Rev. Mol. Cell Biol. *8*, 947–956.

Gong, L., and Yeh, E.T.H. (2006). Characterization of a family of nucleolar SUMO-specific proteases with preference for SUMO-2 or SUMO-3. J. Biol. Chem. *281*, 15869–15877.

Gong, L., Li, B., Millas, S., and Yeh, E.T. (1999). Molecular cloning and characterization of human AOS1 and UBA2, components of the sentrin-activating enzyme complex. FEBS Lett. *448*, 185–189.

Hari, K.L., Cook, K.R., and Karpen, G.H. (2001). The Drosophila Su(var)2-10 locus regulates chromosome structure and function and encodes a member of the PIAS protein family. Genes Dev. *15*, 1334–1348.

Hecker, C.-M., Rabiller, M., Haglund, K., Bayer, P., and Dikic, I. (2006). Specification of SUMO1- and SUMO2-interacting motifs. J. Biol. Chem. *281*, 16117–16127.
Huang, C., Cheng, J., Bawa-Khalfe, T., Yao, X., Chin, Y.E., and Yeh, E.T.H. (2016). SUMOylated ORC2 Recruits a Histone Demethylase to Regulate Centromeric Histone Modification and Genomic Stability. Cell Rep. *15*, 147–157.
Hübner, N.C., Wang, L.H.-C., Kaulich, M., Descombes, P., Poser, I., and Nigg, E.A. (2010). Re-examination of siRNA specificity questions role of PICH and Tao1 in the spindle checkpoint and identifies Mad2 as a sensitive target for small RNAs. Chromosoma *119*, 149–165.
Jeyaprakash, A.A., Basquin, C., Jayachandran, U., and Conti, E. (2011). Structural basis for the recognition of phosphorylated histone h3 by the survivin subunit of the chromosomal passenger complex. Struct. Lond. Engl. 1993 *19*, 1625–1634.
Johnson, E.S., and Blobel, G. (1997). Ubc9p is the conjugating enzyme for the ubiquitin-like protein Smt3p. J. Biol. Chem. *272*, 26799–26802.
Johnson, E.S., Schwienhorst, I., Dohmen, R.J., and Blobel, G. (1997). The ubiquitin-like protein Smt3p is activated for conjugation to other proteins by an Aos1p/Uba2p heterodimer. EMBO J. *16*, 5509–5519.
Kahyo, T., Nishida, T., and Yasuda, H. (2001). Involvement of PIAS1 in the sumoylation of tumor suppressor p53. Mol. Cell *8*, 713–718.
Ke, Y., Huh, J.-W., Warrington, R., Li, B., Wu, N., Leng, M., Zhang, J., Ball, H.L., Li, B., and Yu, H. (2011). PICH and BLM limit histone association with anaphase centromeric DNA threads and promote their resolution. EMBO J. *30*, 3309–3321.
Kelly, A.E., Ghenoiu, C., Xue, J.Z., Zierhut, C., Kimura, H., and Funabiki, H. (2010). Survivin reads phosphorylated histone H3 threonine 3 to activate the mitotic kinase Aurora B. Science *330*, 235–239.
Krenn, V., and Musacchio, A. (2015). The Aurora B Kinase in Chromosome Bi-Orientation and Spindle Checkpoint Signaling. Front. Oncol. *5*, 225.
Kumagi A (2003). Repeated phosphopeptide motifs in Claspin mediate the regulated binding of Chk1. - PubMed - NCBI. Nat Cell Biol.
Lee, G.W., Melchior, F., Matunis, M.J., Mahajan, R., Tian, Q., and Anderson, P. (1998). Modification of Ran GTPase-activating protein by the small ubiquitin-related modifier SUMO-1 requires Ubc9, an E2-type ubiquitin-conjugating enzyme homologue. J. Biol. Chem. *273*, 6503–6507.
Mahajan, R., Delphin, C., Guan, T., Gerace, L., and Melchior, F. (1997). A small ubiquitin-related polypeptide involved in targeting RanGAP1 to nuclear pore complex protein RanBP2. Cell *88*, 97–107.
Matunis, M.J., Coutavas, E., and Blobel, G. (1996). A novel ubiquitin-like modification modulates the partitioning of the Ran-GTPase-activating protein RanGAP1 between the cytosol and the nuclear pore complex. J. Cell Biol. *135*, 1457–1470.
McManus, F.P., Bourdeau, V., Acevedo, M., Lopes-Paciencia, S., Mignacca, L., Lamoliatte, F., Rojas Pino, J.W., Ferbeyre, G., and Thibault, P. (2018). Quantitative SUMO proteomics reveals the modulation of several PML nuclear body associated proteins and an anti-senescence function of UBC9. Sci. Rep. *8*, 7754.
Meluh, P.B., and Koshland, D. (1995). Evidence that the MIF2 gene of Saccharomyces cerevisiae encodes a centromere protein with homology to the mammalian centromere protein CENP-C. Mol. Biol. Cell *6*, 793–807.
Muller, S., Berger, M., Lehembre, F., Seeler, J.S., Haupt, Y., and Dejean, A. (2000). c-Jun and p53 activity is modulated by SUMO-1 modification. J. Biol. Chem. *275*, 13321–13329.
Nacerddine, K., Lehembre, F., Bhaumik, M., Artus, J., Cohen-Tannoudji, M., Babinet, C., Pandolfi, P.P., and Dejean, A. (2005). The SUMO pathway is essential for nuclear integrity and chromosome segregation in mice. Dev. Cell *9*, 769–779.

Narlikar, G.J., Sundaramoorthy, R., and Owen-Hughes, T. (2013). Mechanisms and functions of ATP-dependent chromatin-remodeling enzymes. Cell *154*, 490–503.
Nielsen, C.F., Huttner, D., Bizard, A.H., Hirano, S., Li, T.-N., Palmai-Pallag, T., Bjerregaard, V.A., Liu, Y., Nigg, E.A., Wang, L.H.-C., et al. (2015). PICH promotes sister chromatid disjunction and co-operates with topoisomerase II in mitosis. Nat. Commun. *6*, 8962.
Nishida, T., and Yasuda, H. (2002). PIAS1 and PIASxalpha function as SUMO-E3 ligases toward androgen receptor and repress androgen receptor-dependent transcription. J. Biol. Chem. *277*, 41311–41317.
Nitiss, J.L. (2009). Targeting DNA topoisomerase II in cancer chemotherapy. Nat. Rev. Cancer *9*, 338–350.
Ohkuni, K., Levy-Myers, R., Warren, J., Au, W.-C., Takahashi, Y., Baker, R.E., and Basrai, M.A. (2018). N-terminal Sumoylation of Centromeric Histone H3 Variant Cse4 Regulates Its Proteolysis To Prevent Mislocalization to Non-centromeric Chromatin. G3 Bethesda Md *8*, 1215–1223.
Pandey, N., Keifenheim, D., Yoshida, M.M., Hassebroek, V.A., Soroka, C., Azuma, Y., and Clarke, D.J. (2020). Topoisomerase II SUMOylation activates a metaphase checkpoint via Haspin and Aurora B kinases. J. Cell Biol. *219*.
Petsalaki, E., Akoumianaki, T., Black, E.J., Gillespie, D.A.F., and Zachos, G. (2011). Phosphorylation at serine 331 is required for Aurora B activation. J. Cell Biol. *195*, 449–466.
Pichler, A., Gast, A., Seeler, J.S., Dejean, A., and Melchior, F. (2002). The nucleoporin RanBP2 has SUMO1 E3 ligase activity. Cell *108*, 109–120.
Piskadlo, E., and Oliveira, R.A. (2016). Novel insights into mitotic chromosome condensation. F1000Research *5*.
Ryu, H., Furuta, M., Kirkpatrick, D., Gygi, S.P., and Azuma, Y. (2010). PIASy-dependent SUMOylation regulates DNA topoisomerase IIalpha activity. J. Cell Biol. *191*, 783–794.
Ryu, H., Yoshida, M.M., Sridharan, V., Kumagai, A., Dunphy, W.G., Dasso, M., and Azuma, Y. (2015). SUMOylation of the C-terminal domain of DNA topoisomerase IIα regulates the centromeric localization of Claspin. Cell Cycle Georget. Tex *14*, 2777–2784.
Sachdev, S., Bruhn, L., Sieber, H., Pichler, A., Melchior, F., and Grosschedl, R. (2001). PIASy, a nuclear matrix-associated SUMO E3 ligase, represses LEF1 activity by sequestration into nuclear bodies. Genes Dev. *15*, 3088–3103.
Sapetschnig, A., Rischitor, G., Braun, H., Doll, A., Schergaut, M., Melchior, F., and Suske, G. (2002). Transcription factor Sp3 is silenced through SUMO modification by PIAS1. EMBO J. *21*, 5206–5215.
Saracco, S.A., Miller, M.J., Kurepa, J., and Vierstra, R.D. (2007). Genetic analysis of SUMOylation in Arabidopsis: conjugation of SUMO1 and SUMO2 to nuclear proteins is essential. Plant Physiol. *145*, 119–134.
Schimmel, J., Eifler, K., Sigurðsson, J.O., Cuijpers, S.A.G., Hendriks, I.A., Verlaan-de Vries, M., Kelstrup, C.D., Francavilla, C., Medema, R.H., Olsen, J.V., et al. (2014). Uncovering SUMOylation dynamics during cell-cycle progression reveals FoxM1 as a key mitotic SUMO target protein. Mol. Cell *53*, 1053–1066.
Schmidt, D., and Müller, S. (2002). Members of the PIAS family act as SUMO ligases for c-Jun and p53 and repress p53 activity. Proc. Natl. Acad. Sci. U. S. A. *99*, 2872–2877.
Seufert, W., Futcher, B., and Jentsch, S. (1995). Role of a ubiquitin-conjugating enzyme in degradation of S- and M-phase cyclins. Nature *373*, 78–81.
Shen, Z., Pardington-Purtymun, P.E., Comeaux, J.C., Moyzis, R.K., and Chen, D.J. (1996). UBL1, a human ubiquitin-like protein associating with human RAD51/RAD52 proteins. Genomics *36*, 271–279.

Song, J., Durrin, L.K., Wilkinson, T.A., Krontiris, T.G., and Chen, Y. (2004). Identification of a SUMO-binding motif that recognizes SUMO-modified proteins. Proc. Natl. Acad. Sci. U. S. A. *101*, 14373–14378.

Sridharan, V., and Azuma, Y. (2016). SUMO-interacting motifs (SIMs) in Polo-like kinase 1-interacting checkpoint helicase (PICH) ensure proper chromosome segregation during mitosis. Cell Cycle Georget. Tex *15*, 2135–2144.

Sridharan, V., Park, H., Ryu, H., and Azuma, Y. (2015). SUMOylation regulates polo-like kinase 1-interacting checkpoint helicase (PICH) during mitosis. J. Biol. Chem. *290*, 3269–3276.

Tanaka, K., Nishide, J., Okazaki, K., Kato, H., Niwa, O., Nakagawa, T., Matsuda, H., Kawamukai, M., and Murakami, Y. (1999). Characterization of a fission yeast SUMO-1 homologue, pmt3p, required for multiple nuclear events, including the control of telomere length and chromosome segregation. Mol. Cell. Biol. *19*, 8660–8672.

Wan, J., Subramonian, D., and Zhang, X.-D. (2012). SUMOylation in control of accurate chromosome segregation during mitosis. Curr. Protein Pept. Sci. *13*, 467–481.

Wang, L.H.-C., Mayer, B., Stemmann, O., and Nigg, E.A. (2010). Centromere DNA decatenation depends on cohesin removal and is required for mammalian cell division. J. Cell Sci. *123*, 806–813.

Warburton, P.E., and Earnshaw, W.C. (1997). Untangling the role of DNA topoisomerase II in mitotic chromosome structure and function. BioEssays News Rev. Mol. Cell. Dev. Biol. *19*, 97–99.

Yamano, H. (2019). APC/C: current understanding and future perspectives. F1000Research *8*.

Yoshida, M.M., Ting, L., Gygi, S.P., and Azuma, Y. (2016). SUMOylation of DNA topoisomerase IIα regulates histone H3 kinase Haspin and H3 phosphorylation in mitosis. J. Cell Biol. *213*, 665–678.

Zhang, X.-D., Goeres, J., Zhang, H., Yen, T.J., Porter, A.C.G., and Matunis, M.J. (2008). SUMO-2/3 modification and binding regulate the association of CENP-E with kinetochores and progression through mitosis. Mol. Cell *29*, 729–741.

Zilio, N., Williamson, C.T., Eustermann, S., Shah, R., West, S.C., Neuhaus, D., and Ulrich, H.D. (2013). DNA-dependent SUMO modification of PARP-1. DNA Repair *12*, 761–773.

Chapter 2 Methods for studying essential proteins during mitosis

Introduction

Tools to address the molecular function of a gene by molecular genetic approaches in the field of cell biology have been limited until recently. Groups made use of siRNA mediated knockdown methodology, but this led to its own subset of problems like off targeting effects, incomplete knockdown, and arduous/delayed knockdown. Evidence now indicate that siRNA does not always target a specific gene, resulting in non-specific gene silencing (Jackson et al., 2003; Xu et al., 2006). Non-specificity in siRNA mediated knockdown occur when partial sequence homology allows siRNA to degrade mRNA for genes that were not the original targets (Senthil-Kumar and Mysore, 2011). This issue is especially relevant when discussing PICH because the first siRNAs designed for PICH knockdown showed that it was a checkpoint protein (hence the C in PICH) but, later, was found to be an off-target effect from the siRNA designed and used (Baumann et al., 2007). Upon further analysis Hübner et al., showed that three different PICH siRNA constructs also caused Mad2 and Tao1 depletion (Hübner et al., 2010). The next issue with using siRNA mediated knockdown is incomplete knockdown/length of time to achieve partial knockdown. When using siRNA for PICH depletion in our lab achieved nearly complete knockdown, but it took 3 days (Sridharan and Azuma, 2016). With the recent development of clustered regularly interspaced short-palindromic repeats (CRISPR)/CRISP-associated (Cas) system-based gene-editing technology (CRISPR/Cas9) came the ability to easily knockout a gene of interest (Cong et al., 2013; Mali et al., 2013; O'Connell et al., 2014). CRISPR/Cas9 gene editing was extremely relevant to those studying non-essential genes/gene interactions. But

because PICH is an essential gene for cell viability, and therefore knocking it down for more than one cell cycle can cloud results by multiple cell cycles of chromosome mis-segregation, simply generating a knockout cell line would not suffice. This led me to search for a different method of gene knockdown, which would allow for controllable degradation within a single cell cycle. So, our new system had to enable rapid depletion as well as enable exogenous expression of PICH mutants to delve into the function of PICH on chromosome segregation. This led me to design and implement the Auxin Inducible Degron (AID) system (Natsume et al., 2016).

This system was first discovered and utilized in budding yeast by Dohmen et al. where they achieved conditional depletion by fusing a destabilizing domain (so-called degron) to their proteins of interest (Dohmen et al., 1994). Other groups have gone on to generate other degron technologies by fusion of small molecules (Banaszynski et al., 2006; Bonger et al., 2011; Chung et al., 2015; Iwamoto et al., 2010; Neklesa et al., 2011). With the discovery of CRISPR/Cas9 came the possibility to refine the inducible degron systems. Nishimura et. al. hijacked a plant-specific degradation pathway controlled by a phytohormone called auxin and utilized it in human cells for the first time in 2009. Plants evolved a unique system, which utilizes auxin to directly induce rapid degradation of the AUX/IAA family of transcription repressors through a specific (Skp1-Cullin-F-box) SCF E3 ubiquitin ligase (Teale et al., 2006). Other eukaryotes utilize the same SCF degradation pathway but lack the auxin response. So, Nishimura et al. transplanted the AID system into non-plant cells and use auxin to control depletion of AID-tagged proteins (Figure 2.1). In this chapter I will describe how I adopted this AID

system, as well as CRISPR/Cas9 editing technology, to achieve our goal for establishing molecular genetic approaches in mammalian cells.

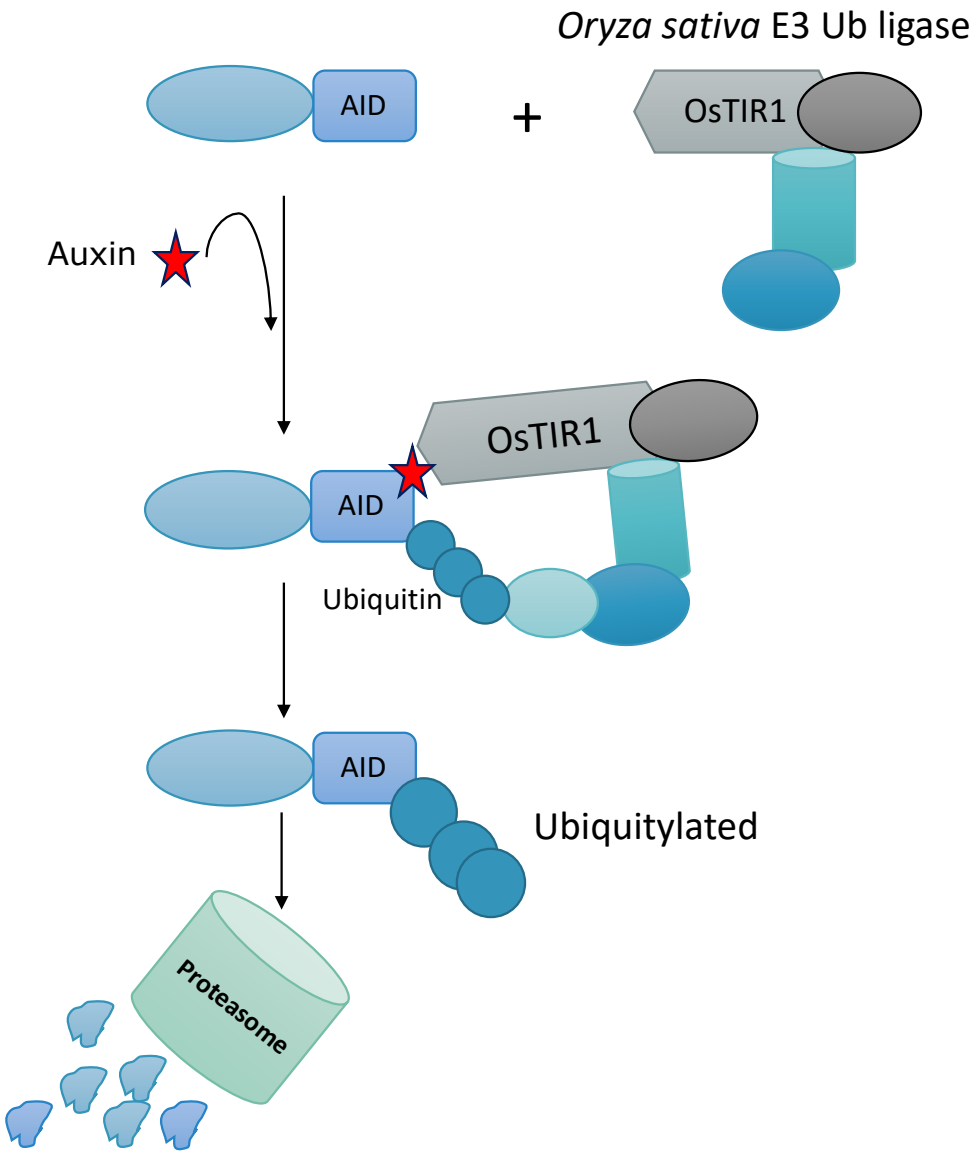

Figure 2.1. Auxin inducible degron system. Schematic illustration of the Auxin inducible degron (AID) system. Expressed Skip-Cullin-F-Box^{OsTIR1} can form a functional E3 ligase complex (Nishimura et al., 2009). In the presence of auxin, the protein of interest with mAID tag is rapidly degraded by the proteasome.

Results

Guide RNA design

The AID system was revolutionized by the discovery of CRISPR/Cas9 technology which enabled precise protein tagging. Cells expressing the F-box protein TIR1, which forms a functional SCF ubiquitin ligase and that have a protein tagged with an AID derived from the IAA17 protein of *Arabidopsis thaliana* can be induced for rapid degradation by the addition of auxin to culture medium (Nishimura et al., 2009). Critically, this AID technology enables rapid degradation with a typical half-life of 10-20 min (Holland AJ, 2012; Lambrus et al., 2015). Much quicker than the other degron technologies described previously in this chapter, which usually have a half-life of several hours (Kanemaki, 2013). This system is also reversible, which enables recovery assays to be optimized as well. But, as I mentioned previously, this technology has been limited until the discovery of CRISPR/Cas9 editing because it was difficult to tag endogenous proteins with an AID.

To overcome this hurdle, Natsume et al. used a CRISPR/Cas9 method for tagging endogenous proteins, using short-homology arm donors. First, a reasonable guide RNA (gRNA) must be identified in the locus of your gene of interest. In my case I wanted to endogenously tag the N-terminus of PICH and used the MIT CRISPR guide website curated by the Zhang lab (Joung et al., 2019). Guide RNAs must fall within 20 nucleotides of the target, for PICH this was 20 nucleotides before the ATG site, and they must not have many off-target sequences falling elsewhere in the genome (Ran et al., 2013). I found a gRNA that was exactly 20 nucleotides from the PICH start site. Next, homology arms must be designed which incorporates the guide site. The

Natsume group found that homology arms could be as short as 125-bp and still deliver the tag to the locus of interest (Natsume et al., 2016). This led me to design 285-bp homology arms. One crucial step in homology arm design is the mutation of protospacer adjacent motifs or PAM sites. PAM sites are short DNA sequences that fall 3-4 bases from the Cas9 cleavable site. Without a mutation in the PAM site which renders it unable to be cut by Cas9, the insert can be continuously put in and cut out again while the Cas9 enzyme is being expressed within the cells, which has been shown to be as long lived as 7 days (Idoko-Akoh et al., 2018).

Oryza sativa (*OsTIR1*) Ubiquitin E3 ligase integration

To begin using this system it is necessary to introduce the *TIR1* gene into your cell line of choice. The Natsume group chose to utilize the *Oryza sativa* (*OsTIR1*) because it was stable at higher temperatures (Nishimura et al., 2009). They then used a safe harbor site called Adeno-associated viral integration site (AAVS1). A safe harbor site is a site in which DNA can be introduced without manipulating expression of the cellular endogenous genome. The AAVS1 safe harbor was one of the first discovered in 2008 by Smith et. al. (Smith et al., 2008). One obstacle that the Natsume et al. paper discovered is that once integrated and after clonal isolation by antibiotic selection, the OsTIR1 protein under constitutive expression controlled by the cytomegalovirus (CMV) promoter was robustly produced (Natsume et al., 2016). This became an issue once they had tagged the protein of interest with an AID, they saw degradation without the presence of auxin. They determined that lower levels of OsTIR1 expression would be needed to maintain controllable induction of degradation. They then utilized a Tet-inducible promoter and donor plasmid with the Tet transactivator in reverse orientation

under a human phosphoglycerate kinase (hPGK) promoter. This enabled them to turn on expression of their OsTIR1 protein at the same time as auxin addition. But expression of the OsTIR1 protein brought up a new obstacle in the system which was that even when treated with doxycycline their clonal isolates began expressing the OsTIR1 mosaically, I will discuss this in more detail in the next section. Uneven expression, of course, meant mosaic degradation of their AID-tagged proteins (Natsume et al., 2016). To overcome the mosaic degradation obstacle, we collaborated with Dr. Mary Dasso at the National Institute of Health (NIH). The Dasso group developed a new method to keep OsTIR1 levels low without using the Tet-ON system. They utilized the promoter of an endogenous housekeeping protein called regulator of chromosome condensation 1 (RCC1). This is a Ran guanine exchange factor that is maintained at consistent expression levels throughout the cell cycle (Moore, 2001). Using CRISPR/Cas9 mediated editing the Dasso group put the *OsTIR1* gene under the *RCC1* promoter separating the two genes and the gene for Blasticidin resistance by a porcine teschovirus-1 2A (P2A) site. This is a self-cleaving peptide that enabled all proteins to be translated together and then cleaved to avoid fusion of the proteins (Kim et al., 2011). After testing, the Dasso group found that levels of OsTIR1 caused no nonspecific degradation in the absence of auxin, and in the presence of auxin all cells rapidly reached knockout levels (undetectable by immunofluorescent and Western blot analysis). This is in contrast to OsTIR1 levels under a CMV promoter which causes nonspecific degradation in the absence of auxin because the expression levels were too high (Natsume et al., 2016).

We began by modifying the plasmid provided by the Dasso group, which had an miRFP tag to label RCC1 which we did not need. The plasmid we generated by modifying the Dasso plasmid is shown in Figure 2.2 which has Blasticidin resistance followed by P2A then the OsTIR1 gene and a myc tag for OsTIR1 visualization. After preparation of the plasmid I began by generating a parental *OsTIR1* cell line in the DLD-1 cell line, kindly provided, along with donor and guide plasmids by the Dasso group. This colon epithelial cell line was chosen for its characteristic euploidy karyotype and because DLD-1 cells transfect with high efficiency and therefore are a good choice when using CRISPR/Cas9 mediated editing. After transfection and 10 days of selection, colonies were isolated. The isolation strategy previously used in our lab involved cloning rings which needed to be coated with Vaseline and autoclaved. Cloning rings can introduce problems such as; incomplete Vaseline seal, inter-clonal contamination, and general contamination. Due to these problems, I sought to incorporate a different method for clonal isolation in our lab.

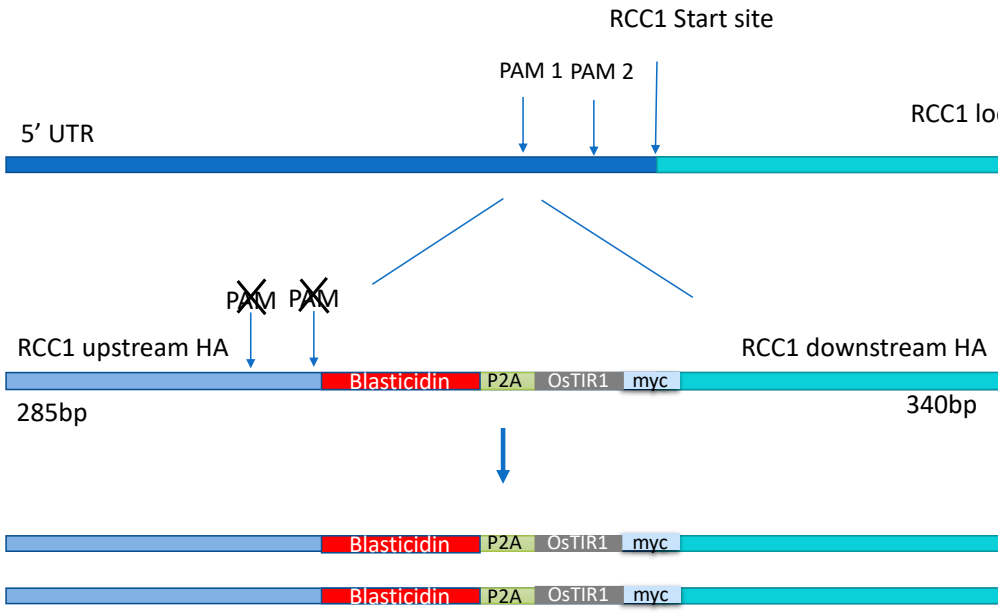

Figure 2.2. RCC1 CRISPR/Cas9 targeting construct. Schematic illustrating CRISPR *OsTIR1* knock-in at the *RCC1* locus.

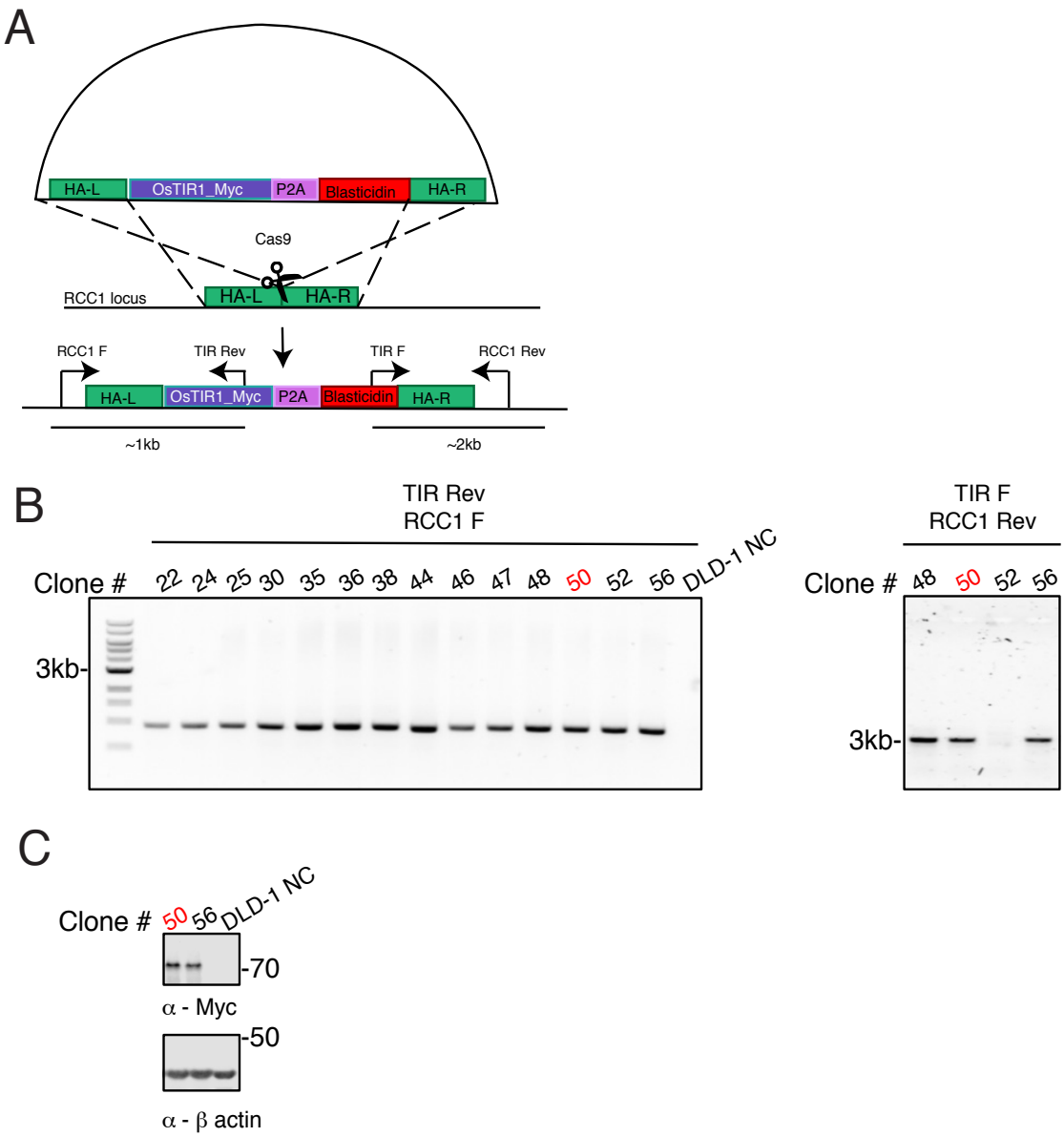

Figure 2.3. Construction of OsTIR1 expressing DLD-1 cell lines.
(A) Experimental schematic for the establishment of OsTIR1 gene expressing DLD1 cell. RCC1-OsTIR1-Myc-P2A-Blasticidin donor plasmid, and two guide RNAs targeting the 3' end of RCC1 were used to integrate the OsTIR1 gene into the RCC1 locus.
(B) After the selection with 2ug/mL Blasticidin, fourteen clones were isolated and subjected to genomic PCR utilizing primers that targeted the 5' end of the construct (upper panel). Non-transfected DLD-1 cells were used as a negative control (DLD-1 NC). Clones #48, 50, 52 and 56 were further verified by genomic PCR using primers for 3' ends of the construct.
(C) Among the positive clones identified in **B**, two clones were chosen to verify the protein expression by Western blotting. Whole cell lysates obtained from asynchronous cell population were subjected to Western blotting. Non-transfected DLD-1 whole cell lysate was used as a negative control (DLD-1 NC). An anti-Myc antibody was used to detect OsTIR1 protein and anti-β-actin was used as a loading control. Clone #50 (marked in red) was chosen to utilize for subsequent AID tagging for TopoIIα and PICH.

I developed and implemented a new clonal isolation method in which clones were picked under the microscope using a 20-200ul pipettor. This enabled complete control of clonal isolation, which eliminated the risk of inter-clonal contamination and was more efficient than the previously described method. After optimization, clones were picked under the microscope and screened for proper integration of the *OsTIR1* gene (Figure 2.3A).

Two screening methods were used, PCR amplification of genomic DNA isolated from clones and Western blot analysis utilizing an anti-myc antibody (Figure 2.3B, C). The PCR construct used amplified both the 5' and 3' of the integration site with one primer falling within integrated sequence and one outside of the integrated sequence. This enabled us to screen clones for proper integration of the transgene as well as for protein product. We saw an integration rate of 93% where 14/14 clones showed 5' integration and 13/14 showed 3' integration. Now that OsTIR1 parental cells were generated, the next step was to endogenously tag PICH with an AID.

Targeting Auxin Inducible Degron (AID) tag to gene of interest

The AID I chose to use is a mini-AID which was a 68-aa fragment modified from the original AID/IAA7 tag, the molecular weight is 7.4kDa (Nishimura and Kanemaki, 2014). DLD-1 parental cells (with confirmed OsTIR1 integration) were transfected with the PICH donor and gRNA. After clonal isolation I found that none of my isolated clones had the AID tag. After troubleshooting and determining that the donor plasmid and transfection protocol was not the issue, I designed additional guide RNAs, as this had shown increased efficiency of tagging in the OsTIR1 step. Parental cells were

transfected with a donor plasmid and three gRNAs all targeting the N-terminus of PICH (Figure 2.4).

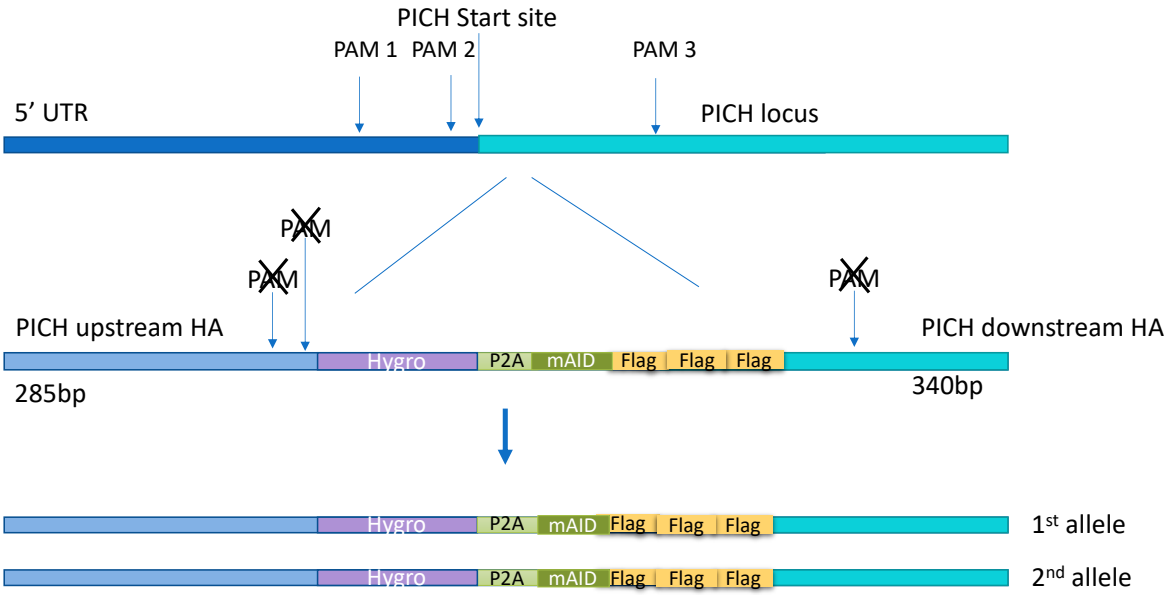

Figure 2.4. PICH CRISPR/Cas9 targeting construct. Schematic illustrating CRISPR *mAID* knock-in at the *PICH* locus.

After clonal isolation, I found that nearly all isolated clones were homozygously tagged with the mAID by Western blot and PCR amplification showed proper integration at the 5' end of my insertion site (Figure 2.5B, C). Cells were then treated with auxin to examine degradation efficiency and timing.

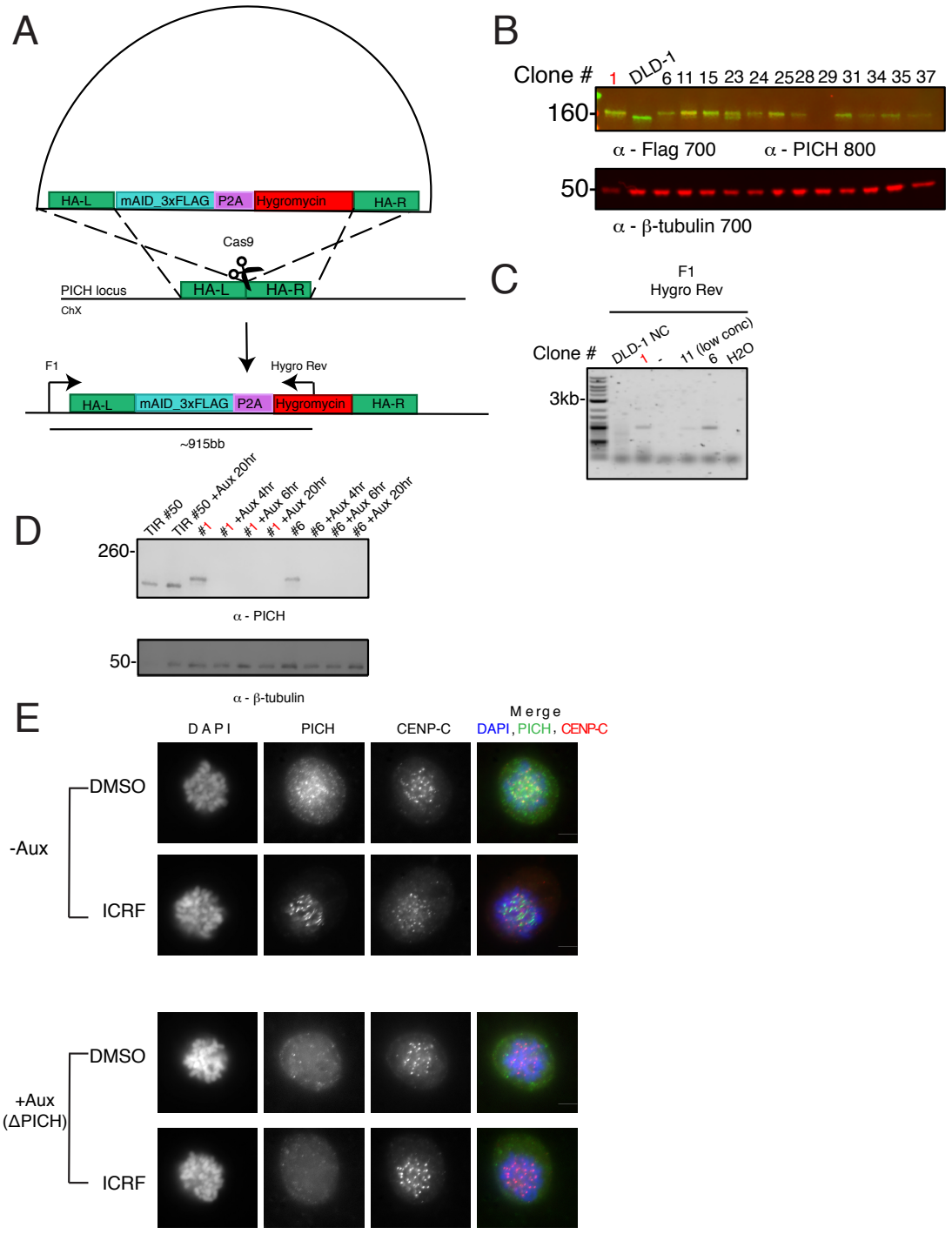

Figure 2.5. Construction of PICH-AID cell line.
(A) Experimental schematic of donor plasmid used to tag the 5' end of endogenous PICH locus with AID tag. Cells were transfected with PICH-mAID-3xFlag-P2A-Hygromycin donor and two

different guide RNAs. After selection with 400ug/mL hygromycin clones were isolated, whole cell lysates were collected from asynchronous populations, and Western blotting was performed.
(B) Representative Western blot for hygromycin-resistant clone screening is shown. An anti-Flag antibody was used to detect AID-Flag tagged PICH (~180kDa) in the 700 channel (colored red) and anti-PICH antibodies were used to detect both AID-Flag tagged PICH (~180kDa) and untagged PICH (~150kDa) in the 800 channel (colored green). Non-transfected DLD-1 TIR1#50 parental cell line (labeled DLD-1) was used as a negative control. Anti-β-tubulin was used as a loading control. Among thirteen samples analyzed, the clones which showed a single yellow PICH band were chosen for genomic PCR analysis (clones #1, 6 and 11).
(C) Genomic DNA was isolated and subjected to PCR using an F1 primer located upstream of the left homology arm and Hygro Rev PCR primer located within the insert. Non-transfected DLD-1 TIR#50 parental cell DNA was used as a control (DLD-1 NC).
(D) The clones 1 and 6 were tested for further depletion of PICH protein by auxin addition at 4, 6, and 20-hour time points. The non-transfected DLD-1 TIR1#50 parental cells were used as a control with either non-treated (TIR#50) or treated with auxin for 20 hours (TIR#50 +Aux 20 hours). The whole cell lysates were subjected to Western blotting analysis. Anti-PICH antibodies were used to detect PICH (~150kDa) or PICH-AID (~180kDa), anti-β-tubulin antibodies were used as a loading control. Clone #1 (marked in red) was chosen to utilize for subsequent experiments showed in Figure 5 and Figure S6.
(E) DLD-1 cells with endogenous PICH tagged with an auxin inducible degron (AID) were synchronized in mitosis and treated with DMSO or ICRF-193. Auxin was added 6 hours after Thymidine release. Mitotic cells obtained by shake-off were plated onto fibronectin coated coverslips and subsequently stained with indicated antibodies. DNA was labeled with DAPI. PICH foci on mitotic chromosomes were completely eliminated with auxin in both DMSO and ICRF-193 treated cells.

Two PICH clones were seen to be degraded to undetectable levels within 4 hours of treatment with auxin (the shortest time-point tested) by Western blot and immunofluorescent analysis (Figure 2.5D, E). The foci observed in Figure 2.5E were observed to be non-specific binding of PICH antibody as the foci do not occur on the chromosomes where PICH localizes. This rapid depletion enabled the loss of PICH within a single cell cycle, which was important because PICH siRNA not only ran the risk of having off-target effects but also took 3 days to achieve the same level of depletion. Time of depletion using siRNA then clouded phenotypes as PICH depletion causes chromosome segregation defects. By achieving knockout levels of PICH in 4 hours, I was able to study the effect of loss of PICH in a single cell cycle. To further

study the role PICH plays in chromosome segregation during mitosis, the introduction of different PICH mutants under a controllable promoter would also become necessary.

Safe harbor selection, Tet-inducible gene insertion, and screening

To introduce inducible PICH mutants into OsTIR1-mAID-PICH cells we utilized donor constructs deposited by Kanekami et al. which had the Tet transactivator under the human phosphoglycerate kinase (hPGK) promoter and gene of interest under the control of a tet-inducible promoter (Natsume et al., 2016). These CRISPR/Cas9 constructs targeted the AAVS1 safe harbor locus (Figure 2.6). PICH mutants with an mCherry tag were integrated into the donor construct and OsTIR1-mAID-PICH cells were transfected. After 12 clones were isolated each clone was treated with auxin and doxycycline for 14 hours to induce degradation of PICH and expression of exogenous PICH mCherry. Three clones were seen to have mCherry expression, albeit low. But, after passaging no mCherry signal could be detected. PCR amplification of both 5' and 3' integration sites showed that the transgene had integrated properly but Western blot analysis showed low levels of PICH and mCherry signals. After troubleshooting doses of doxycycline and time of induction for expression we came to the conclusion that the integrated genes might have been silenced. This was supported by Klatt et al. who showed that high CpG methylation of promoters introduced into AAVS1 sites can occur (Klatt et al., 2020). To overcome this issue other safe harbor sites were sought out.

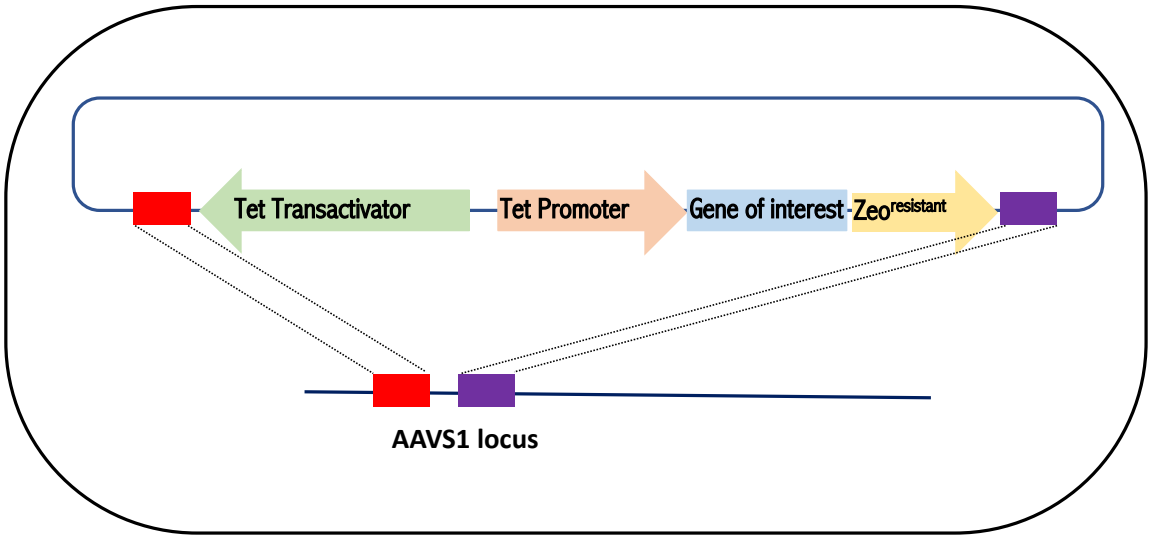

Figure 2.6. Tet-inducible CRISPR/Cas9 AAVS1 targeting construct. Schematic illustrating CRISPR knock-in at the *AAVS1* safe harbor locus.

The second safe harbor site identified was a well-studied site called *chemokine receptor 5* (*CCR5*). CCR5 has been studied for decades as it was found to give humans resistance to human immunodeficiency virus infection (HIV) (Lopalco, 2010). This site was a reasonable candidate as a safe harbor site as there are populations of humans who naturally occur without this receptor and therefore, knock-in at this locus, although it may disrupt CCR5 protein product, seemingly does not affect other surrounding genes or lead to organismic nonviability (Figure 2.7) (Pellenz et al., 2019). We began by designing our guide RNAs. Due to having higher knock-in efficiency at the PICH and RCC1 locus with multiple guides, I designed two gRNAs for *CCR5* using the CRISPR MIT design site (Figure 2.8A). After transfecting TIR1-mAID-PICH cells with inducible PICH mCherry mutants and performing clonal isolation, DNA was isolated for PCR and the expression levels were tested by addition of doxycycline by Western blot analysis with an mCherry antibody (Figure 2.8B, C). Clones with positive expression and PCR

verified integration were then examined for immunofluorescent expression of mCherry and used for subsequent experiments (discussed in Chapters three and four) (Figure 2.8D).

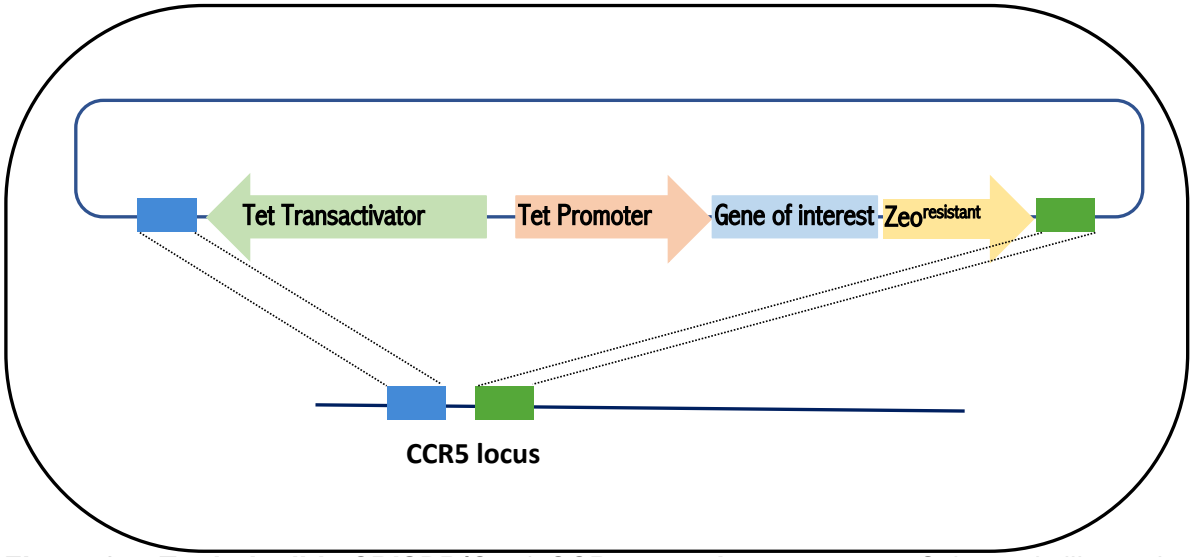

Figure 2.7. Tet-inducible CRISPR/Cas9 CCR5 targeting construct. Schematic illustrating CRISPR knock-in at the *CCR5* safe harbor locus.

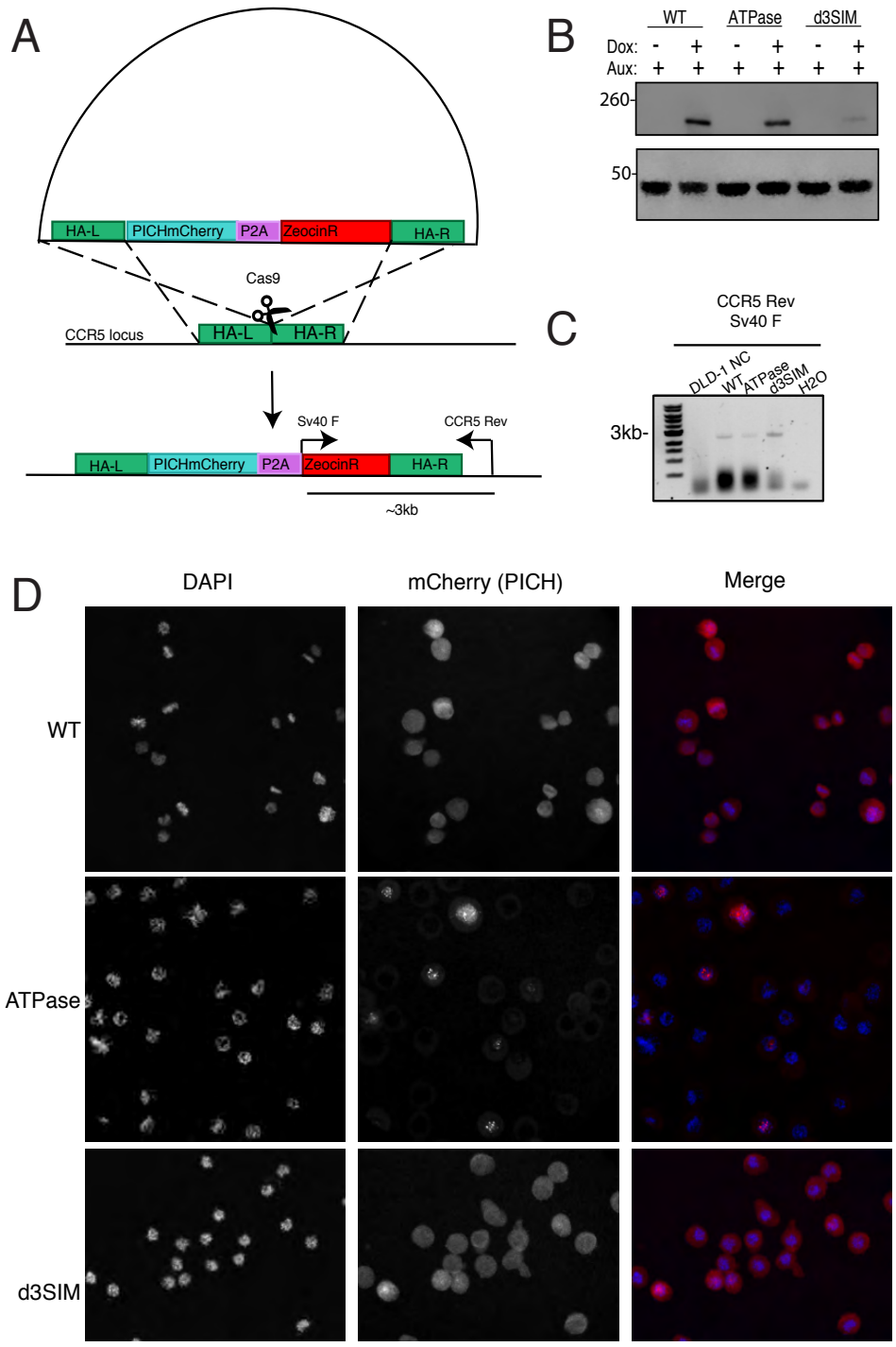

Figure 2.8. Construction of Tet-inducible PICH mCherry mutants.
(A) Experimental schematic of donor plasmid used to introduce PICH mCherry mutants into the CCR5 safe harbor locus. Cells were transfected with PICH- mCherry-P2A-Zeocin donor and two different guide RNAs.

(B) After selection with 400ug/mL Zeocin clones were isolated, cells were treated with doxycycline and auxin for 14 hours, whole cell lysates were collected from asynchronous populations, and Western blotting was performed.
(C) Genomic DNA was isolated and subjected to PCR using a Sv40 F primer located within the insert and CCR5 Rev located outside of the right homology arm. Non-transfected DLD-1 TIR#50 parental cell DNA was used as a control (DLD-1 NC).
(D) DLD-1 cells with endogenous PICH tagged with an auxin inducible degron (AID) and PICH mCherry mutants introduced into the CCR5 locus were synchronized in mitosis and treated with auxin and doxycycline for 22hours. Mitotic cells obtained by shake-off were plated onto fibronectin coated coverslips and subsequently stained with DAPI to label DNA and mCherry to label PICH expressing cells.

Discussion

I sought out to fill a gap in the field and avoid using siRNA mediated protein depletion. This method is problematic as siRNA can lead to the degradation of proteins it was not designed to target. This has been demonstrated by many groups with many different proteins, and specifically with PICH, which is revealed by its name as a "checkpoint" protein. siRNA mediated degradation is also problematic in terms of length of time it takes to reach knockout levels. This was seen to be true in our lab when siRNA knockdown of PICH took 3 days (Sridharan and Azuma, 2016). Due to PICH's essential role in chromosome segregation, knocking it down over 3 cell cycles can cause confounded results, for example observed defects could be from any stage of previous cell cycles. To avoid this using siRNA, I sought to incorporate a different degradation methodology into our lab. This led me to utilize the Auxin Inducible Degron technology to study my scientific questions. The AID technology enables rapid and complete degradation of AID-tagged proteins upon the addition of a phytohormone called auxin (Natsume et al., 2016). Rapid degradation is important in the PICH field for two reasons; one being the aforementioned issues with siRNA mediated knockdown, and the second being that PICH is a necessary protein for proper chromosome segregation (Biebricher et al., 2013; Nielsen et al., 2015). The latter making phenotypes

complicated as the level of chromosomal defects increase each cell cycle that PICH is depleted or knocked out in cells. The rapid elimination of PICH by auxin enables the avoidance of this issue. Rapid depletion of PICH also led to novel findings in the role of PICH in cell cycle progression, as mentioned in Chapter four.

This system is not without its limitations, guide RNA design being a critical challenge in experimental design. I began trying to tag the N-terminus of PICH utilizing one high scoring gRNA, designed using the MIT CRISPR Design website. This gRNA had a score of 98%, which meant that it had very few off-target binding sites that occurred within genes. But, even after optimization of transfection and selection protocols, I was still unsuccessful at adding a mAID tag to the PICH N-terminus. I found that incorporating more than one gRNA increased tagging efficiency to nearly 100%, where all 30 clones isolated had mAID-PICH and only two were heterozygous for this tag. But, as research continues to perfect Cas9 editing, new methods for guide selection are being generated (Tsai et al., 2015). One example being, identifying new motifs which can cause inefficient targeting/cutting are limiting the need for multiple guides (Graf et al., 2019).

The last limitation was found to be the selection of safe harbor used. I began by using the previously described AAVS1 safe harbor site and found that although clones were shown to have proper integration of the transgene, after passaging no expression could be observed. The lack of expression was found to be likely due to CpG methylation (Pellenz et al., 2019), which effectively silenced expression in most cells. Currently, many labs are using the AAVS1 site and facing similar challenges. We found that by using a different safe harbor locus, CCR5, which had known protein products,

protein expression was uniform, and did not become silenced after cell passaging. Another safe harbor, human Hipp11 (H11) was used in Chapter three of this dissertation. The H11 locus is situated between the DRG1 and EIF4ENIF1 genes found in many organisms, including humans (Chi et al., 2019). This offers great potential for stable gene knock-in as it has robust ubiquitous gene expression which has been demonstrated in mice, pigs, human embryonic stem cells, as well as induced pluripotent stem cells (Hippenmeyer et al., 2010; Tasic et al., 2011; Zhu et al., 2014).

Together, by designing and implementing CRISPR/Cas9 editing and inducible degradation and subsequent mutant expression, we have created cell lines that enable us to ask questions previously thought too fundamentally difficult to describe. Until now, the ability to perform relatively simple molecular genetic approaches gave model organisms a large advantage over mammalian cell culture. Now, this robust system enables rapid production of cell lines with tagged proteins to enable acquisition of clean phenotypic data and can be easily adapted for use across many different labs and disciplines.

Materials and Methods

Plasmids, constructs, and site-directed mutagenesis

The original plasmid for OsTIR1 targeting to RCC1 locus was created by inserting the TIR1 sequence amplified from pBABE TIR1-9Myc (Addgene #47328; (Holland AJ, 2012) plasmid, Blasticidin resistant gene (BSD) amplified from pQCXIB with ires-blast (Takara/Clontech), and miRFP670 amplified from pmiRFP670-N1 plasmid (Addgene #79987; (Shcherbakova et al., 2016) into the pEGFP-N1 vector (Takara/Clontech) with homology arms for RCC1 C-terminal locus. Using genomic DNA obtained from DLD-1 cell as a template DNA, the homology arms were amplified using primers listed in supplemental information (Supporting information Table 1). Further, OsTIR1 targeting plasmid was modified by eliminating the miRFP670 sequence by PCR amplification of left homology arm and TIR/BSD/right homology arm for inserting into pMK292 obtained from Addgene (#72830) (Natsume et al., 2016) using XmaI/BstBI sites. Three copies of codon optimized micro AID tag (50 amino-acid each (Morawska and Ulrich, 2013)) was synthesized by the IDT company, and hygromycin resistant gene/ P2A sequence was inserted upstream of the 3x micro AID sequence. The 3xFlag sequence from p3xFLAG-CMV-7.1 plasmid (Sigma) was inserted downstream of the AID sequence. The homology arms sequences for PICH N-terminal insertion was amplified using primers listed in supplemental information (Supporting Information Table 2.1) from genomic DNA of DLD-1 cell, then inserted into the plasmid by using PciI/SalI and SpeI/NotI sites. The CCR5 locus targeting donor plasmids for inducible expression of PICH mCherry proteins were created by modifying pMK243 (Tet-OsTIR1-PURO) plasmid (Natsume et al., 2016). pMK243 (Tet-OsTIR1-PURO) was purchased from Addgene (#72835) and the OsTIR1

fragment was removed by BglII and MluI digestion, followed by an insertion of a multi-cloning site. Homology arms for each locus were amplified from DLD-1 genomic DNA using the primers listed in supplemental information. The PICH mCherry cDNA were inserted at the MluI and SalI sites of the modified pMK243 plasmid. For CCR5 targeting plasmid, the antibiotic resistant gene was changed from Puromycin-resistant to Zeocin-resistant. In all the RCC1 locus, PICH locus, and CCR5 locus genome editing cases, the guide RNA sequences listed in Supporting information Table 2.1 were designed using CRISPR Design Tools from https://figshare.com/articles/CRISPR_Design_Tool/1117899 (Rafael Casellas laboratory, NIH) and http://crispr.mit.edu:8079 (Zhang laboratory, MIT) inserted into pX330 (Addgene #42230). Mutations were introduced in PAM sequences on the homology arms.

Cell culture, Transfection, and Colony Isolation

Targeted insertion using the CRISPR/Cas9 system was used for all integration of exogenous sequences into the genome. DLD-1 cells were transfected with guide plasmids and donor plasmid using ViaFect™ (#E4981, Promega) on 3.5cm dishes. Two days later the cells were split and re-plated on 10cm dishes at ~20% confluency, the cells were then subjected to antibiotic selection by maintaining (OsTIR1 selection) 1μg/ml Blasticidin (#ant-bl, Invivogen), (PICH mCherry) 400μg/ml Zeocin (#ant-zn, Invivogen), or (PICH mAID) 200μg/ml Hygromycin B Gold (#ant-hg, Invivogen)). The cells were cultured for 10 to 14 days with a selection medium, 20ul of the colonies were isolated under a bright field microscope in the hood using 10x magnification and a 20-200ul pipettor by aspiration with medium pipette tips and cultured in 48 well plates, then split into increasing sized dishes. After propagation the remaining cells were then scraped and prepared for

Western blotting and genomic DNA to verify the insertion of the transgene. Specifically, for the Western blotting analysis, the cells were pelleted, 1X SDS PAGE sample buffer was added, and boiled/vortexed. Samples were separated on an 8-16% gel and then blocked with Casein and probed using the indicated antibody described in each figure legend. Signals were acquired using the LI-COR Odyssey Fc imager. To perform genomic PCR, the cells were pelleted, genomic DNA was extracted using lysis buffer (100mM Tris-HCl pH 8.0, 200mM NaCl, 5mM EDTA, 1% SDS, and 0.6mg/mL proteinase K (#P8107S, NEB)), and purified by ethanol precipitation followed by resuspension with TE buffer containing 50ug/mL RNase A (#EN0531,ThermoFisher). Primers used for confirming the proper integrations are listed in the supplemental information.

To establish AID cell lines, as an initial step, the *Oryza sativa* E3 ligase (OsTIR1) gene was inserted into the 3' end of a housekeeping gene, RCC1, using CRISPR/Cas9 system in the DLD-1 cell line. The RCC1 locus was an appropriate locus to accomplish the modest but sufficient expression level of the OsTIR1 protein so that it would not induce a non-specific degradation without the addition of Auxin. We then introduced DNA encoding for AID-3xFlag tag into the PICH locus using CRISPR/Cas9 editing into the OsTIR1 expressing parental line. The isolated candidate clones were subjected to genomic PCR and Western blotting analysis to validate integration of the transgene. Once clones were established and the transgene integration was validated, the depletion of the protein in the auxin-treated cells was confirmed by Western blotting and immunostaining.

Introducing DNA encoding Tet inducible PICH mCherry into the CCR5 locus was accomplished by CRISPR/Cas9 editing into the desired locus. The OsTIR1 expressing,

mAID PICH parental cell line was used for introduction of the PICH mCherry mutants targeted to the CCR5 locus. The isolated candidate clones were subjected to genomic PCR and Western blotting analysis to validate integration of the transgene. Once clones were established and the transgene integration was validated, the expression of the transgenes was induced by the addition of doxycycline.

Cell fixation and staining

To fix the mitotic cells on fibronectin coated cover slips, cells were incubated with 4% paraformaldehyde for 10 minutes at room temperature, and subsequently washed three times with 1X PBS containing 10mM Tris-HCl to quench PFA. Following the fixation, the cells were permeabilized using 100% ice cold Methanol in -20°C freezer for 5 minutes. Cells were then blocked using 2.5% hydrolyzed gelatin for 30 minutes at room temperature. Following blocking the cells were stained with primary antibodies for 1 hour at room temperature, washed 3 times with 1X PBS containing 0.1% tween20, and incubated with secondary for 1 hour at room temperature. Following secondary incubation cells were washed 3 times with 1x PBS-T and mounted onto slide glass using VECTASHIELD® Antifade Mounting Medium with DAPI (#H-1200, Vector laboratory) and sealed with nail polish. Images were acquired using an UltraView VoX spinning disk confocal system (PerkinElmer) mounted on an Olympus IX71 inverted microscope. The microscope was equipped with a software-controlled piezoelectric stage for rapid Z-axis movement. Images were collected using a 60 × 1.42 NA planapochromatic objective (Olympus) and an ORCA ERAG camera (Hamamatsu Photonics). Solid state 405, 488, and 561 nm lasers were used for excitation. Fluorochrome-specific emission filters were used to prevent emission bleed through between fluorochromes. This system was

controlled by Volocity software (PerkinElmer). Minimum and maximum intensity cutoffs (black and white levels) for each channel were chosen in Volocity before images were exported. Images are presented as extended focus, meaning z-stacks were deconvoluted into one 2D image. No other adjustments were made to the images. Figures were prepared from exported images in Adobe illustrator.

The following primary antibodies were used for staining: Rabbit anti-PICH 1:800 (described in Chapter three), and Rat anti-RFP (#RMA5F8, Bulldog Bio Inc), and Guinea Pig anti-CNEP-C 1:2,000 (#PD030, MBL).

Collaborations and workload allocations

For all experiments designed in this chapter Victoria Hassebroek designed, conducted, and analyzed data except the following:

Figure 2.3 – Vasalisa Aksenova and Alexei Arnaoutov designed original OsTIR1 plasmid targeted to RCC1 locus.

Figure 2.6-2.7. –Hyewon Park modified the original AAVS1 and CCR5 plasmids

References

Banaszynski, L.A., Chen, L.-C., Maynard-Smith, L.A., Ooi, A.G.L., and Wandless, T.J. (2006). A rapid, reversible, and tunable method to regulate protein function in living cells using synthetic small molecules. Cell *126*, 995–1004.

Baumann, C., Körner, R., Hofmann, K., and Nigg, E.A. (2007). PICH, a centromere-associated SNF2 family ATPase, is regulated by Plk1 and required for the spindle checkpoint. Cell *128*, 101–114.

Biebricher, A., Hirano, S., Enzlin, J.H., Wiechens, N., Streicher, W.W., Huttner, D., Wang, L.H.-C., Nigg, E.A., Owen-Hughes, T., Liu, Y., et al. (2013). PICH: a DNA translocase specially adapted for processing anaphase bridge DNA. Mol. Cell *51*, 691–701.

Bonger, K.M., Chen, L., Liu, C.W., and Wandless, T.J. (2011). Small-molecule displacement of a cryptic degron causes conditional protein degradation. Nat. Chem. Biol. *7*, 531–537.

Chi, X., Zheng, Q., Jiang, R., Chen-Tsai, R.Y., and Kong, L.-J. (2019). A system for site-specific integration of transgenes in mammalian cells. PloS One *14*, e0219842.

Chung, H.K., Jacobs, C.L., Huo, Y., Yang, J., Krumm, S.A., Plemper, R.K., Tsien, R.Y., and Lin, M.Z. (2015). Tunable and reversible drug control of protein production via a self-excising degron. Nat. Chem. Biol. *11*, 713–720.

Cong, L., Ran, F.A., Cox, D., Lin, S., Barretto, R., Habib, N., Hsu, P.D., Wu, X., Jiang, W., Marraffini, L.A., et al. (2013). Multiplex genome engineering using CRISPR/Cas systems. Science *339*, 819–823.

Dohmen, R.J., Wu, P., and Varshavsky, A. (1994). Heat-inducible degron: a method for constructing temperature-sensitive mutants. Science *263*, 1273–1276.

Graf, R., Li, X., Chu, V.T., and Rajewsky, K. (2019). sgRNA Sequence Motifs Blocking Efficient CRISPR/Cas9-Mediated Gene Editing. Cell Rep. *26*, 1098-1103.e3.

Hippenmeyer, S., Youn, Y.H., Moon, H.M., Miyamichi, K., Zong, H., Wynshaw-Boris, A., and Luo, L. (2010). Genetic mosaic dissection of Lis1 and Ndel1 in neuronal migration. Neuron *68*, 695–709.

Holland AJ (2012). Inducible, reversible system for the rapid and complete degradation of proteins in mammalian cells. - PubMed - NCBI. Proc. Natl. Acad. Sci. U. S. A.

Hübner, N.C., Wang, L.H.-C., Kaulich, M., Descombes, P., Poser, I., and Nigg, E.A. (2010). Re-examination of siRNA specificity questions role of PICH and Tao1 in the spindle checkpoint and identifies Mad2 as a sensitive target for small RNAs. Chromosoma *119*, 149–165.

Idoko-Akoh, A., Taylor, L., Sang, H.M., and McGrew, M.J. (2018). High fidelity CRISPR/Cas9 increases precise monoallelic and biallelic editing events in primordial germ cells. Sci. Rep. *8*, 15126.

Iwamoto, M., Björklund, T., Lundberg, C., Kirik, D., and Wandless, T.J. (2010). A general chemical method to regulate protein stability in the mammalian central nervous system. Chem. Biol. *17*, 981–988.

Jackson, A.L., Bartz, S.R., Schelter, J., Kobayashi, S.V., Burchard, J., Mao, M., Li, B., Cavet, G., and Linsley, P.S. (2003). Expression profiling reveals off-target gene regulation by RNAi. Nat. Biotechnol. *21*, 635–637.

Joung, J., Konermann, S., Gootenberg, J.S., Abudayyeh, O.O., Platt, R.J., Brigham, M.D., Sanjana, N.E., and Zhang, F. (2019). Author Correction: Genome-scale CRISPR-Cas9 knockout and transcriptional activation screening. Nat. Protoc. *14*, 2259.

Kanemaki, M.T. (2013). Frontiers of protein expression control with conditional degrons. Pflugers Arch. *465*, 419–425.

Kim, J.H., Lee, S.-R., Li, L.-H., Park, H.-J., Park, J.-H., Lee, K.Y., Kim, M.-K., Shin, B.A., and Choi, S.-Y. (2011). High cleavage efficiency of a 2A peptide derived from porcine teschovirus-1 in human cell lines, zebrafish and mice. PloS One *6*, e18556.

Klatt, D., Cheng, E., Hoffmann, D., Santilli, G., Thrasher, A.J., Brendel, C., and Schambach, A. (2020). Differential Transgene Silencing of Myeloid-Specific Promoters in the AAVS1 Safe Harbor Locus of Induced Pluripotent Stem Cell-Derived Myeloid Cells. Hum. Gene Ther. *31*, 199–210.

Lambrus, B.G., Uetake, Y., Clutario, K.M., Daggubati, V., Snyder, M., Sluder, G., and Holland, A.J. (2015). p53 protects against genome instability following centriole duplication failure. J. Cell Biol. *210*, 63–77.

Lopalco, L. (2010). CCR5: From Natural Resistance to a New Anti-HIV Strategy. Viruses *2*, 574–600.

Mali, P., Yang, L., Esvelt, K.M., Aach, J., Guell, M., DiCarlo, J.E., Norville, J.E., and Church, G.M. (2013). RNA-guided human genome engineering via Cas9. Science *339*, 823–826.

Moore, J.D. (2001). The Ran-GTPase and cell-cycle control. BioEssays News Rev. Mol. Cell. Dev. Biol. *23*, 77–85.

Morawska, M., and Ulrich, H.D. (2013). An expanded tool kit for the auxin-inducible degron system in budding yeast. Yeast Chichester Engl. *30*, 341–351.

Natsume, T., Kiyomitsu, T., Saga, Y., and Kanemaki, M.T. (2016). Rapid Protein Depletion in Human Cells by Auxin-Inducible Degron Tagging with Short Homology Donors. Cell Rep. *15*, 210–218.

Neklesa, T.K., Tae, H.S., Schneekloth, A.R., Stulberg, M.J., Corson, T.W., Sundberg, T.B., Raina, K., Holley, S.A., and Crews, C.M. (2011). Small-molecule hydrophobic tagging-induced degradation of HaloTag fusion proteins. Nat. Chem. Biol. *7*, 538–543.

Nielsen, C.F., Huttner, D., Bizard, A.H., Hirano, S., Li, T.-N., Palmai-Pallag, T., Bjerregaard, V.A., Liu, Y., Nigg, E.A., Wang, L.H.-C., et al. (2015). PICH promotes sister chromatid disjunction and co-operates with topoisomerase II in mitosis. Nat. Commun. *6*, 8962.

Nishimura, K., and Kanemaki, M.T. (2014). Rapid Depletion of Budding Yeast Proteins via the Fusion of an Auxin-Inducible Degron (AID). Curr. Protoc. Cell Biol. *64*, 20.9.1-16.

Nishimura, K., Fukagawa, T., Takisawa, H., Kakimoto, T., and Kanemaki, M. (2009). An auxin-based degron system for the rapid depletion of proteins in nonplant cells. Nat. Methods *6*, 917–922.

O'Connell, M.R., Oakes, B.L., Sternberg, S.H., East-Seletsky, A., Kaplan, M., and Doudna, J.A. (2014). Programmable RNA recognition and cleavage by CRISPR/Cas9. Nature *516*, 263–266.

Pellenz, S., Phelps, M., Tang, W., Hovde, B.T., Sinit, R.B., Fu, W., Li, H., Chen, E., and Monnat, R.J. (2019). New Human Chromosomal Sites with "Safe Harbor" Potential for Targeted Transgene Insertion. Hum. Gene Ther. *30*, 814–828.

Ran, F.A., Hsu, P.D., Wright, J., Agarwala, V., Scott, D.A., and Zhang, F. (2013). Genome engineering using the CRISPR-Cas9 system. Nat. Protoc. *8*, 2281–2308.

Senthil-Kumar, M., and Mysore, K.S. (2011). Caveat of RNAi in plants: the off-target effect. Methods Mol. Biol. Clifton NJ *744*, 13–25.

Shcherbakova, D.M., Baloban, M., Emelyanov, A.V., Brenowitz, M., Guo, P., and Verkhusha, V.V. (2016). Bright monomeric near-infrared fluorescent proteins as tags and biosensors for multiscale imaging. Nat. Commun. *7*, 12405.

Smith, J.R., Maguire, S., Davis, L.A., Alexander, M., Yang, F., Chandran, S., ffrench-Constant, C., and Pedersen, R.A. (2008). Robust, persistent transgene expression in human embryonic stem cells is achieved with AAVS1-targeted integration. Stem Cells Dayt. Ohio *26*, 496–504.

Sridharan, V., and Azuma, Y. (2016). SUMO-interacting motifs (SIMs) in Polo-like kinase 1-interacting checkpoint helicase (PICH) ensure proper chromosome segregation during mitosis. Cell Cycle Georget. Tex *15*, 2135–2144.

Tasic, B., Hippenmeyer, S., Wang, C., Gamboa, M., Zong, H., Chen-Tsai, Y., and Luo, L. (2011). Site-specific integrase-mediated transgenesis in mice via pronuclear injection. Proc. Natl. Acad. Sci. U. S. A. *108*, 7902–7907.

Teale, W.D., Paponov, I.A., and Palme, K. (2006). Auxin in action: signalling, transport and the control of plant growth and development. Nat. Rev. Mol. Cell Biol. *7*, 847–859.

Tsai, S.Q., Zheng, Z., Nguyen, N.T., Liebers, M., Topkar, V.V., Thapar, V., Wyvekens, N., Khayter, C., Iafrate, A.J., Le, L.P., et al. (2015). GUIDE-seq enables genome-wide profiling of off-target cleavage by CRISPR-Cas nucleases. Nat. Biotechnol. *33*, 187–197.

Xu, P., Zhang, Y., Kang, L., Roossinck, M.J., and Mysore, K.S. (2006). Computational estimation and experimental verification of off-target silencing during posttranscriptional gene silencing in plants. Plant Physiol. *142*, 429–440.

Zhu, F., Gamboa, M., Farruggio, A.P., Hippenmeyer, S., Tasic, B., Schüle, B., Chen-Tsai, Y., and Calos, M.P. (2014). DICE, an efficient system for iterative genomic editing in human pluripotent stem cells. Nucleic Acids Res. *42*, e34.

Primers used for amplification of homology arms

RCC1 Left HA Forward	GGAATTCCATATGGGAGGCAATGGGACTGGAACCC
RCC1 Left HA Reverse	GAAGATCTAGACTGCTCTTTGTCCTTGACCAAGAGTACAGTATGCTG ACCTCCAGAGCTAACGCTCAGAACAACTCTATTCTCCAGCTGTTTGC CCATCA
RCC1 Right HA Forward	CCGCTCGAGTGATGAAGCCTCTGAGGGCCTGG
RCC1 Right HA Reverse	ATAGTTTAGCGGCCGCCTATATCCTATTTTCTCAGCCACTGTACAAG
PICH Left HA Forward	CGGACATGTACACTCCGTGTCTCGAAGGCAG
PICH Left HA Reverse	GCCGTCGACGACCCTCGGATTGGGTTTCAGTTACC
PICH Right HA Forward	GAACTAGTATGGAGGCATCCCGAAGGTTTCCGGAAGCCGATGCC
PICH Right HA Reverse	GCGGCCGCCTCTTGCCACGCCATCCCT
CCR5 Left HA Forward	gtactcaaaagctcccccaggcctcc
CCR5 Left HA Reverse	CTGCGAACACTGGTGAGAGGCCG
CCR5 Right HA Forward	GAACCTGCCATGACAGTCACGGTG
CCR5 Right HA Reverse	ctccccgtcccactctcttccc

gRNA sequences used for Cas9 targeting of RCC1, PICH, or CCR5 loci

gRNA Rcc1-1	GACACAGATAAGACCACA
gRNA Rcc1-2	CTTATCTGTGTCCAGCGG
gRNA PICH-1	CCTCGGATTGGGTTCCAGTT
gRNA PICH-2	CCGAAGGTTTCCGGAAGCCG
gRNA CCR5	CCACCCGCTGATTCAATACG

Primers used for genomic PCR

CCR5 F	cgagctcagggaccaactgaaataaag
Pause Site R	gttttgatggagagcgtatgttagtac
Sv40 F	ccgAGATCTctctagaggatctttgtgaag
CCR5 R	cagtttggggttaaacttgtcctcctc
RCC1 F	gccatggaggtcctgtagaa
RCC1 Rev	ACACCTGAGGGGCAAGAGTA
TIR Rev	TGAAGTCGGCGAAGT
TIR F	TCTTCACTGGTGTCAATGTAT
PICH F1	acggggtgtcaccattttagcc
Hygro Rev	TCAGCGAGAGCCTGACCTAT

Supporting Information Table 2.1

Chapter 3 PICH translocase activity is required for proper distribution of SUMOylated proteins on mitotic chromosomes

Introduction

Accurate chromosome segregation is a complex and highly regulated process during mitosis. Sister chromatid cohesion is necessary for proper chromosome alignment and is mediated by both Cohesin and catenated DNA at centromeric regions (Bauer et al., 2012; Losada et al., 1998; Michaelis et al., 1997). Compared to the well-described regulation of Cohesin (Morales and Losada, 2018), the regulation of catenated DNA cleavage by DNA Topoisomerase IIα (TopoIIα) is not fully understood despite its critical role in chromosome segregation. ATP-dependent DNA decatenation by TopoIIα takes place during the metaphase-to-anaphase transition and this allows for proper chromosome segregation (Gómez et al., 2014; Shamu and Murray, 1992; Wang et al., 2010). Failure in resolution of catenanes by TopoIIα leads to the formation of chromosome bridges, and ultra-fine DNA bridges (UFBs) to which PICH localizes (Spence et al., 2007). PICH is a SNF2 family DNA translocase (Baumann et al., 2007; Biebricher et al., 2013), and its binding to UFBs recruits other proteins to UFBs (Chan et al., 2007; Hengeveld et al., 2015). In addition to the role in UFB binding during anaphase, PICH has been shown to play a key role in chromosome segregation at the metaphase to anaphase transition (Baumann et al., 2007; Nielsen et al., 2015; Sridharan and Azuma, 2016).

Previously, we demonstrated that PICH binds SUMOylated proteins using its three SUMO interacting motifs (SIMs) (Sridharan et al., 2015). PICH utilizes ATPase activity to translocate DNA similar to known nucleosome remodeling enzymes (Whitehouse et al.,

2003), thus it is a putative remodeling enzyme for chromosomal proteins. But, the nucleosome remodeling activity of PICH was shown to be limited as compared to established nucleosome remodeling factors (Ke et al., 2011). Therefore, the target of PICH remodeling activity has not yet been determined. Importantly, both loss of function PICH mutants in either SUMO-binding activity or translocase activity showed chromosome bridge formation (Sridharan and Azuma, 2016), suggesting that both of these activities cooperate to accomplish proper chromosome segregation although the molecular mechanism linking these two functions is unknown. Previous studies demonstrated that proper regulation of mitotic chromosomal SUMOylation is required for faithful chromosome segregation (Cubeñas-Potts et al., 2013; Díaz-Martínez et al., 2006; Nacerddine et al., 2005). Studies using C. elegans demonstrated the dynamic nature of SUMOylated proteins during mitosis and its critical role in chromosome segregation (Pelisch et al., 2014). Several SUMOylated chromosomal proteins were identified for their potential role in chromosome segregation, for example; TopoIIα, CENP-A, CENP-E, FoxM1, and Orc2 (Bachant et al., 2002; Huang et al., 2016; Ohkuni et al., 2018; Schimmel et al., 2014; Zhang et al., 2008). Because PICH is able to specifically interact with SUMO moieties (Sridharan et al., 2015), these SUMOylated chromosomal proteins could be a target of the SIM-dependent function of PICH in mediating faithful chromosome segregation. Among the known SUMOylated chromosomal proteins, TopoIIα has been shown to functionally interact with PICH. PICH-knockout cells have increased sensitivity to ICRF-193, a potent TopoII catalytic inhibitor, accompanied with increased incidences of chromosome bridges, binucleation, and micronuclei formation (Kurasawa and Yu-Lee, 2010; Nielsen et al., 2015; Wang et al., 2008). ICRF-193 stalls TopoIIα at the last step of

the strand passage reaction (SPR) in which two DNA strands are trapped within the TopoIIα molecule without DNA strand breaks (Patel et al., 2000; Roca et al., 1994). In addition to that specific mode of inhibition, ICRF-193 has been shown to increase SUMOylation of TopoIIα (Agostinho et al., 2008; Pandey et al., 2020). Because PICH has SUMO binding ability, it is possible that increased SUMOylation of TopoIIα contributes to interactions with PICH under ICRF-193 treatment. However, no study has shown a linkage between SUMOylation of TopoIIα and PICH function.

To elucidate possible functional interactions of PICH with SUMOylated chromosomal proteins, we established the connection between PICH and chromosomal SUMOylation by utilizing specific TopoII inhibitors and genome edited cell lines. Our results demonstrate that increased SUMOylation by ICRF-193 treatment leads to the recruitment of and enrichment of PICH on chromosomes. Depletion of SUMOylation abrogates this enrichment, suggesting PICH specifically targets SUMOylated chromosomal proteins. Depletion of PICH led to the retention of SUMOylated proteins including SUMOylated TopoIIα on the chromosomes in ICRF-193 treated cells. Replacing endogenous PICH with a translocase deficient PICH mutant resulted in increased SUMO2/3 foci on chromosomes where PICH was located, suggesting that PICH utilizes its translocase activity to remodel SUMOylated proteins on the chromosomes. *In vitro* assays showed that PICH specifically interacts with SUMOylated TopoIIα to attenuate SUMOylated TopoIIα activity in a SIM dependent manner. Taken together, we propose a novel mechanism for PICH in promoting proper chromosome segregation during mitosis by remodeling SUMOylated proteins on mitotic chromosomes including TopoIIα.

Results

Upregulation of SUMO2/3 modification by treatment with TopoIIα inhibitor ICRF-193 causes increased PICH foci on mitotic chromosomes.

We previously reported that PICH utilized its SIMs for proper chromosome segregation and for its mitotic chromosomal localization (Sridharan and Azuma, 2016). We wished to examine whether modulating mitotic SUMOylation affected PICH localization on mitotic chromosomes. Treatment with ICRF-193, a catalytic inhibitor of TopoII which blocks TopoII at the last stage of its SPR, after DNA decatenation but before DNA release, increases SUMO2/3 modification of TopoIIα on mitotic chromosomes. In contrast, treatment with another catalytic TopoII inhibitor, Merbarone, which blocks TopoII before the cleavage step of the SPR, does not affect the level of SUMO2/3 modification of TopoIIα (Agostinho et al., 2008; Pandey et al., 2020). We utilized these two contrasting inhibitors to assess whether TopoIIα inhibition and/or SUMOylation changes PICH distribution on mitotic chromosomes. DLD-1 cells were synchronized in prometaphase, and mitotic cells were collected by mitotic shake off, then chromosomes were isolated. To assess the effects of the TopoII inhibitors specifically during mitosis, the inhibitors were added to cells after mitotic shake off. Consistent with previous reports (Agostinho et al., 2008; Pandey et al., 2020), Western blot analysis of isolated chromosomes showed that treatment with ICRF-193 significantly increased the overall SUMO2/3 modification of chromosomal proteins including SUMOylated TopoIIα (marked by red asterisks in Figure 3.1A). Intriguingly, when PICH levels on mitotic chromosomes were measured they were found to be significantly increased upon treatment with ICRF-193. In contrast, Merbarone did not increase the level of these proteins on the chromosomes suggesting that there is

a specificity of ICRF-193 that causes increased levels of PICH and SUMOylation of TopoIIα (Figure 3.1A).

To investigate the localization of PICH on mitotic chromosomes under treatment with ICRF-193, mitotic cells were subjected to immunofluorescence staining. Synchronized cells were collected by mitotic shake off, treated with inhibitors, then plated onto fibronectin coated coverslips. Cells were fixed after a 20-minute incubation and subjected to immunofluorescence staining. As seen in Western blot analysis, SUMO2/3 foci intensity were present on the chromosomes, where they overlapped with TopoIIα foci upon ICRF-193 treatment (Figure 3.1B enlarged images). Although, the TopoIIα signal changed slightly under Merbarone treatment, no enrichment of SUMO2/3 foci were observed (Figure 3.1B). We noted for the first time that PICH foci were also found to be enriched on the chromosomes where they overlapped with SUMO2/3 foci upon ICRF-193 treatment, but, treatment with Merbarone did not affect PICH localization (Figure 3.1C). These data show that treatment with ICRF-193, but not Merbarone, causes increased TopoIIα SUMOylation and enrichment of PICH and SUMO2/3 foci on the chromosomes.

A

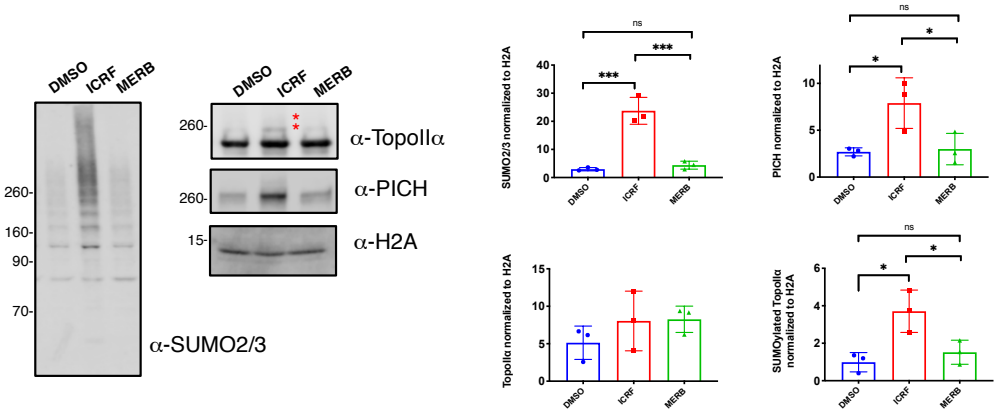
DMSO
ICRF
MERB
260-
160-
90-
70-
α-SUMO2/3
260-
α-TopoIIα
260-
α-PICH
15-
α-H2A
SUMO2/3 normalized to H2A
PICH normalized to H2A
TopoIIα normalized to H2A
SUMOylated TopoIIα normalized to H2A
ns
*
***

B

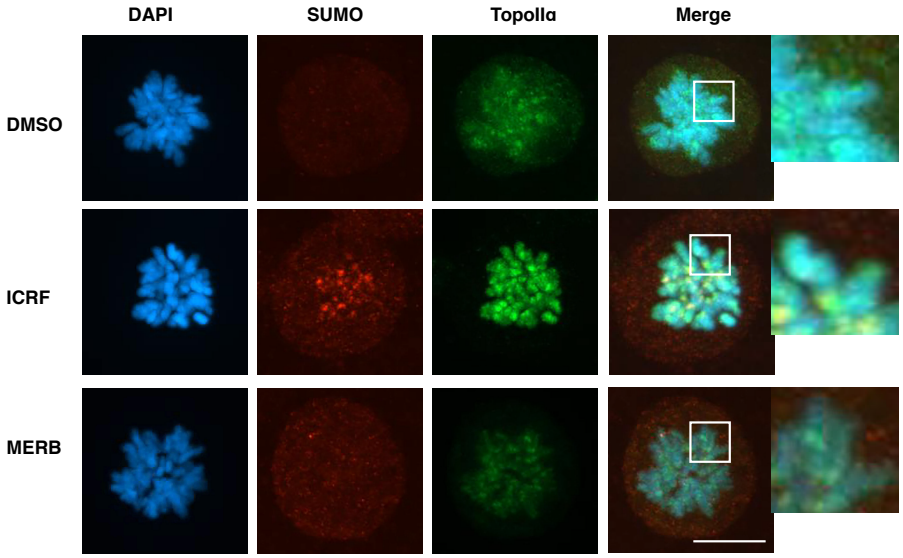
DAPI
SUMO
TopoIIα
Merge
DMSO
ICRF
MERB

C

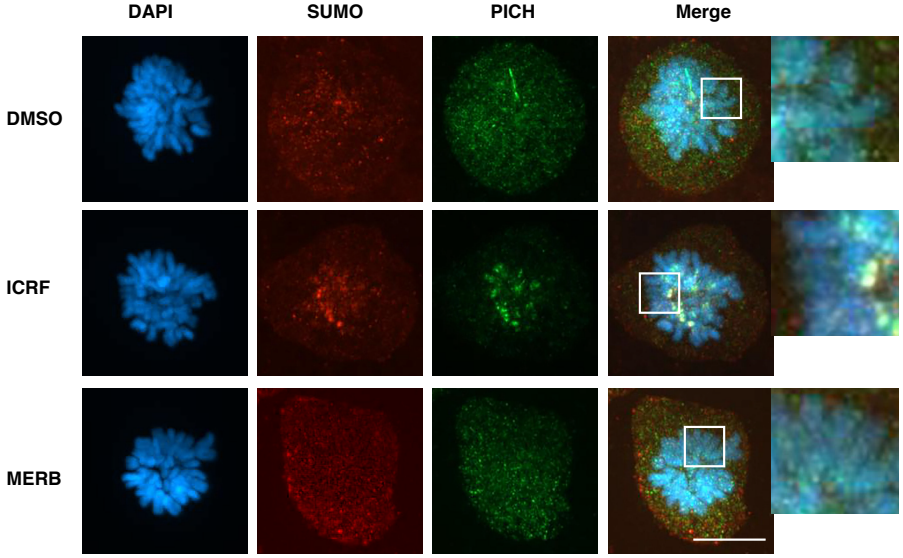
DAPI
SUMO
PICH
Merge
DMSO
ICRF
MERB

Figure 3.1. TopoIIα inhibition by ICRF-193 leads to increased PICH, SUMO2/3 and TopoIIα levels on mitotic chromosomes.
(A) DLD-1 cells were synchronized and treated with indicated inhibitors (7μM ICRF-193: ICRF, and 40μM Merbarone: Merb), DMSO was used as a control. Mitotic chromosomes were isolated and subjected to Western blotting with indicated antibodies. * indicates SUMOylated TopoIIα. p values for comparison among three experiments were calculated using a one-way ANOVA analysis of variance with Tukey multi-comparison correction.
ns: not significant; *: $p \leq 0.05$; ***: $p < 0.001$
(B) Mitotic cells treated with DMSO (control), ICRF-193, and Merbarone were stained with antibodies against: TopoIIα (green) and SUMO2/3 (red). DNA was stained with DAPI (blue). Scale bar = 11μm. The white square indicates enlarged area.
(C) Mitotic cells were treated as in **B** and stained with antibodies against: PICH (green), SUMO2/3 (red). DNA was stained with DAPI (blue). Scale bar = 11μm. The white square indicates enlarged area.

Mitotic SUMOylation is required for PICH enrichment in ICRF-193 treated cells.

Although results obtained from inhibiting TopoIIα suggest that increased SUMOylation plays a critical role in PICH enrichment, the distinct effects of the different inhibitor treatments, for example differences in TopoII conformation, could also play a role. To determine if mitotic SUMOylation is critical for PICH enrichment in ICRF-193 treated cells we developed a novel method to inhibit mitotic SUMOylation in cells. First, we generated a fusion protein, called Py-S2, which consists of the N-terminal region of human PIASy (Ryu and Azuma, 2010), and the SENP2-catalytic domain (required for deSUMOylation) (Reverter, David, 2004; Ryu and Azuma, 2010; Sridharan et al., 2015). The N-terminal region of PIASy localizes to mitotic chromosomes, in part, via its specific interaction with the RZZ (Rod-Zw10-Zwilch) complex (Ryu and Azuma, 2010). Thus, the fusion protein is expected to bring deSUMOylation activity where mitotic SUMOylation occurs on chromosomes by recruitment of PIASy via its N-terminal region. As a negative control, we substituted a cysteine to alanine at position 548 of SENP2 (called Py-S2 Mut) to create a loss of function mutant (Reverter and Lima, 2006; Reverter, David, 2004) (Figure 3.4A). The activity of the recombinant fusion proteins on

chromosomal SUMOylation was verified in Xenopus egg extract (XEE) assays (Figure 3.2). As predicted, addition of the Py-S2 protein to XEE completely eliminated mitotic chromosomal SUMOylation. To our surprise, the Py-S2 Mut protein stabilized SUMOylation of chromosomal proteins, thus acting as a dominant negative mutant against endogenous deSUMOylation enzymes. We believe this is because the Py-S2 Mut can still bind SUMOylated proteins but because it no longer has cleavage activity it remains bound, protecting them from deSUMOylation by other SENPs.

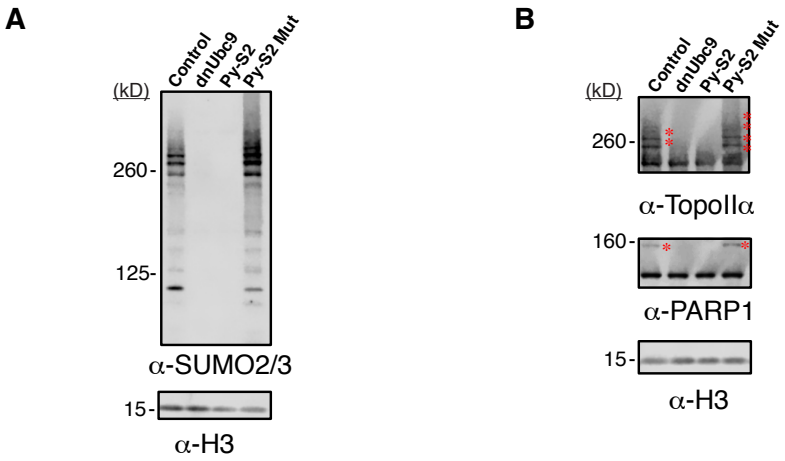

Figure 3.2. Testing SUMO modulating proteins in the *Xenopus laevis* egg extract system.
(A) Recombinant Py-S2 or Py-S2 Mut proteins were added to *Xenopus laevis* egg extract upon induction of mitosis, and the chromosomes were isolated. Chromosome samples were subjected to Western blotting with anti-SUMO2/3 antibody.
(B) Chromosome samples in A were subjected to Western blotting with anti-Xenopus TopoIIα antibody to detect both TopoIIα (~160kDa) and SUMOylated TopoIIα (marked with red asterisks), and anti-Xenopus PARP1 antibody to detect both PARP1 (~100kDa) and SUMOylated PARP1 (marked with red asterisks). Anti-histone H3 antibody was used as a loading control.

30nM of Py-S2 protein was sufficient to eliminate chromosomal SUMOylation, which is the equivalent concentration of endogenous PIASy protein in XEE, suggesting that the Py-S2

effectively deSUMOylates SUMOylated chromosomal proteins at a physiologically relevant concentration. Note that the concentration of dnUbc9 required for complete inhibition of chromosomal SUMOylation is 5μM in XEE, which is not within the physiological range and is difficult to induce a high expression level of dnUbc9 in cells. Addition of the Py-S2 C548A mutant (Py-S2 Mut) increased SUMO2/3 modification in chromosomal samples, including both TopoIIα SUMOylation and PARP1 SUMOylation. This suggests that the Py-S2 Mut acts as a dominant mutant for stabilizing SUMOylation.

To express the fusion proteins in cells, we created inducible expression cell lines using the Tetracycline inducible system (Figure 3.2) (Natsume et al., 2016). We utilized CRISPR/Cas9 genome editing to integrate each of the fusion genes into the human H11 (hH11) safe harbor locus (Ruan et al., 2015; Zhu et al., 2014) in DLD-1 cells.

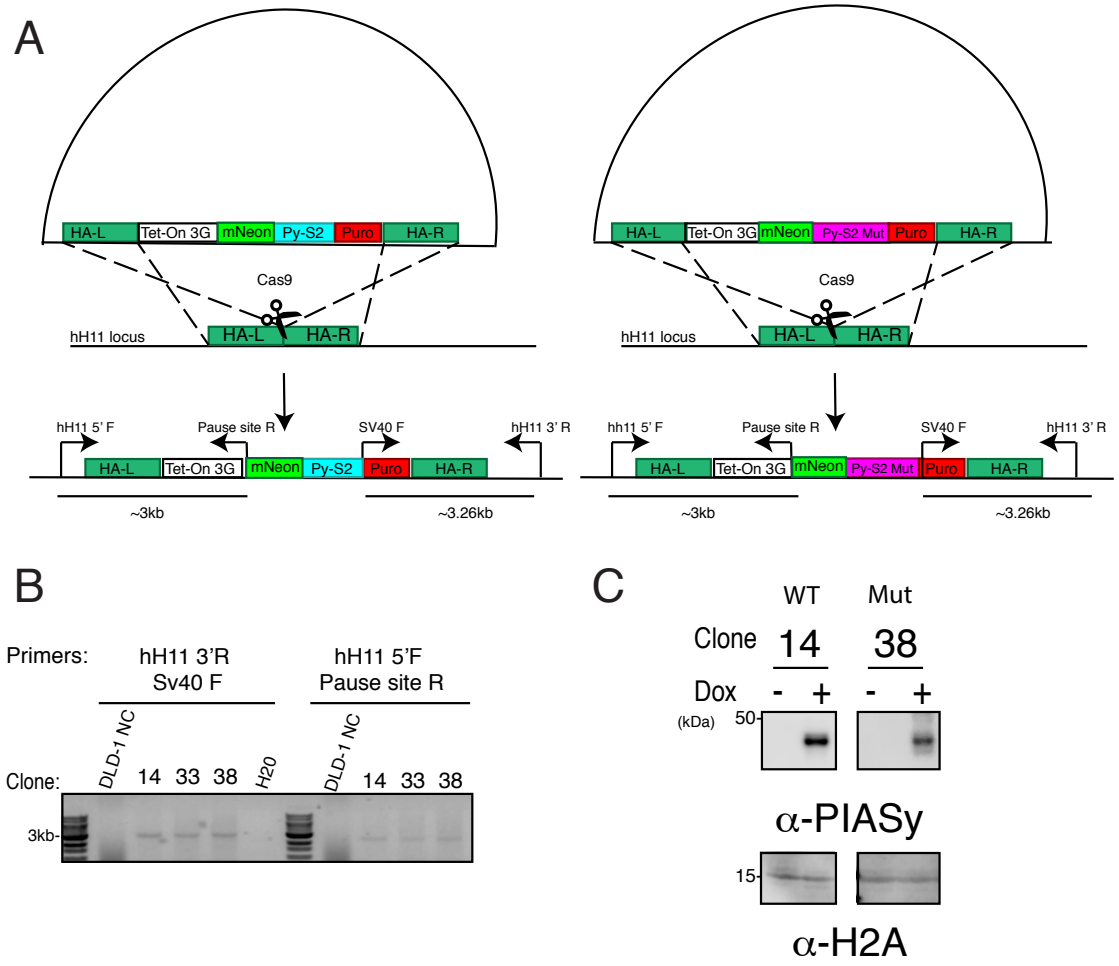

Figure 3.3. Construction of Py-S2 and Py-S2 Mut DLD-1 cell lines.
(A) Experimental scheme to introduce inducible Py-S2 and Py-S2 Mut into hH11 locus of DLD-1 cells. Cells were transfected with a donor plasmid with homology arms directed to the CCR5 locus (CCR5-TetON3G-mNeonPyS2-PuroR) and two gRNAs to target CCR5 locus. For the screening of the transgene integrated clones, primers were designed to amplify the 5' region (~3kb) and 3' region (~3.26kb) of the integration site.
(B) After the selection using 1ug/mL Puromycin, 1 clone each per construct were further subjected to genomic PCR to confirm the integration of the transgene.
(C) The whole cell lysates obtained from the candidate clones were subjected to Western Blotting to confirm the inducible expression of Py-S2 and Py-S2 Mut proteins. Anti-PIASy antibodies were used to detect expression of fusion proteins (+Dox) or not (-Dox), anti-H2A antibodies were used as a loading control.

To test whether the novel Py-S2 fusion protein worked as expected, cells were synchronized, and doxycycline was added after release from a Thymidine block. After treatment with ICRF-193, chromosomes were isolated and subjected to Western blot analysis. The Py-S2 expressing cells had nearly undetectable levels of chromosomal SUMOylation and SUMOylated TopoIIα (Figure 3.4B). Intriguingly in Py-S2 expressing cells, PICH levels on chromosomes were no longer affected by ICRF-193 treatment, suggesting that the response of PICH to ICRF-193 depends on the cell's ability to SUMOylate chromosomal proteins including TopoIIα (Figure 3.4B).

To determine how deSUMOylation affects PICH and TopoIIα distribution, Py-S2 expressing mitotic cells were stained. Immunofluorescent analysis of Py-S2 expressing cells reiterated what was observed in Western blot analysis. Even under ICRF-193 treatment, Py-S2 expressing cells had nearly undetectable levels of SUMO2/3 and clear reduction of PICH levels (Figure 3.4C, D +Dox panels). But, TopoIIα signals remained unaffected, in agreement with our previous observations in XEE assays, which showed that TopoIIα localization is independent of SUMOylation (Azuma et al., 2005) (Figure 3.4E).

The role of SUMOylation in the enrichment of PICH on mitotic chromosomes is further supported by the Py-S2 Mut expressing cells. Western blot analysis of mitotic chromosomes expressing Py-S2 Mut revealed increased levels of overall SUMOylation as well as SUMOylated TopoIIα in the absence of ICRF-193 (Figure 3.5A lane 1 vs. lane 3). This suggests that a similar stabilization of SUMOylation occurs in cells as was observed in the XEE assays, albeit with less penetrance. PICH levels were also slightly increased in the Py-S2 Mut expressing cells in the absence of ICRF-193 (Figure 3.5A). This slight increase of both PICH and SUMO2/3 seen in Western blots was even more apparent with immunofluorescence analysis. In the absence of ICRF-193, Py-S2 Mut expressing cells had increased signals of PICH and SUMO2/3 on the chromosomes (Figure 3.5B, C comparing DMSO/-Dox and DMSO/+Dox). Similar to Figure 3.4E, TopoIIα localization and signal intensity did not change upon Py-S2 Mut expression (Figure 3.5D). In all, these data reinforce the indication that the enrichment of PICH foci on mitotic chromosomes in ICRF-193 treated cells is dependent on increased SUMOylation.

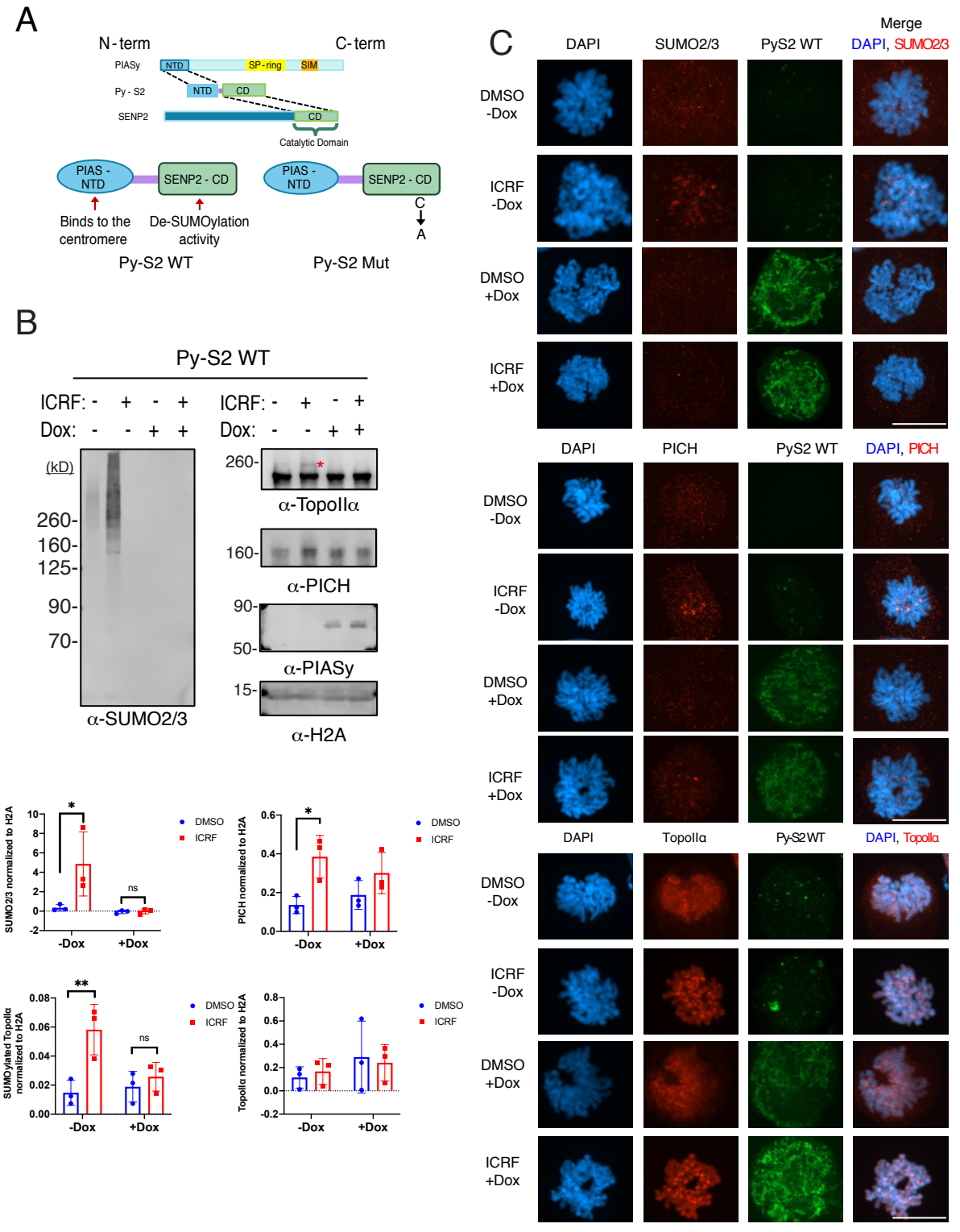
A
N-term
C-term
PIASy
NTD
SP-ring
SIM
Py-S2
NTD
CD
SENP2
CD
Catalytic Domain
PIAS - NTD
SENP2 - CD
Binds to the centromere
De-SUMOylation activity
Py-S2 WT
PIAS - NTD
SENP2 - CD
C
A
Py-S2 Mut
B
Py-S2 WT
ICRF: - + - +
Dox: - - + +
(kD)
260-
160-
125-
90-
70-
α-SUMO2/3
ICRF: - + - +
Dox: - - + +
260-
α-TopoIIα
160-
α-PICH
90-
50-
α-PIASy
15-
α-H2A
SUMO2/3 normalized to H2A
DMSO
ICRF
-Dox
+Dox
ns
PICH normalized to H2A
SUMOylated TopoIIα normalized to H2A
TopoIIα normalized to H2A
C
DAPI
SUMO2/3
PyS2 WT
Merge
DAPI, SUMO2/3
DMSO -Dox
ICRF -Dox
DMSO +Dox
ICRF +Dox
DAPI
PICH
PyS2 WT
DAPI, PICH
DAPI
TopoIIα
Py-S2WT
DAPI, TopoIIα

Figure 3.4. DeSUMOylation enzyme eliminates PICH response to ICRF-193.
(A) Schematic of fusion proteins generated for modulating SUMOylation on mitotic chromosomes.
(B) Mitotic chromosomes were subjected to Western blotting with indicated antibodies. * indicates SUMOylated TopoIIα. p values for comparison among three experiments were calculated using a two-way ANOVA analysis of variance with Tukey multi-comparison correction;
ns: not significant; *: $p \leq 0.05$; **: $p < 0.01$
(C) Mitotic cells were fixed and stained with antibodies against: SUMO2/3 (red), PICH (red), TopoIIα (red), and mNeon (green). DNA was stained by DAPI (blue). Scale bar = 11μm.

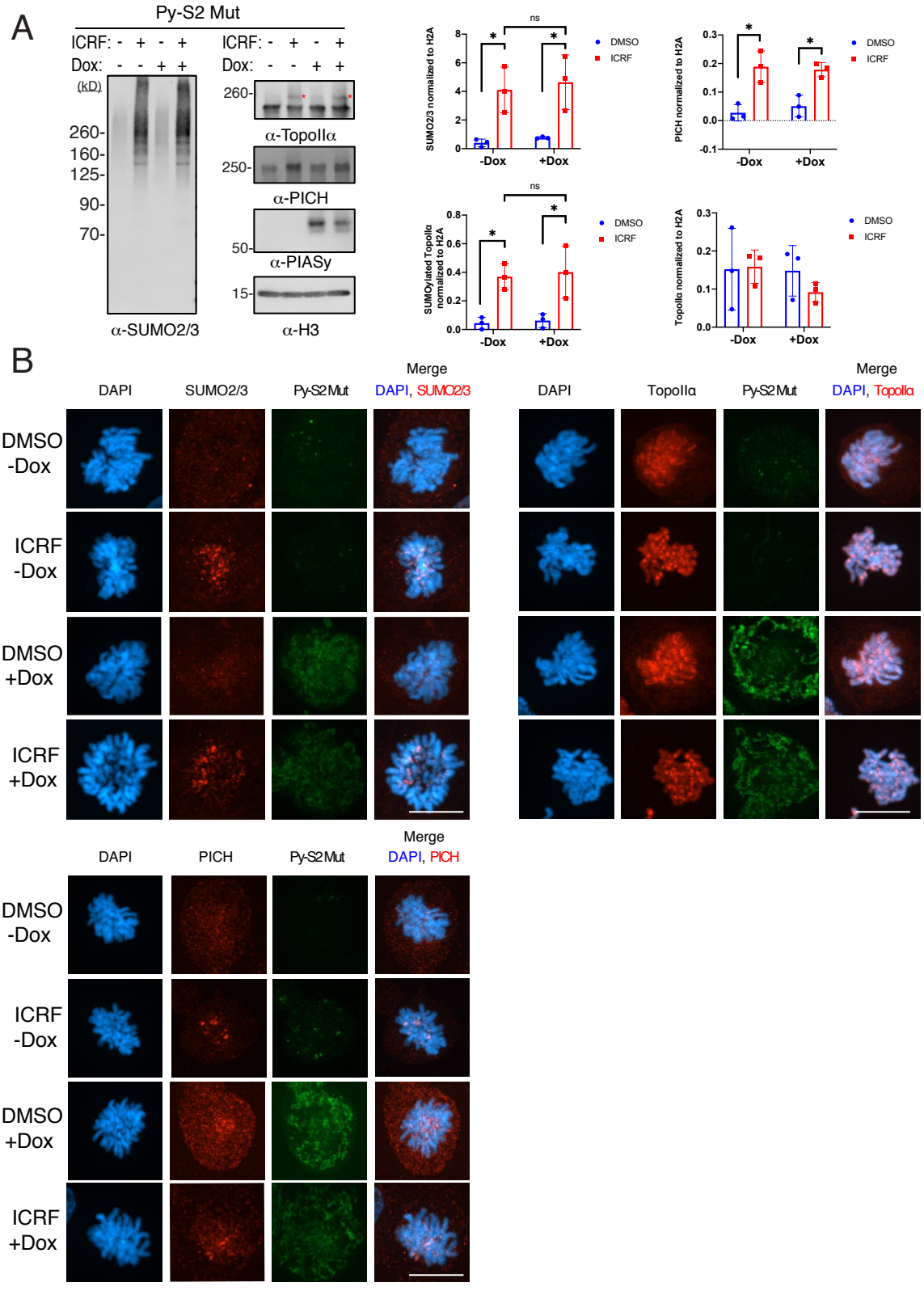
A
Py-S2 Mut
ICRF: - + - +
Dox: - - + +
(kD)
260-
160-
125-
90-
70-
α-SUMO2/3
ICRF: - + - +
Dox: - - + +
260-
α-TopoIIα
250-
α-PICH
50-
α-PIASy
15-
α-H3
SUMO2/3 normalized to H2A
PICH normalized to H2A
SUMOylated TopoIIα normalized to H2A
TopoIIα normalized to H2A
ns
*
DMSO
ICRF
-Dox
+Dox
B
DAPI
SUMO2/3
Py-S2Mut
Merge
DAPI, SUMO2/3
TopoIIα
DAPI, TopoIIα
PICH
DAPI, PICH
DMSO -Dox
ICRF -Dox
DMSO +Dox
ICRF +Dox

Figure 3.5. Mutant form of deSUMOylation enzyme promotes PICH and SUMO2/3 foci in both control and ICRF-193 treated cells.
(A) Mitotic chromosomes were isolated and subjected to Western blotting with indicated antibodies.
* indicates SUMOylated TopoIIα. p values for comparison among three experiments were calculated using a two-way ANOVA analysis of variance with Tukey multi-comparison correction.
ns: not significant; *: $p \leq 0.05$
(B) Mitotic cells were fixed and stained with antibodies against: SUMO2/3 (red), TopoIIα (red), PICH (red), and mNeon (green). DNA was stained with DAPI (blue). Scale bar = 11μm.

Increased PICH levels observed in ICRF-193 treatment lost upon TopoIIα depletion.

Since increasing mitotic SUMOylation enriches PICH on the chromosomes, we tested whether the PICH response to ICRF-193 is due to TopoIIα SUMOylation. To accomplish this, we generated a mAID-TopoIIα cell line, which enables rapid and complete elimination of TopoIIα in the presence of auxin (Natsume et al., 2016; Nishimura et al., 2009). As previously mentioned in Chapter two, we first established a cell line that has integration of an auxin-dependent Ubiquitin E3 ligase, *OsTIR1* gene, at the promoter of a housekeeping (*RCC1)* gene (Figure 2.3) using CRISPR/Cas9 editing technology. Using the established OsTIR1 expressing DLD-1 cell line, DNA encoding a mAID-Flag tag was inserted into both TopoIIα loci (Figure 3.6A-C). After 6-hour treatment with auxin, TopoIIα was degraded to undetectable levels in all cells analyzed (Figure 3.6D and E). This rapid elimination allowed us to examine the effect of TopoIIα depletion in a single cell cycle.

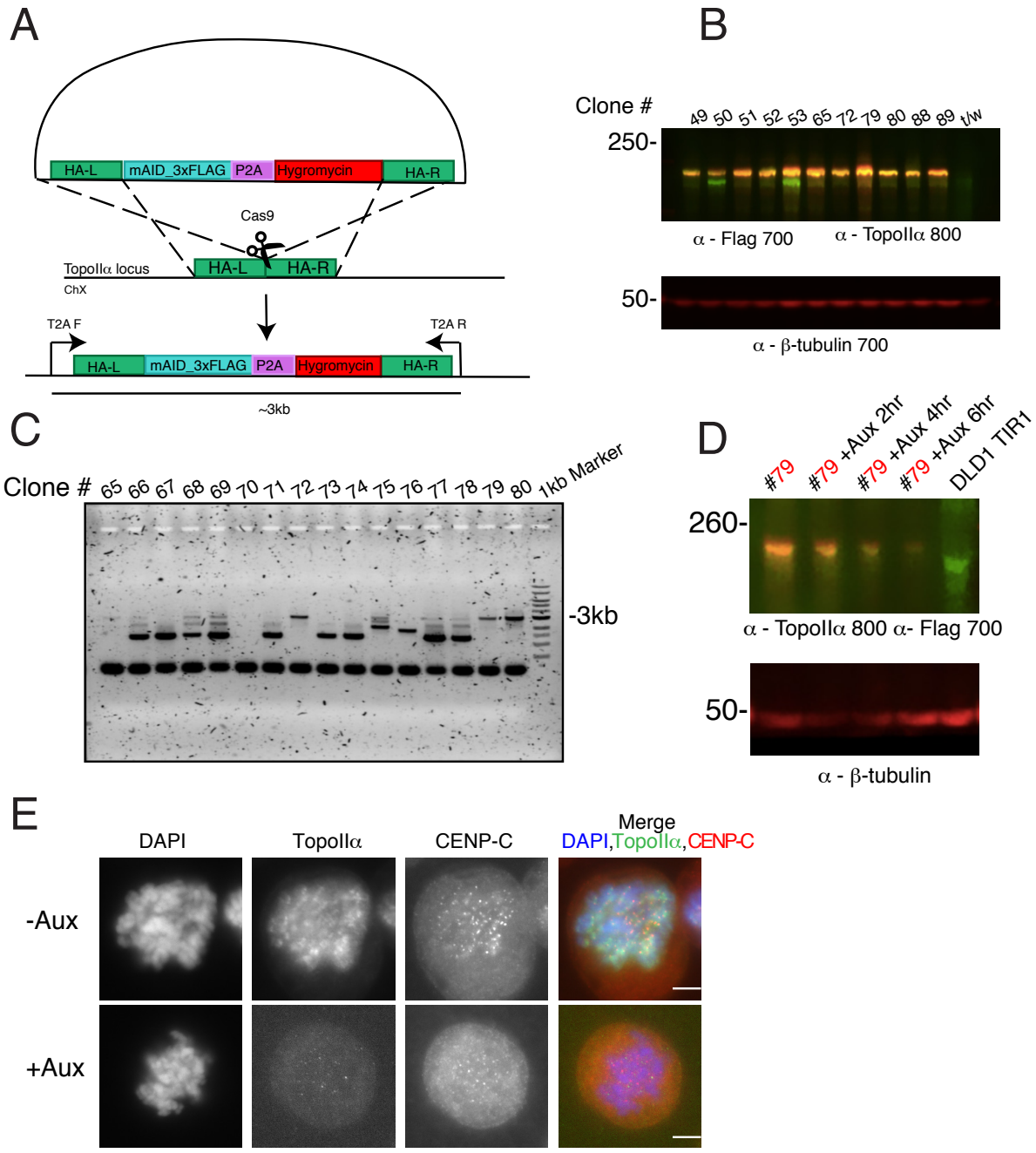

Figure 3.6. Construction of TopoIIα-AID cell line.
(A) Experimental schematic of donor plasmid tagging the 5' end of endogenous TopoIIα with AID. Cells were transfected with the donor plasmid together with two different guide RNAs.
(B) After selection with 400ug/mL hygromycin, resistant clones were isolated. Whole cell lysate was obtained from cells and the expression of the transgene was screened by Western blotting. Representative Western blotting of clones is shown. An anti-Flag antibody was used to detect AID-Flag tagged TopoIIα (~190kDa) in the 700 channel (red) and anti-TopoIIα antibodies were used to detect both AID-Flag tagged TopoIIα and untagged TopoIIα (~160kDa) in the 800 channel (green). Anti-β-tubulin was used as a loading control.

(C) Genomic DNA from hygromycin resistant clones was extracted for PCR analysis using indicated primers shown in A. Representative result of PCR amplification was shown. Clones showing only 3kbp DNA fragment are homozygous AID integrated clones (#72, #79 and #80).
(D) The clone #79 was treated with auxin for 2, 4, and 6-hours, and evaluated the TopoIIα depletion by Western blotting. As a control, DLD-1 OsTIR1#50 parental cells were treated with auxin for 6 hours (DLD1 TIR1). Whole cell lysates were subjected to Western blotting analysis using indicated antibodies. Clone #79 was chosen for further analysis in the subsequent experiments showed in Figure 3.4.
(E) DLD-1 cells with endogenous TopoIIα tagged with an auxin inducible degron (AID) were synchronized in mitosis and treated with auxin 6 hours after Thymidine release. Cells were plated onto fibronectin coated coverslips and subsequently stained with anti-TopoIIα, anti-CENP-C, and DNA was labeled with DAPI. TopoIIα foci on mitotic chromosomes are completely eliminated with auxin treatment.

To deplete TopoIIα, the cells were treated with auxin after release from a Thymidine block. After mitotic shake off and treatment with ICRF-193, isolated chromosomes were subjected to Western blotting with anti-SUMO2/3, anti-TopoIIα, and anti-PICH antibodies. ICRF-193 treatment still increased overall SUMOylation in ΔTopoIIα cells, suggesting that ICRF-193 affects SUMOylation of other chromosomal proteins, as such TopoIIβ (Figure 3.7A). Notably, ΔTopoIIα cells treated with ICRF-193 showed no changes in PICH levels on the chromosomes. This suggests that increased levels of PICH seen in ICRF-193 treatment is a SUMOylated TopoIIα-dependent response (Figure 3.7A). Immunofluorescent analysis of ΔTopoIIα cells showed a clear reduction of PICH foci even in the presence of ICRF-193 (Figure 3.7B). In ΔTopoIIα cells, SUMO2/3 foci were no longer increased at the centromere (marked by CENP-C) in response to ICRF-193 (Figure 3.7C). These results suggest that TopoIIα SUMOylation caused by ICRF-193 critically contributes to the enrichment of PICH foci on chromosomes.

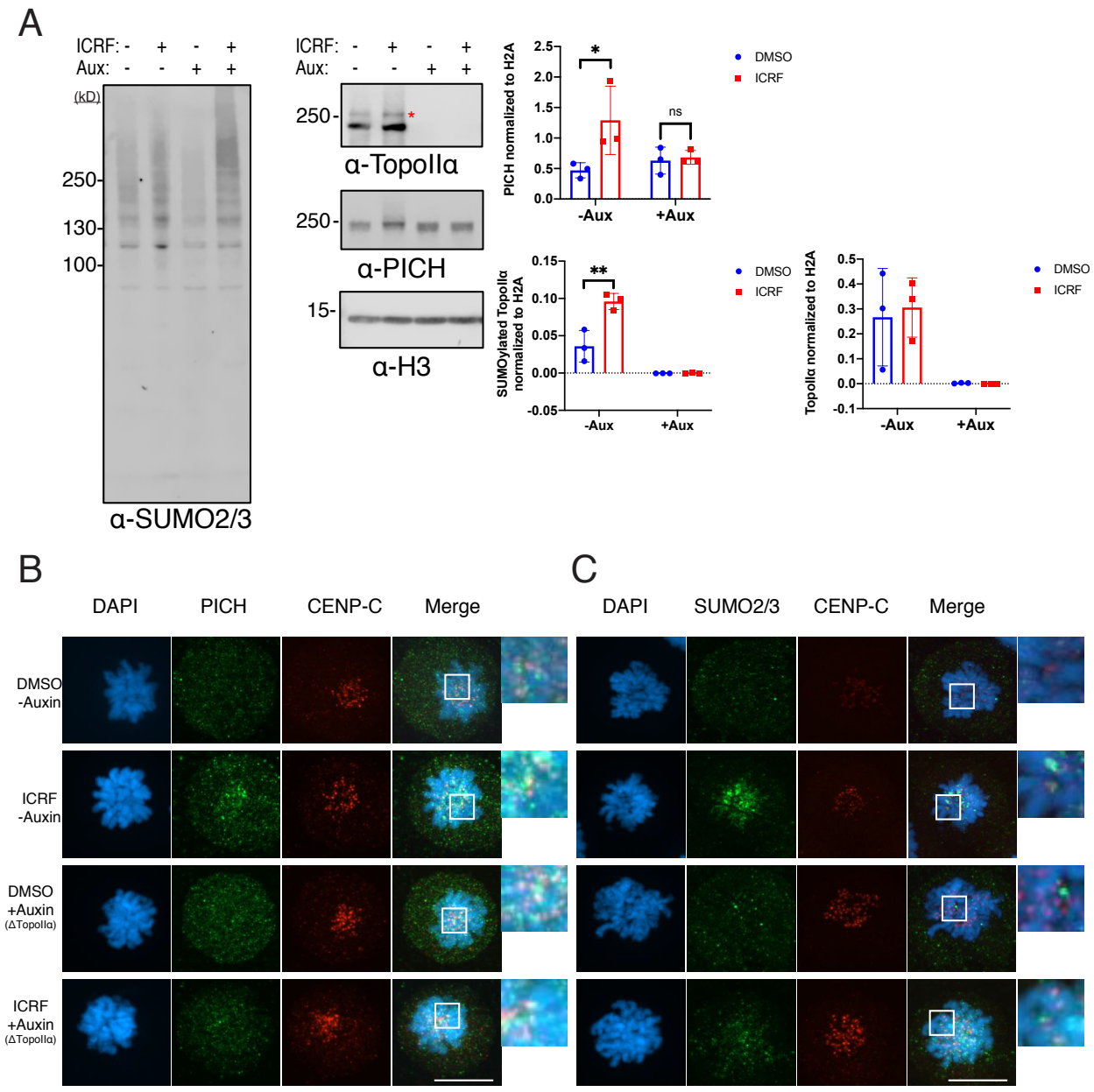

Figure 3.7. Depletion of TopoIIα attenuates SUMO2/3 modification and eliminates PICH response in ICRF-193 treated cells.

(A) DLD-1 cells with endogenous TopoIIα tagged with a mAID were synchronized in mitosis and treated with DMSO (control) and ICRF-193. Auxin was added to the cells after release from Thymidine for 6 hours. Mitotic chromosomes were isolated and subjected to Western blotting with indicated antibodies.

* indicates SUMOylated TopoIIα.

p values for comparison among three experiments were calculated using a two-way ANOVA analysis of variance with Tukey multi-comparison correction; ns: not significant; *: $p \leq 0.05$; **: $p < 0.01$

(B) Mitotic cells were fixed and stained with antibodies against: PICH (green), CENP-C (red). DNA was stained with DAPI (blue). Scale bar = 11μm. The white square indicates enlarged area.
(C) Mitotic cells were fixed and stained with antibodies against: SUMO2/3 (green), CENP-C (red). DNA was stained with DAPI (blue). Scale bar = 11μm. The white square indicates enlarged area.

Loss of PICH leads to enrichment of SUMOylated proteins at mitotic centromeres.

So far, the results indicate that PICH targets SUMOylated chromosomal proteins, mainly SUMOylated TopoIIα, in ICRF-193 treated cells. Because the ability of PICH to interact with SUMO via its SUMO-interacting motifs is required for proper chromosome segregation, we wished to determine if PICH is required for regulating distribution of SUMOylated chromosomal proteins. To examine this, mAID-PICH cells were generated as described in Chapter two. To deplete PICH, auxin was added to the cells after release from a Thymidine block, then mitotic cells were collected by mitotic shake off. Isolated chromosomes were then subjected to Western blot analysis. Intriguingly, ΔPICH control cells showed a significant increase in SUMOylated TopoIIα compared to -Auxin cells, shown by the appearance of a second upshifted band marked by an asterisk (Figure 3.8A). This suggests that PICH is involved in the reduction of SUMOylated TopoIIα on chromosomes. Immunofluorescent staining further supported this novel role of PICH. In agreement with the Western blot results analysis of ΔPICH cells showed an enrichment of TopoIIα signal at the centromere in both control and ICRF-193 treated cells (Figure 3.8B enlarged images). In addition, increased SUMO2/3 foci were observed in both control and ICRF-193 treated cells (Figure 3.8C enlarged images). This increased SUMO2/3 in control cells without PICH is consistent with the Western bolt result that showed increased SUMO2/3 signals in same condition (Figure 3.8A comparing lane 1

and 3). Together, the results suggest that PICH functions in the regulation and proper localization of SUMOylated chromosomal proteins, including SUMOylated TopoIIα.

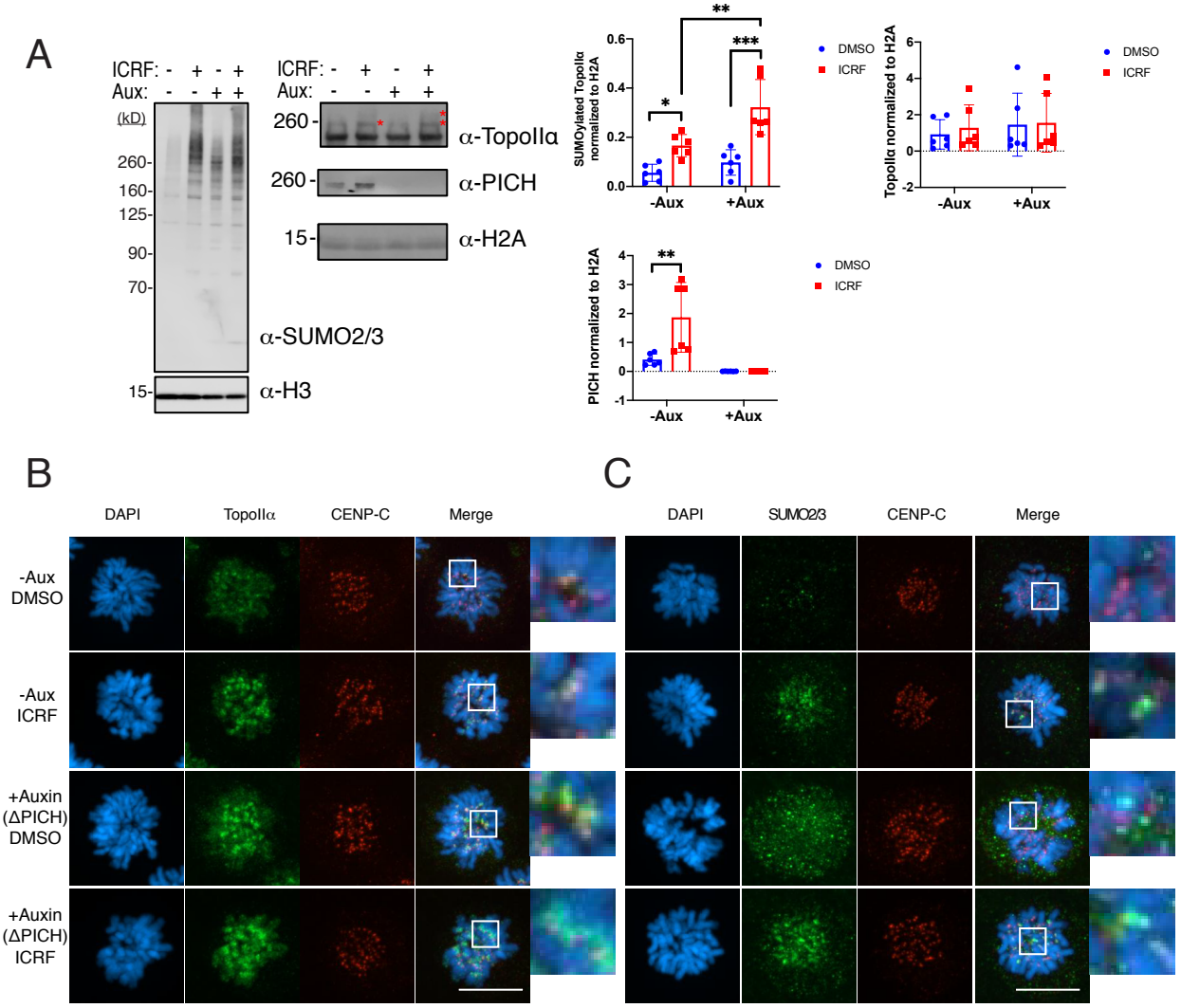

Figure 3.8. PICH-depleted chromosomes show increased levels of SUMOylated TopoIIα.
(A) DLD-1 cells with endogenous PICH tagged with a mAID were synchronized in mitosis and treated with DMSO (control) and ICRF-193. Auxin was added to the cells after release from Thymidine for 6 hours. Mitotic chromosomes were isolated and subjected to Western blotting with indicated antibodies.
* indicates SUMOylated TopoIIα.
p values for comparison among six experiments were calculated using a two-way ANOVA analysis of variance and Tukey multi-comparison correction; ns: not significant; *: $p \leq 0.05$; **: $p < 0.01$; ***: $p < 0.001$; ****: $p < 0.0001$.
(B) Mitotic cells were fixed and stained with antibodies against: TopoIIα (green), CENP-C (red). DNA was stained with DAPI (blue). Scale bar = 11μm. The white square indicates enlarged area.

(C) Mitotic cells were fixed and stained with antibodies against: SUMO2/3 (green), CENP-C (red). DNA was stained with DAPI (blue). Scale bar = 11μm. The white square indicates enlarged area.

ATP-dependent translocase activity of PICH is required for regulating SUMOylated chromosomal proteins.

To identify which function of PICH is required for the redistribution of SUMOylated proteins including TopoIIα, we created a PICH-replacement cell line by combining mAID-mediated PICH depletion and inducible expression of exogenous PICH mutants. The mAID-PICH cells had CRISPR/Cas9 targeted integration of either Tet-inducible WT PICH-mCherry, an ATPase dead mutant (K128A-mCherry), or non-SUMO interacting form of PICH (d3SIM-mCherry) into the CCR5 safe harbor locus (Papapetrou and Schambach, 2016). After clonal isolation and validation (Figure 2.8), PICH-mCherry expression was tested in asynchronous cells by treating with auxin and doxycycline for 14 hours, and the whole cell lysates were used for Western blot analysis. Although the expression level of the exogenous proteins was variable, we were able to replace endogenous PICH with exogenous PICH (Figure 3.9A). We did observe variation of mCherry expression within each clonal isolate (Figure 2.8D) and this may explain the variation in expression levels observed in Western blot analysis. The PICH-replacement for mitotic cell analysis was achieved by incubating cells with auxin or auxin and doxycycline for 22 hours before mitotic shake off. The mitotic cells were treated with DMSO (control) and ICRF-193 then mitotic chromosomes were isolated. Western blot analysis was performed to determine how translocase activity and SIMs contribute to PICH binding to mitotic chromosomes (Figure 3.9B). The PICH WT-mCherry was observed to have a similar response to ICRF-193 as endogenous PICH, showing

increased binding with ICRF-193 treatment. The K128A mutant also showed increased binding under ICRF-193 treatment. In contrast, the d3SIM mutant could not bind to chromosomes, consistent with our previous observations (Sridharan and Azuma, 2016).

To further examine how the PICH mutants affect localization of TopoIIα and SUMO2/3, immunofluorescent analysis of prometaphase cells was performed. PICH WT-mCherry showed the same staining patterns as endogenous PICH and its response to ICRF-193 was similar to Figure 3.1. Both SUMO2/3 and TopoIIα staining was consistent with that seen in Figure 3.1 (Figure 3.9C), further validating that mCherry tagged exogenous PICH functions the same as endogenous PICH. When the K128A mutant, which cannot translocate on DNA, was expressed in both control and ICRF-193 treated cells, strong mCherry foci were observed on the chromosomes. Importantly, these foci overlap with SUMO2/3 foci (Figure 3.9D). This suggests that the PICH K128A mutant interacts with SUMOylated targets but due to its inability to translocate remains stably associated with the chromosomes where the SUMOylated proteins are located. TopoIIα signals were enriched on the chromosomes, where signals had increased intensity and were more punctate than those in Figure 3.9C. This indicates that PICH translocase activity regulates the association of TopoIIα with chromosomes and is involved in the proper localization of TopoIIα. As observed by Western blot analysis, the PICH d3SIM-mCherry mutant did not show any chromosomal signal, but rather a diffuse signal was observed throughout the cell. Interestingly, even cells treated with ICRF-193 did not show an increased chromosomal SUMO2/3 signal. This was unexpected because depletion of PICH did not affect the increase of SUMO2/3 foci induced by ICRF-193 treatment. This observation suggests that the PICH d3SIM mutant has a dominant negative effect on

chromosomal SUMOylation, but the molecular mechanism of that phenomenon is currently unidentified. TopoIIα in PICH d3SIM expressing cells was also affected showing a slight loss of chromosomal signal in control cells and more diffuse/non-punctate staining with ICRF-193 treatment (Figure 3.9E). This suggests that the SIM-dependent chromosomal association of PICH is required for proper organization of mitotic chromosomes, including proper distribution of SUMOylated proteins and TopoIIα on mitotic chromosomes.

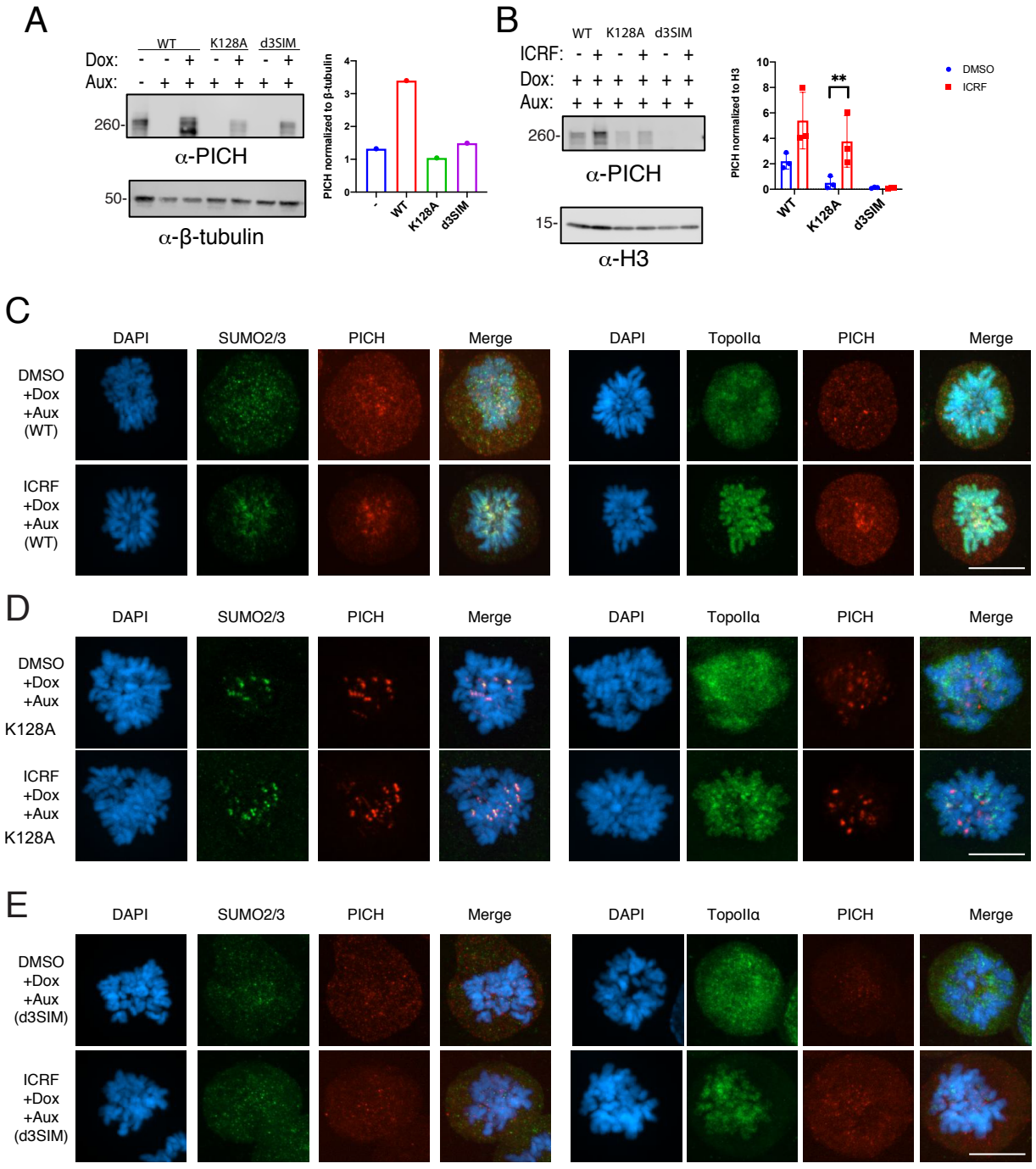
A
WT
K128A
d3SIM
Dox:
Aux:
260-
α-PICH
50-
α-β-tubulin
PICH normalized to β-tubulin
B
WT
K128A
d3SIM
ICRF:
Dox:
Aux:
260-
α-PICH
15-
α-H3
PICH normalized to H3
**
DMSO
ICRF
C
DAPI
SUMO2/3
PICH
Merge
DAPI
TopoIIα
PICH
Merge
DMSO +Dox +Aux (WT)
ICRF +Dox +Aux (WT)
D
DMSO +Dox +Aux K128A
ICRF +Dox +Aux K128A
E
DMSO +Dox +Aux (d3SIM)
ICRF +Dox +Aux (d3SIM)

Figure 3.9. Translocase function of PICH is necessary for redistribution of SUMOylated proteins and SUMOylated TopoIIα on mitotic chromosomes.
(A) DLD-1 cells with endogenous PICH tagged with a mAID and exogenous PICH mCherry mutants were treated with auxin or auxin and doxycycline for 14 hours. Whole cell lysates were subjected to Western blotting with indicated antibodies.
(B) DLD-1 cells with endogenous PICH tagged with a mAID and exogenous PICH mCherry mutants were treated with auxin or auxin and doxycycline for 22 hours. Mitotic chromosomes were isolated and subjected to Western blotting with indicated antibodies.
p values for comparison among three experiments were calculated. ns: not significant; **: $p < 0.01$.
(C) WT PICH mCherry mitotic cells were fixed and stained with antibodies against: SUMO2/3 (green), TopoIIα (green), mCherry (red). DNA was stained with DAPI (blue). Scale bar = 11μm.
(D) K128A PICH mCherry mitotic cells were fixed and stained with antibodies against: SUMO2/3 (green), TopoIIα (green), mCherry (red). DNA was stained with DAPI (blue). Scale bar = 11μm.
(E) d3SIM PICH mCherry mitotic cells were fixed and stained with antibodies against: SUMO2/3 (green), TopoIIα (green), mCherry (red). DNA was stained with DAPI (blue). Scale bar = 11μm.

PICH interacts with SUMOylated TopoIIα through its SIMs.

To examine whether PICH can interact with SUMOylated TopoIIα and determine the potential role of the translocase activity and SUMO binding ability of PICH on the interaction with SUMOylated TopoIIα, we performed an *in vitro* DNA decatenation assay. The assay was designed to compare non-SUMOylated and SUMOylated TopoIIα in the presence of recombinant PICH (Figure 3.10A). Using the conditions established in our previous study, recombinant *Xenopus laevis* TopoIIα was SUMOylated *in vitro*, then its DNA decatenation activity was analyzed by using catenated kDNA as the substrate (Ryu et al., 2010b). The decatenation activity was measured by calculating the percentage of decatenated kDNA separated by gel electrophoresis. On average, 70% of kDNA is decatenated at the five and ten-minute time-point when non-SUMOylated TopoIIα is present in the reaction (Figure 3.10B PICH lanes marked by (i)). As we have previously shown, the decatenation activity of SUMOylated TopoIIα was reduced compared to non-SUMOylated TopoIIα (Figure 3.10B lanes marked by (ii)). Importantly, when we added PICH to each of the reaction at concentrations equimolar to TopoIIα (200nM), the

decatenation activity of SUMOylated TopoIIα was further attenuated (Figure 3.10B marked by (iii), C). The reduction of decatenation activity of SUMOylated TopoIIα was statistically significant at both the five and ten-minute time-points (Figure 3.10C light grey bars). A dose-dependent effect of PICH on SUMOylated TopoIIα decatenation activity was observed but that was not the case for non-SUMOylated TopoIIα. The concentration of TopoIIα in the reaction was 200nM, and PICH significantly reduced decatenation activity of SUMOylated TopoIIα ranging between 200nM (equimolar) up to 400nM (Figure 3.10D, E). Only SUMOylated TopoIIα was inhibited by PICH dose-dependently which is distinct from the PICH/non-SUMOylated TopoIIα interaction.

To determine which activity of PICH is required for inhibiting SUMOylated TopoIIα decatenation activity, we utilized a PICH mutant that has defects in either the SUMO-binding ability (PICH-d3SIM) or in translocase activity (PICH-K128A) (Figure 3.11A) (Sridharan and Azuma, 2016). If PICH/SUMO interaction is critical for inhibiting the decatenation activity of SUMOylated TopoIIα, the PICH-d3SIM mutant would lose its inhibitory function. In addition, we also expect that the PICH translocase activity deficient (PICH-K128A) mutant would lose its inhibitory function on SUMOylated TopoIIα, because this mutant could not remove SUMOylated TopoIIα from kDNA. Supporting our hypothesis, PICH-d3SIM lost its inhibitory function and SUMOylated TopoIIα decatenation activity returned to levels similar to no PICH addition (Figure 3.11C comparing ST to ST + PICH d3SIM). This suggests that direct SUMO/SIM interactions between PICH and SUMOylated TopoIIα play a key role in this inhibition. In contrast, the translocase deficient PICH mutant did not attenuate SUMOylated TopoIIα decatenation activity compared to WT PICH (Figure 3.11C comparing ST + PICH WT and ST + PICH

K128A). Notably, neither of the PICH mutants showed any apparent effect on non-SUMOylated TopoIIα (Figure 3.11B) compared to PICH WT. This suggests that PICH binding to DNA does not inhibit the decatenation activity of TopoIIα, but rather it forms a complex with SUMOylated TopoIIα and prevents its decatenation activity. Taken together, our results suggest that PICH recognizes the SUMO moieties on TopoIIα through its SIMs to attenuate decatenation activity.

In conclusion, our results show a novel function of PICH on the redistribution of SUMOylated chromosomal proteins during mitosis. This activity is dependent on PICH translocase activity and *in vitro* data suggests that SUMO interacting ability of PICH is important in the recognition of SUMOylated proteins, like TopoIIα (Figure 3.12).

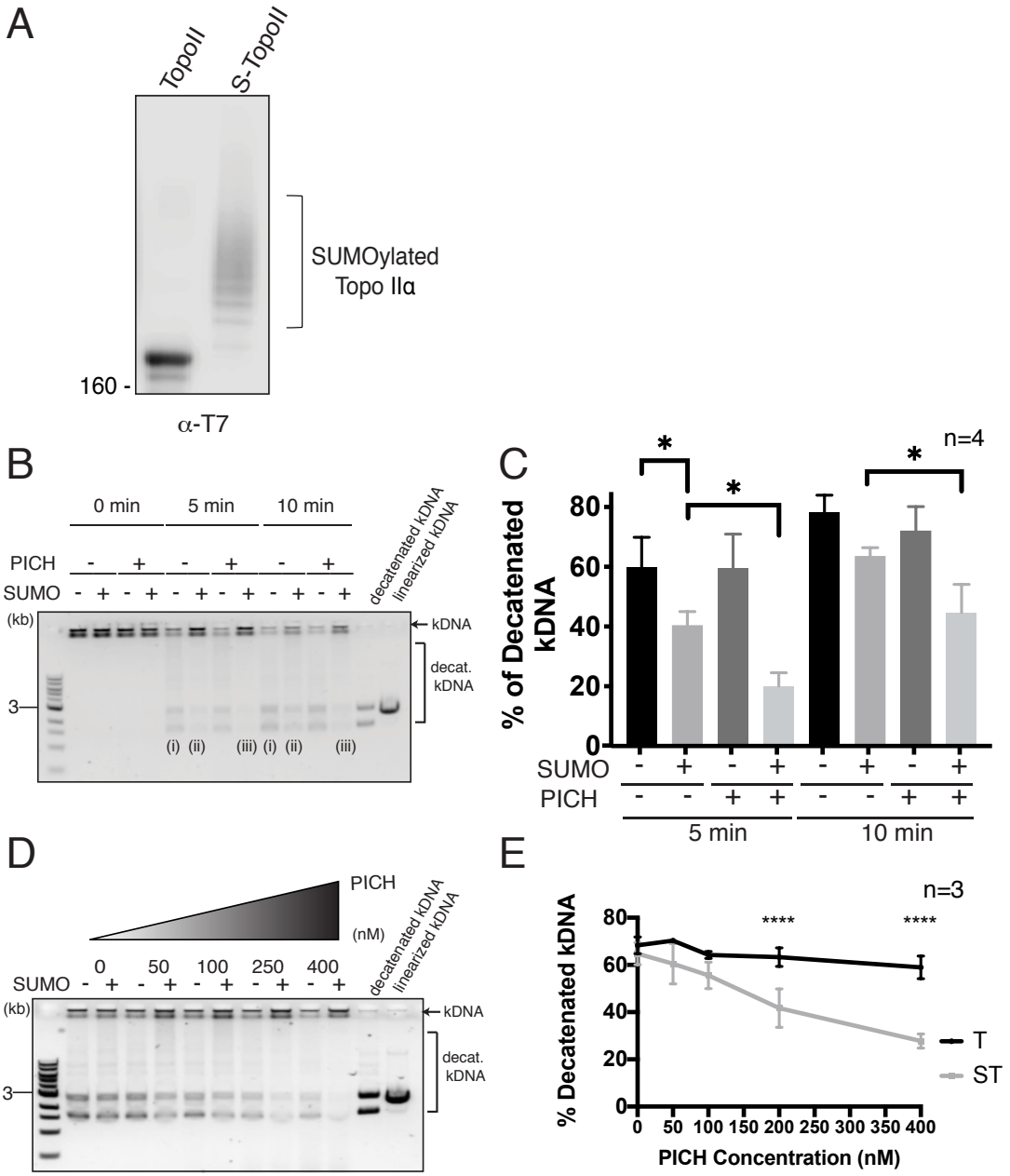

Figure 3.10. PICH inhibits SUMOylated TopoIIα decatenation activity.
(A) Recombinant T7 tagged TopoIIα proteins were SUMOylated *in vitro*. Samples were subjected to Western blotting using anti-T7 tag antibody. The bracket indicates SUMOylated TopoIIα.
(B) Representative gel after decatenation reactions with non-SUMOylated TopoIIα (— SUMO lane (i)) or SUMOylated TopoIIα (+ SUMO lane (ii)) (+PICH lane (iii)) Catenated kDNA is indicated by an arrow. The bracket indicates the decatenated kDNA species.
(C) The decatenation activity of reactions in B was calculated as a percentage of decatenated kDNA.

(D) Representative gel after decatenation reactions with SUMOylated and non-SUMOylated TopoIIα with increasing concentrations of PICH. Catenated kDNA is indicated by an arrow. The bracket indicates decatenated kDNA species.
(E) The decatenation activity of SUMOylated (ST) and non-SUMOylated TopoIIα (T) in D was calculated as a percentage of decatenated kDNA.
Statistical analysis of **C** (n=4) and **E** (n=3) were performed by using a two-way ANOVA analysis of variance with Tukey multi-comparison correction; p values for comparison among the experiments were calculated. ns: not significant; *: $p \leq 0.05$; **: $p < 0.01$; ***: $p < 0.001$; ****: $p < 0.0001$.

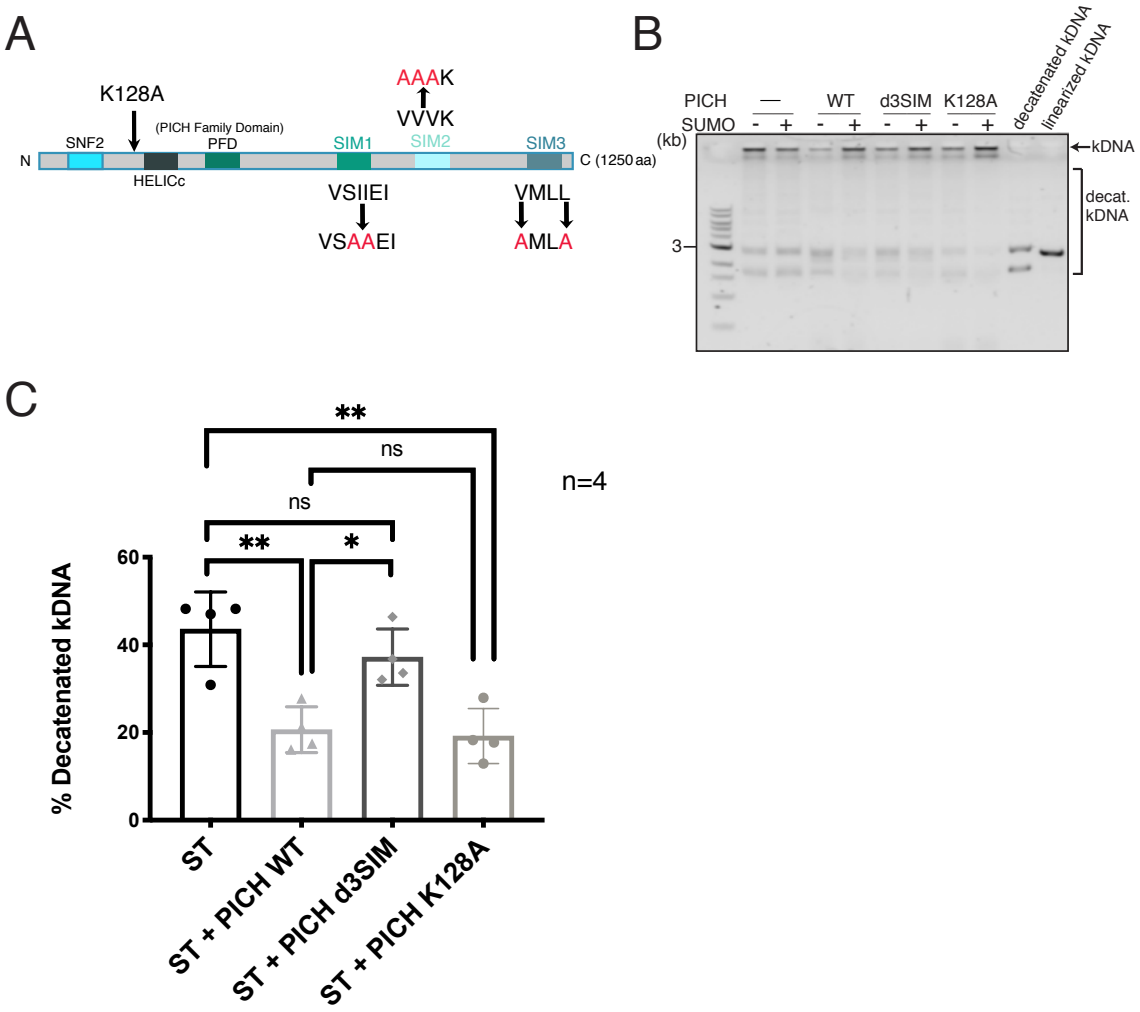

Figure 3.11. PICH SUMO-binding ability involved in suppression of SUMOylated TopoIIα decatenation activity.
(A) Schematic of PICH protein with known functional motifs. The introduced mutations in SIMs and in the ATPase domain (K128A) are indicated.
(B) Representative gel showing non-SUMOylated (-SUMO) and SUMOylated TopoIIα (+SUMO) activity with PICH WT, a non-SUMO-binding mutant (d3SIM), and a translocase deficient mutant (K128A) or no PICH protein (-PICH). Catenated kDNA is indicated with an arrow. The bracket indicates decatenated kDNA species.

(C) Decatenation activity of SUMOylated TopoIIα (ST) with indicated PICH (ST: no PICH, ST + PICH WT: PICH wild-type, ST + PICH d3SIM: PICH-d3SIM mutant, and ST + PICH K128A: PICH-K128A mutant). Statistical analysis of **C** was performed by using a one-way ANOVA analysis of variance with Tukey multi-comparison correction; p values for comparison among four experiments were calculated.
ns: not significant; *: $p \leq 0.05$; **: $p < 0.01$.

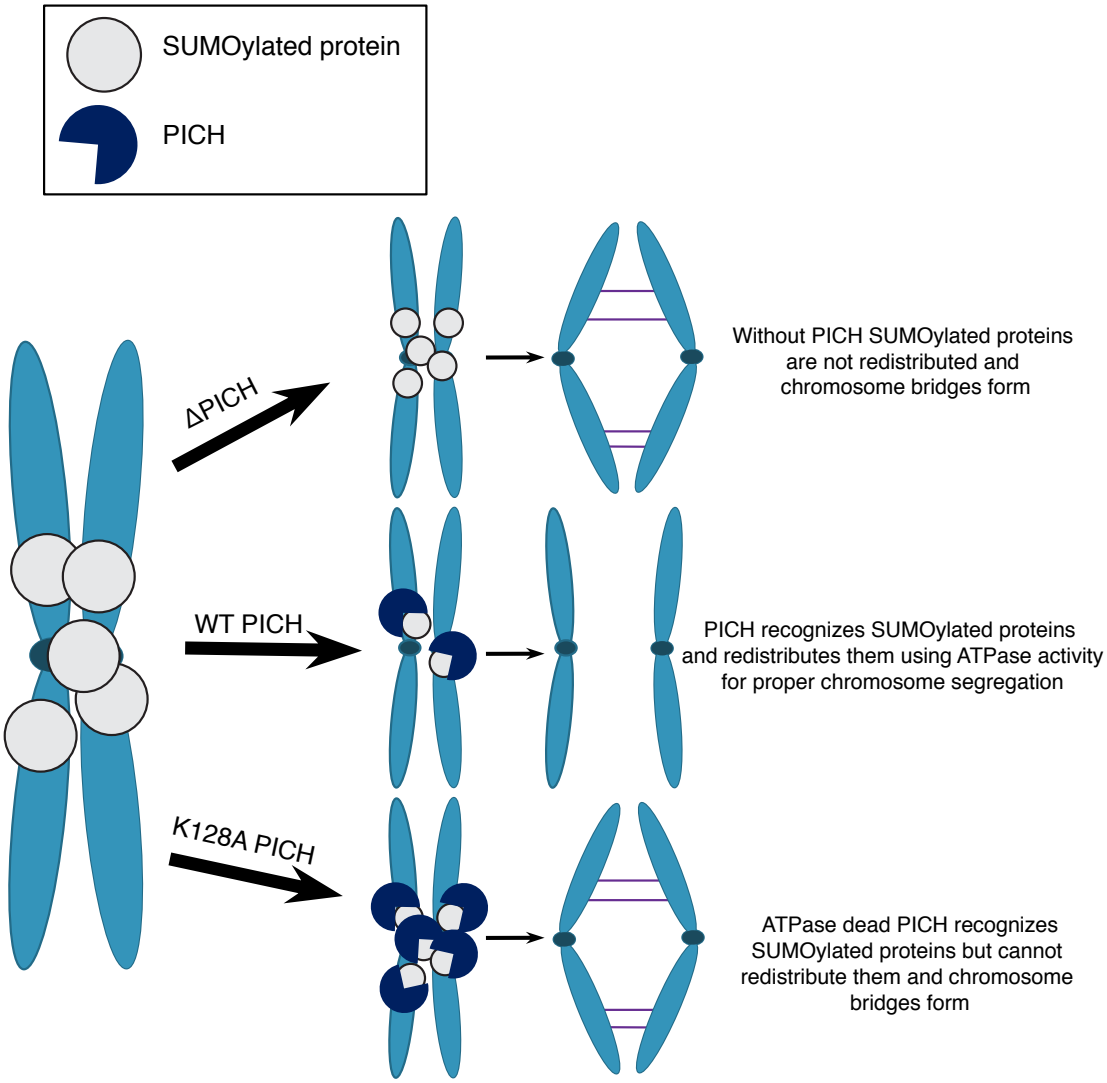

Figure 3.12. Model for demonstrating the role of PICH on the redistribution of SUMOylated proteins like TopoIIα to promote sister chromatid disjunction.
SUMOylation plays a critical role in mitotic regulation and timing, this is due in part by regulating the activity and mediating binding of critical proteins. During mitosis proteins become SUMOylated and PICH recognizes and binds these proteins using its three SUMO interacting motifs, then using its translocase activity it redistributes SUMOylated proteins on the chromosomes and this enables proper chromosome segregation. Without PICH we see an accumulation of SUMOylated proteins on the chromosomes. PICH without translocase activity also shows this similar accumulation of SUMOylated proteins on the chromosomes.

Discussion

We previously demonstrated that both PICH DNA translocase activity and SUMO interacting ability are required for its essential function in proper chromosome segregation (Sridharan and Azuma, 2016). The results presented in this report provide the link between these two functions of PICH during mitosis. Collectively, the results indicate that PICH interacts with chromosomal proteins and increased SUMOylation, whether by modulating enzymes or a specific inhibitor of TopoII mediates the enrichment of PICH foci on mitotic chromosomes. The PICH-replacement to mutant forms demonstrated that PICH DNA translocase activity is required for proper localization of SUMOylated proteins on chromosomes. Our results suggest that both PICH DNA translocase activity and SUMO interacting ability cooperate to remodel chromosomal proteins to accomplish faithful chromosome segregation.

PICH targets and redistributes chromosomal SUMOylated proteins using its SUMO binding ability and translocase activity.

SUMOylation has been shown to play a role in complex assembly by mediating SUMO/SIM interactions (Guzzo et al., 2012; Lin et al., 2006; Matmati et al., 2018; Pelisch et al., 2017). It has been demonstrated that numerous proteins are SUMOylated on mitotic chromosomes (Cubeñas-Potts et al., 2015; Huang et al., 2016; Schimmel et al., 2014). Proper regulation of SUMOylation on chromosomal proteins is apparently key to promote faithful chromosome segregation shown by modulating enzymes for controlling SUMOylation (Cubeñas-Potts et al., 2013; Díaz-Martínez et al., 2006; Hari et al., 2001; Pelisch et al., 2014). Our current study demonstrates that SUMOylated chromosomal proteins are targeted by PICH through its SIMs. Increased SUMO2/3 modification either

by ICRF-193 (Figure 3.1) or expression of the novel deSUMOylation enzyme mutant (Figure 3.5) promotes enrichment of PICH and SUMO2/3 foci on chromosomes, and this suggests PICH efficiently targets SUMOylated chromosomal proteins including TopoIIα. Given the fact that PICH can interact with SUMO moieties (Sridharan et al., 2015) using its three SIMs, this enrichment of PICH foci and SUMO2/3 foci suggests PICH can target multiple SUMOylated chromosomal proteins. More importantly, the translocase deficient mutant of PICH showed enrichment of SUMO2/3 foci on chromosomes without treatments to increase SUMOylation (Figure 3.9). Increased SUMO2/3 foci under expression of the mutant suggests that loss of translocase activity of PICH stabilized SUMOylated protein(s), presumably forming a stable complex on the chromosomes. Until now, the role of PICH DNA translocase activity in chromosome segregation has not been clearly determined on a cellular level. PICH primary structure suggests that it acts as a nucleosome remodeling enzyme, however, PICH has not been shown to have robust nucleosome remodeling activity towards nucleosomes composed of canonical histones (Ke et al., 2011). Our observations suggest that PICH utilizes its translocase activity to remodel chromosomal proteins. Identification of which SUMOylated chromosomal proteins are targeted by PICH will advance our understanding of the role of mitotic SUMOylation and the function of PICH in promoting faithful chromosome segregation.

SUMOylated TopoIIα is a target of PICH.

Although PICH has the ability to interact with multiple SUMOylated proteins, SUMOylated TopoIIα is undoubtedly a primary target. This notion is supported by our observations in TopoIIα-depleted cells (Figure 3.7). Depleting TopoIIα abrogates the enrichment of PICH foci even in the presence of ICRF-193. TopoIIα-depleted

chromosomes also showed an ICRF-193 dependent increase in overall SUMOylation on chromosomes, however, staining for SUMO2/3 showed no clear increase in SUMO2/3 foci. This suggests that the SUMO2/3 foci observed in ICRF-193 treated cells mainly correspond with SUMOylated TopoIIα and PICH could more effectively target SUMOylated TopoIIα over other SUMOylated proteins. It is notable that TopoIIα-depletion increases PICH binding with mitotic chromosomes even without upregulation of SUMOylation. This might represent the formation of PICH threads in TopoIIα-depleted prometaphase chromosomes (Antoniou-Kourounioti et al., 2019), which are observed in ICRF-193 treated cells (Wang et al., 2008). Therefore, increased PICH foci under ICRF-193 could be the result of the formation of PICH threads on prometaphase chromosomes. However, the results from Py-S2 expression (Figure 3.4) and PICH d3SIM mutant replacement (Figure 3.9) suggest that the increased PICH binding to chromosomes under ICRF-193 treatment is mainly controlled by the upregulation of SUMOylation. PICH binding to TopoIIα has been shown to increase the activity of TopoIIα (Nielsen et al., 2015). In contrast to that role, PICH binding to SUMOylated TopoIIα has different consequences, i.e. inhibition of decatenation activity (Figure 3.10). The inhibition of activity requires SIMs suggesting that direct interaction of PICH and SUMOylated TopoIIα is critical (Figure 3.11). The mechanism of how both WT PICH and translocase-deficient mutants similarly inhibit decatenation activity of SUMOylated TopoIIα is currently unclear. From cellular analyses, PICH could remodel the SUMOylated TopoIIα using its translocase activity, therefore it might be possible that WT PICH promotes the removal of SUMOylated TopoIIα from catenated DNAs and that action results in inhibition of decatenation activity towards catenated kDNA substrate. Conversely, the translocase-

deficient mutant could inhibit decatenation activity by forming a stable complex with SUMOylated TopoIIα on DNA. Further analysis of the complex formation of PICH and SUMOylated TopoIIα *in vitro* or in cells is our next goal to elucidate the mechanism of this inhibition.

Broader implications of the novel function of PICH as a SUMOylated protein remodeler.

These novel findings lead to a more mechanistic understanding of the interaction between SUMOylated TopoIIα and PICH and provide insight into why PICH knockout cells were found to be sensitive to ICRF-193. PICH can increase TopoIIα decatenation activity *in vitro* and that helps to resolve tangled DNA during anaphase (Nielsen et al., 2015). In addition, recent studies indicate that the translocase activity of PICH can be used to control the supercoiling status of DNA together with Topoisomerase IIIα (Bizard et al., 2019). This increased supercoiling of DNA provides a more suitable substrate for TopoIIα and thus increases its decatenation activity. Both models can explain how PICH promotes decatenation on tangled DNA at centromeres to prevent UFB formation or resolve existing UFBs by stimulating TopoIIα activity. One unanswered question is how ICRF-193 mediated stalled TopoIIα is removed to prevent the formation of chromosome bridges. ICRF-193 treatment is known to induce a closed clamp conformation of TopoIIα with both detangled DNA strands bound within it (Morris et al., 2000; Roca et al., 1994). It is interesting to hypothesize from our current study that PICH SUMO-binding ability and translocase activity are able to recognize and bind SUMOylated TopoIIα and remove it from DNA. Analysis of PICH function using a TopoIIα-replaced cell line, utilizing the same methodology as the PICH mutant cell lines, will provide insight for this model. Recently,

we demonstrated that SUMOylation of TopoIIα plays a critical role in controlling the progression of mitosis. ICRF-193 treatment resulted in a mitotic arrest in cells that requires SUMOylated TopoIIα and subsequent Aurora B activation (Pandey et al., 2020). Because PICH can control SUMOylated TopoIIα on chromosomes, it is possible that PICH can control stalled TopoIIα-dependent mitotic checkpoint by attenuating SUMOylated TopoIIα on chromosomes. This can be tested using PICH depletion or replacement cell lines as well as modulating PICH activity in TopoIIα-replaced cell lines with a non-SUMOylatable mutant.

This novel role for PICH during mitosis leads to a better understanding of how chromosomal proteins are regulated by SUMOylation and how that might affect chromosome segregation when left unregulated. Although a precise molecular mechanism remains to be determined for the specific SUMOylated protein targeted by PICH, one potential mechanism of how PICH could function with SUMOylated TopoIIα using both translocase activity and SUMO binding ability is presented from this study. A formal test of this model would greatly benefit the PICH field as its function during mitosis remains elusive. This would also shed light on how cells utilize PICH and TopoIIα to deal with the tangled DNA for proper chromosome segregation during mitosis.

Materials and Methods

Plasmids, constructs, and site-directed mutagenesis

The Py-S2 fusion DNA construct of human PIASy-NTD (amino acid 1-135) and SENP2-CD (amino acid 363-589) was created by fusion PCR method using a GA linker between the two fragments. Then, the Py-S2 fusion DNA fragment was subcloned into a recombinant expression pET28a plasmid at the BamHI/XhoI sites. To generate the Py-S2 Mut fusion DNA construct, substitution of Cysteine to Alanine at 548 in Py-S2 was introduced using a site-directed mutagenesis QuikChangeII kit (Agilent) by following the manufacturer's instructions. hH11 locus and CCR5 locus targeting donor plasmids for inducible expression of Py-S2 proteins were created by modifying pMK243 (Tet-OsTIR1-PURO) plasmid (Natsume et al., 2016). pMK243 (Tet-OsTIR1-PURO) was purchased from Addgene (#72835) and the OsTIR1 fragment was removed by BglII and MluI digestion, followed by an insertion of a multi-cloning site. Homology arms for each locus were amplified from DLD-1 genomic DNA using the primers listed in the Supporting Information Table 3.1. The Py-S2 fused with mNeon cDNA and PICH-mCherry fused cDNA were inserted at the MluI and SalI sites of the modified pMK243 plasmid. For CCR5 targeting plasmid, the antibiotics resistant gene was changed to Zeocin-resistant from Puromycin-resistant. Three copies of codon optimized micro AID tag (50 amino-acid each (Morawska and Ulrich, 2013)) was synthesized by the IDT company, and hygromycin resistant gene/ P2A sequence was inserted upstream of the 3x micro AID sequence. The 3xFlag sequence from p3xFLAG-CMV-7.1 plasmid (Sigma) was inserted downstream of the AID sequence. The homology arms sequences for TopoIIα N-terminal insertion were amplified using primers listed in Supporting Information Table 3.1 from genomic DNA of

DLD-1 cells, then inserted into the plasmid by using PciI/SalI and SpeI/NotI sites. In TopoIIα locus and hH11 locus genome editing cases, the guide RNA sequences listed in Supporting Information Table 3.1 were designed using CRISPR Design Tools from https://figshare.com/articles/CRISPR_Design_Tool/1117899 (Rafael Casellas laboratory, NIH) and http://crispr.mit.edu:8079 (Zhang laboratory, MIT) inserted into pX330 (Addgene #42230). Mutations were introduced in PAM sequences on the homology arms. The *X. laevis* TopoIIα cDNA and human PICH cDNA were subcloned into a pPIC 3.5K vector in which calmodulin-binding protein CBP-T7 tag sequences were inserted as previously described (Ryu et al., 2010b, Sridharan and Azuma, 2016). All mutations in the plasmids were generated by site-directed mutagenesis using a QuikChangeII kit (Agilent) according to the manufacturer's instructions. All constructs were verified by DNA sequencing.

Recombinant protein expression and purification, and preparation of antibodies

Recombinant TopoIIα and PICH proteins were prepared as previously described (Ryu et al., 2010b, Sridharan and Azuma, 2016). In brief, the pPIC 3.5K plasmids carrying TopoIIα or PICH cDNA fused with Calmodulin binding protein-tag were transformed into the GS115 strain of *Pichia pastoris* yeast and expressed by following the manufacturer's instructions (Thermo/Fisher). Yeast cells expressing recombinant proteins were frozen and ground with a coffee grinder that contained dry ice, and suspended with lysis buffer (50 mM Tris-HCl, pH 7.5, 150 mM NaCl, 2 mM $CaCl_2$, 1 mM $MgCl_2$, 0.1% Triton X-100, 5% glycerol, 1 mM DTT, complete EDTA-free Protease inhibitor tablet (Roche), and 10 mM PMSF). The lysed samples were centrifuged at 25,000 *g* for 40 min. To capture the CBP-tagged proteins, the supernatant was mixed with calmodulin-sepharose resin (GE

Healthcare) for 90 min at 4°C. The resin was then washed with lysis buffer, and proteins were eluted with buffer containing 10 mM EGTA. In the case of PICH, the elution was concentrated with a centrifugal concentrator (Amicon ultra with a 100kDa molecular weight cut-off). In the case of TopoIIα, the elution was further purified by Hi-trap Q anion-exchange chromatography (GE Healthcare). Recombinant Py-S2 proteins fused to a hexa-histidine tag were expressed in Rossetta2 (DE3) (EMD Millipore/Novagen) and purified with hexa-histidine affinity resin (Talon beads from Takara/Clontech). Fractions obtained by imidazole-elution were subjected to Hi-trap SP cation-exchange chromatography. The peak fractions were pooled then concentrated by centrifugal concentrator (Amicon ultra with a 30kDa molecular weight cut-off). The E1 complex (Aos1/Uba2 heterodimer), PIASy, Ubc9, dnUbc9, and SUMO paralogues were expressed in Rosetta2(DE3) and purified as described previously (Ryu et al., 2010a).

To generate the antibody for human PICH, the 3'end (coding for amino acids 947~1250) was amplified from PICH cDNA by PCR. The amplified fragment was subcloned into pET28a vector (EMD Millipore/Novagen) then the sequence was verified by DNA sequencing. The recombinant protein was expressed in Rossetta2(DE3) strain (EMD Millipore/Novagen). Expressed protein was found in inclusion bodies and thus, the proteins were solubilized by 8M urea containing buffer (20mM Hepes pH7.8, 300mM NaCl, 1mM MgCl2, 0.5mM TCEP). The solubilized protein was purified by Talon-resin (Clontech/Takara) using the hexa-histidine-tag fused at the N-terminus of the protein. The purified protein was separated by SDS-PAGE and protein was excised after Instant*Blue*™ (Sigma-Aldrich) staining. The gel slice was used as an antigen and immunization of rabbits was made by Pacific Immunology Inc., CA, USA. To generate the primary

antibody for human TopoIIα, the 3'end of TopoIIα (coding for amino acids 1359~1589) was amplified from TopoIIα cDNA by PCR. The amplified fragment was subcloned into pET28a and pGEX-4T vectors (GE Healthcare) then the sequence was verified by DNA sequencing. The recombinant protein was expressed in Rossetta2(DE3). The expressed protein was purified using a hexa-histidine-tag or GST-tag by Talon-resin (Clontech/Takara) or Glutathione-sepharose (GE healthcare) following the manufacture's protocol. The purified proteins were further separated by cation-exchange column. Purified hexa-histidine-tagged TopoIIα protein as used as an antigen and immunization of rabbits was made by Pacific Immunology Inc., CA, USA. For both PICH and TopoIIα antigens, antigen affinity columns were prepared by conjugating purified antigens (hexa-histidine-tagged PICH C-terminus fragment or GST-tagged TopoIIα C-terminus fragment) to the NHS-Sepharose resin following manufacture's protocol (GE healthcare). The rabbit antisera were subjected to affinity purification using antigen affinity columns. Secondary antibodies used for this study and their dilution rates were: for Western blotting; Goat anti-Rabbit (IRDye®680RD, 1/20000, LI-COR) and Goat anti-Mouse (IRDye®800CW, 1/20000, LI-COR), and for immunofluorescence staining; Goat anti-mouse IgG Alexa Fluor 568 (#A11031, 1:500, Invitrogen), goat anti-rabbit IgG Alexa Fluor 568 (#A11036, 1:500, Thermo/Fisher), goat anti-rabbit IgG Alexa Fluor 488 (#A11034, 1:500, Thermo/Fisher), goat anti-guinea pig IgG Alexa Fluor 568 (#A21450, 1:500, Thermo/Fisher). Unless otherwise stated, all chemicals were obtained from Sigma-Aldrich.

***In vitro* SUMOylation assays and decatenation assays**

The SUMOylation reactions were performed in the Reaction buffer (20 mM Hepes, pH 7.8, 100 mM NaCl, 5 mM $MgCl_2$, 0.05% Tween 20, 5% glycerol, 2.5mM ATP, and 1 mM DTT) by adding 15 nM E1, 15 nM Ubc9, 45 nM PIASy, 500 nM T7-tagged TopoIIα, and 5 μM SUMO2-GG—the SUMO isoform which is able to be conjugated to substrates. For the non-SUMOylated TopoIIα control, 5 μM SUMO2-G mutant was used instead of SUMO2-GG. After the reaction with the incubation for one hour at 25°C, it was stopped with the addition of EDTA at a final concentration of 10mM. For the analysis of the SUMOylation profile of TopoIIα 3X SDS-PAGE sample buffer was added to reaction, and the samples were resolved on 8–16% Tris-HCl gradient gels (#XP08165BOX, Thermo/Fisher) by SDS-PAGE, then analyzed by Western blotting with HRP-conjugated anti-T7 monoclonal antibody (#T3699, EMD Millipore/Novagen).

Decatenation assays were performed in decatenation buffer (50 mM Tris-HCl, pH 8.0, 120 mM NaCl, 5 mM $MgCl_2$, 0.5 mM DTT, 30 μg BSA/ml, and 2 mM ATP) with SUMOylated TopoIIα and non-SUMOylated TopoIIα and with 6.2 ng/μl of kDNA (TopoGEN, Inc.). The reaction was performed at 25°C with the conditions indicated in each of the figures. The reactions were stopped by adding one third volume of 6X DNA dye (30% glycerol, 0.1% SDS, 10 mM EDTA, and 0.2 μg/μl bromophenol blue). The samples were loaded on a 1% agarose gel containing SYBR™ Safe DNA Gel stain (#S33102, Invitrogen) with 1kb ladder (#N3232S, NEB), and electrophoresed at 100 V in TAE buffer (Tris-acetate-EDTA) until the marker dye reached the middle of the gel. The amount of kDNA remaining in the wells was measured using ImageStudio, and the percentage of decatenated DNA was calculated as (Intensity of initial kDNA [at 0 minutes incubation] - intensity of remaining catenated DNA)/Intensity of initial kDNA. Obtained

percentages of catenated DNA was plotted and analyzed for the statistics by using GraphPad Prism 8 Software.

Cell culture, Transfection, and Colony Isolation

Targeted insertion using the CRISPR/Cas9 system was used for all integration of exogenous sequences into the genome. DLD-1 cells were transfected with guide plasmids and donor plasmid using ViaFect^{TM} (#E4981, Promega) on 3.5cm dishes. The cells were split and re-plated on 10cm dishes at ~20% confluency, two days after, the cells were subjected to a selection process by maintaining them in the medium in the presence of an appropriate selection reagent (1µg/ml Blasticidin (#ant-bl, Invivogen), 400µg/ml Zeocin (#ant-zn, Invivogen), 200µg/ml Hygromycin B Gold (#ant-hg, Invivogen)). The cells were cultured for 10 to 14 days with a selection medium, the colonies were isolated and grown in 48 well plates, and prepared Western blotting and genomic DNA samples to verify the insertion of the transgene. Specifically, for the Western blotting analysis, the cells were pelleted, 1X SDS PAGE sample buffer was added, and boiled/vortexed. Samples were separated on an 8-16% gel and then blocked with Casein and probed using the indicated antibody described in each figure legend. Signals were acquired using the LI-COR Odyssey Fc imager. To perform genomic PCR, the cells were pelleted, genomic DNA was extracted using lysis buffer (100mM Tris-HCl pH 8.0, 200mM NaCl, 5mM EDTA, 1% SDS, and 0.6mg/mL proteinase K (#P8107S, NEB)), and purified by ethanol precipitation followed by resuspension with TE buffer containing 50ug/mL RNase A (#EN0531,ThermoFisher). Primers used for confirming the proper integrations are listed in the Supporting Information Table 3.1.

To establish AID cell lines, as an initial step, the *Oryza sativa* E3 ligase (OsTIR1) gene was inserted into the 3' end of a housekeeping gene, RCC1, using CRISPR/Cas9 system in the DLD-1 cell line as described in Chapter two. (Figure 2.3). We then introduced DNA encoding for AID-3xFlag tag into the TopoIIα or PICH locus using CRISPR/Cas9 editing into the OsTIR1 expressing parental line. The isolated candidate clones were subjected to genomic PCR and Western blotting analysis to validate integration of the transgene. Once clones were established and the transgene integration was validated, the depletion of the protein in the auxin-treated cells was confirmed by Western blotting and immunostaining (Figure 3.6 and 2.5).

Introducing DNA encoding Tet inducible PICH mCherry into the CCR5 locus or inducible Py-S2 into hH11 were made by CRISPR/Cas9 editing into the desired locus (Figure 2.8 and 3.3). The OsTIR1 expressing, mAID PICH parental cell line was used for introduction of the PICH mCherry mutants targeted to the CCR5 locus. The isolated candidate clones were subjected to genomic PCR and Western blotting analysis to validate integration of the transgene. Once clones were established and the transgene integration was validated, the expression of the transgenes was confirmed by the addition of doxycycline (Figure 2.8).

Xenopus egg extract assay for mitotic chromosomal SUMOylation analysis

Low speed cytostatic factor (CSF) arrested Xenopus egg extracts (XEEs) and demembraned sperm nuclei were prepared following standard protocols (Murray, 1991; Powers et al., 2001). To prepare the mitotic replicated chromosome, CSF extracts were driven into interphase by adding 0.6mM $CaCl_2$. Demembraned sperm nuclei were added to interphase extract at 4000 sperm nuclei/μl, then incubated for ~60 min to complete

DNA replication confirmed by the morphology of nuclei. Then, equal volume of CSF XEE was added to the reactions to induce mitosis. To confirm the activities of Py-S2 proteins on mitotic SUMOylation, the Py-S2 proteins or dnUbC9 were added to XEEs at a final concentration of 30nM and 5μM, respectively, at the onset of mitosis-induction. After mitotic chromosome formation was confirmed by microscopic analysis of condensed mitotic chromosomes, chromosomes were isolated by centrifugation using a 40% glycerol cushion as previously described (Yoshida et al., 2016) then the isolated mitotic chromosomes were boiled in SDS-PAGE sample buffer. Samples were resolved on 8-16% gradient gels and subjected to Western blotting with indicated antibodies. Signals were acquired using a LI-COR Odyssey Fc digital imager and the quantification was performed using Image Studio Lite software.

The following primary antibodies were used for Western blotting: Rabbit anti-Xenopus TopoIIα (1:10,000), Rabbit anti-Xenopus PARP1 (1:10,000), Rabbit anti-SUMO2/3 (1:1,000) (all prepared as described previously (Ryu et al., 2010a)), anti-Histone H3 (#14269, Cell Signaling).

Preparation of mitotic cells and chromosome isolation

DLD-1 cells were grown in McCoy's 5A 1x L-glutamine 10% FBS media for no more than 10 passages. To analyze mitotic chromosomes, cells were synchronized by a Thymidine/Nocodazole cell cycle arrest protocol. In brief, cells were arrested with 2mM Thymidine for 17 hours, were released from the Thymidine block by performing three washes with non-FBS containing McCoy's 5A 1x L-glutamine media and placed in fresh 10% FBS containing media. 6 hours after the Thymidine release, 0.1ug/mL Nocodazole was added to the cells for 4 additional hours, mitotic cells were isolated by performing a

mitotic shake-off and washed 3 times using McCoy's non-FBS containing media to release the Nocodazole block. The cells were then resuspended with 10% FBS containing fresh media and 7uM of ICRF-193, 40uM Merbarone, or an equal volume of DMSO, were plated on Fibronectin coated cover slips, and incubated for 20 minutes (NEUVITRO, #GG-12-1.5-Fibronectin). To isolate mitotic chromosomes, the cells were lysed with lysis buffer [250mM Sucrose, 20mM HEPES, 100mM NaCl, 1.5mM $MgCl_2$, 1mM EDTA, 1mM EGTA, 0.2% TritonX-100, 1:2000 LPC (Leupeptin, Pepstatin, Chymostatin, 20mg each/ml in DMSO; Sigma-Aldrich), and 20mM Iodoacetamide (Sigma-Aldrich #I1149)] incubated for 5 minutes on ice. Lysed cells were then placed on a 40% glycerol cushion containing 0.25% Triton-X-100, and spun at 10,000xg for 5 minutes, twice. Isolated chromosomes were then boiled with SDS-PAGE sample buffer, resolved on an 8-16% gradient gel and subjected to Western blotting with indicated antibodies. Signals of the blotting were acquired using the LI-COR Odyssey Fc machine.

The following primary antibodies were used for Western blotting: Rabbit anti-PICH (1:1,000), Rabbit anti-TopoIIα (1:20,000) (both are prepared as described above), Rabbit anti-SUMO2/3 (1:1,000), Rabbit anti-Histone H2A (1:2,000) (#18255, Abcam), Rabbit anti-Histone H3 (1:2,000) (#14269, Cell Signaling), Rabbit anti-PIASy (1:500) (as described in (Azuma et al., 2005)), Mouse anti-β-actin (1:2,000) (#A2228, Sigma-Aldrich), Mouse anti-myc (1:1,000) (#9E10, Santa Cruz), Mouse anti-β-tubulin (1:2,000) (#, Sigma-Aldrich), Mouse anti-Flag (1:1,000) (#F1804, Sigma-Aldrich).

Cell fixation and staining

To fix the mitotic cells on fibronectin coated cover slips, cells were incubated with 4% paraformaldehyde for 10 minutes at room temperature, and subsequently washed three

times with 1X PBS containing 10mM Tris-HCl to quench PFA. Following the fixation, the cells were permeabilized using 100% ice cold Methanol in a -20°C freezer for 5 minutes. Cells were then blocked using 2.5% hydrolyzed gelatin for 30 minutes at room temperature. Following blocking the cells were stained with primary antibodies for 1 hour at room temperature, washed 3 times with 1X PBS containing 0.1% tween20, and incubated with secondary for 1 hour at room temperature. Following secondary incubation, cells were washed 3 times with 1x PBS-T and mounted onto a glass slide using VECTASHIELD® Antifade Mounting Medium with DAPI (#H-1200, Vector laboratory) and sealed with nail polish. Images were acquired using an UltraView VoX spinning disk confocal system (PerkinElmer) mounted on an Olympus IX71 inverted microscope. It was equipped with a software-controlled piezoelectric stage for rapid Z-axis movement. Images were collected using a 60 × 1.42 NA planapochromatic objective (Olympus) and an ORCA ERAG camera (Hamamatsu Photonics). Solid state 405, 488, and 561 nm lasers were used for excitation. Fluorochrome-specific emission filters were used to prevent emission bleed through between fluorochromes. This system was controlled by Volocity software (PerkinElmer). Minimum and maximum intensity cutoffs (black and white levels) for each channel were chosen in Volocity before images were exported. Images are presented as extended focus. No other adjustments were made to the images. Figures were prepared from exported images in Adobe illustrator.

The following primary antibodies were used for staining: Rabbit anti-PICH 1:800, Rabbit anti-human TopoIIα 1:1000 (both are prepared as described above), Mouse anti-human TopoIIα 1:300 (#Ab 189342, Abcam), Mouse anti-SUMO2/3 (#12F3, Cytoskeleton Inc),

Guinea Pig anti-SUMO2/3 (1:300) (prepared as previously described (Ryu et al., 2010), and Rat anti-RFP (#RMA5F8, Bulldog Bio Inc).

Statistical analysis

All statistical analyses were performed with either 1- or 2-way ANOVA, followed by the appropriate post-hoc analyses using GraphPad Prism 8 software. Graphs are presented as mean with standard deviation.

Collaborations and workload allocations

For all experiments designed in this chapter Victoria Hassebroek designed, conducted, and analyzed data except the following:

Figure 3.2 – Dr. Yoshiaki Azuma purified the protein and Hyewon Park performed egg extract experiment

Figure 3.6 –Hyewon Park created the mAID-TopoIIα cell line

In addition, Dr. Nootan Pandey and Brooklyn Lerbakken performed initial validation of Py-S2 WT and Mut cell lines

References

Agostinho M, Santos V, Ferreira F, Costa R, Cardoso J, Pinheiro I, Rino J, Jaffray E, Hay RT, Ferreira J. 2008. Conjugation of human topoisomerase 2 alpha with small ubiquitin-like modifiers 2/3 in response to topoisomerase inhibitors: cell cycle stage and chromosome domain specificity. *Cancer Res* **68**:2409–2418. doi:10.1158/0008-5472.CAN-07-2092

Antoniou-Kourounioti M, Mimmack ML, Porter ACG, Farr CJ. 2019. The Impact of the C-Terminal Region on the Interaction of Topoisomerase II Alpha with Mitotic Chromatin. *Int J Mol Sci* **20**. doi:10.3390/ijms20051238

Azuma Y, Arnaoutov A, Anan T, Dasso M. 2005. PIASy mediates SUMO-2 conjugation of Topoisomerase-II on mitotic chromosomes. *EMBO J* **24**:2172–2182. doi:10.1038/sj.emboj.7600700

Bachant J, Alcasabas A, Blat Y, Kleckner N, Elledge SJ. 2002. The SUMO-1 isopeptidase Smt4 is linked to centromeric cohesion through SUMO-1 modification of DNA topoisomerase II. *Mol Cell* **9**:1169–1182.

Bauer DLV, Marie R, Rasmussen KH, Kristensen A, Mir KU. 2012. DNA catenation maintains structure of human metaphase chromosomes. *Nucleic Acids Res* **40**:11428–11434. doi:10.1093/nar/gks931

Baumann C, Körner R, Hofmann K, Nigg EA. 2007. PICH, a centromere-associated SNF2 family ATPase, is regulated by Plk1 and required for the spindle checkpoint. *Cell* **128**:101–114. doi:10.1016/j.cell.2006.11.041

Biebricher A, Hirano S, Enzlin JH, Wiechens N, Streicher WW, Huttner D, Wang LH-C, Nigg EA, Owen-Hughes T, Liu Y, Peterman E, Wuite GJL, Hickson ID. 2013. PICH: a DNA translocase specially adapted for processing anaphase bridge DNA. *Mol Cell* **51**:691–701. doi:10.1016/j.molcel.2013.07.016

Bizard AH, Allemand J-F, Hassenkam T, Paramasivam M, Sarlós K, Singh MI, Hickson ID. 2019. PICH and TOP3A cooperate to induce positive DNA supercoiling. *Nat Struct Mol Biol* **26**:267–274. doi:10.1038/s41594-019-0201-6

Chan K-L, North PS, Hickson ID. 2007. BLM is required for faithful chromosome segregation and its localization defines a class of ultrafine anaphase bridges. *EMBO J* **26**:3397–3409. doi:10.1038/sj.emboj.7601777

Cubeñas-Potts C, Goeres JD, Matunis MJ. 2013. SENP1 and SENP2 affect spatial and temporal control of sumoylation in mitosis. *Mol Biol Cell* **24**:3483–3495. doi:10.1091/mbc.E13-05-0230

Cubeñas-Potts C, Srikumar T, Lee C, Osula O, Subramonian D, Zhang X-D, Cotter RJ, Raught B, Matunis MJ. 2015. Identification of SUMO-2/3-modified proteins associated with mitotic chromosomes. *Proteomics* **15**:763–772. doi:10.1002/pmic.201400400

Díaz-Martínez LA, Giménez-Abián JF, Azuma Y, Guacci V, Giménez-Martín G, Lanier LM, Clarke DJ. 2006. PIASgamma is required for faithful chromosome segregation in human cells. *PloS One* **1**:e53. doi:10.1371/journal.pone.0000053

Gómez R, Viera A, Berenguer I, Llano E, Pendás AM, Barbero JL, Kikuchi A, Suja JA. 2014. Cohesin removal precedes topoisomerase IIα-dependent decatenation at centromeres in male mammalian meiosis II. *Chromosoma* **123**:129–146. doi:10.1007/s00412-013-0434-9

Guzzo CM, Berndsen CE, Zhu J, Gupta V, Datta A, Greenberg RA, Wolberger C, Matunis MJ. 2012. RNF4-dependent hybrid SUMO-ubiquitin chains are signals for RAP80 and

thereby mediate the recruitment of BRCA1 to sites of DNA damage. *Sci Signal* **5**:ra88. doi:10.1126/scisignal.2003485
Hari KL, Cook KR, Karpen GH. 2001. The Drosophila Su(var)2-10 locus regulates chromosome structure and function and encodes a member of the PIAS protein family. *Genes Dev* **15**:1334–1348. doi:10.1101/gad.877901
Hengeveld RCC, de Boer HR, Schoonen PM, de Vries EGE, Lens SMA, van Vugt MATM. 2015. Rif1 Is Required for Resolution of Ultrafine DNA Bridges in Anaphase to Ensure Genomic Stability. *Dev Cell* **34**:466–474. doi:10.1016/j.devcel.2015.06.014
Huang C, Cheng J, Bawa-Khalfe T, Yao X, Chin YE, Yeh ETH. 2016. SUMOylated ORC2 Recruits a Histone Demethylase to Regulate Centromeric Histone Modification and Genomic Stability. *Cell Rep* **15**:147–157. doi:10.1016/j.celrep.2016.02.091
Ke Y, Huh J-W, Warrington R, Li B, Wu N, Leng M, Zhang J, Ball HL, Li B, Yu H. 2011. PICH and BLM limit histone association with anaphase centromeric DNA threads and promote their resolution. *EMBO J* **30**:3309–3321. doi:10.1038/emboj.2011.226
Kurasawa Y, Yu-Lee L. 2010. PICH and cotargeted Plk1 coordinately maintain prometaphase chromosome arm architecture. *Mol Biol Cell* **21**:1188–1199. doi:10.1091/mbc.e09-11-0950
Lin D-Y, Huang Y-S, Jeng J-C, Kuo H-Y, Chang C-C, Chao T-T, Ho C-C, Chen Y-C, Lin T-P, Fang H-I, Hung C-C, Suen C-S, Hwang M-J, Chang K-S, Maul GG, Shih H-M. 2006. Role of SUMO-interacting motif in Daxx SUMO modification, subnuclear localization, and repression of sumoylated transcription factors. *Mol Cell* **24**:341–354. doi:10.1016/j.molcel.2006.10.019
Losada A, Hirano M, Hirano T. 1998. Identification of Xenopus SMC protein complexes required for sister chromatid cohesion. *Genes Dev* **12**:1986–1997.
Matmati S, Vaurs M, Escandell JM, Maestroni L, Nakamura TM, Ferreira MG, Géli V, Coulon S. 2018. The fission yeast Stn1-Ten1 complex limits telomerase activity via its SUMO-interacting motif and promotes telomeres replication. *Sci Adv* **4**:eaar2740. doi:10.1126/sciadv.aar2740
Michaelis C, Ciosk R, Nasmyth K. 1997. Cohesins: chromosomal proteins that prevent premature separation of sister chromatids. *Cell* **91**:35–45.
Morales C, Losada A. 2018. Establishing and dissolving cohesion during the vertebrate cell cycle. *Curr Opin Cell Biol* **52**:51–57. doi:10.1016/j.ceb.2018.01.010
Morawska M, Ulrich HD. 2013. An expanded tool kit for the auxin-inducible degron system in budding yeast. *Yeast Chichester Engl* **30**:341–351. doi:10.1002/yea.2967
Morris SK, Baird CL, Lindsley JE. 2000. Steady-state and rapid kinetic analysis of topoisomerase II trapped as the closed-clamp intermediate by ICRF-193. *J Biol Chem* **275**:2613–2618.
Murray AW. 1991. Cell cycle extracts. *Methods Cell Biol* **36**:581–605.
Nacerddine K, Lehembre F, Bhaumik M, Artus J, Cohen-Tannoudji M, Babinet C, Pandolfi PP, Dejean A. 2005. The SUMO pathway is essential for nuclear integrity and chromosome segregation in mice. *Dev Cell* **9**:769–779. doi:10.1016/j.devcel.2005.10.007
Natsume T, Kiyomitsu T, Saga Y, Kanemaki MT. 2016. Rapid Protein Depletion in Human Cells by Auxin-Inducible Degron Tagging with Short Homology Donors. *Cell Rep* **15**:210–218. doi:10.1016/j.celrep.2016.03.001
Nielsen CF, Huttner D, Bizard AH, Hirano S, Li T-N, Palmai-Pallag T, Bjerregaard VA, Liu Y, Nigg EA, Wang LH-C, Hickson ID. 2015. PICH promotes sister chromatid disjunction and co-operates with topoisomerase II in mitosis. *Nat Commun* **6**:8962. doi:10.1038/ncomms9962

Nishimura K, Fukagawa T, Takisawa H, Kakimoto T, Kanemaki M. 2009. An auxin-based degron system for the rapid depletion of proteins in nonplant cells. *Nat Methods* **6**:917–922. doi:10.1038/nmeth.1401

Ohkuni K, Levy-Myers R, Warren J, Au W-C, Takahashi Y, Baker RE, Basrai MA. 2018. N-terminal Sumoylation of Centromeric Histone H3 Variant Cse4 Regulates Its Proteolysis To Prevent Mislocalization to Non-centromeric Chromatin. *G3 Bethesda Md* **8**:1215–1223. doi:10.1534/g3.117.300419

Pandey N, Keifenheim D, Yoshida MM, Hassebroek VA, Soroka C, Azuma Y, Clarke DJ. 2020. Topoisomerase II SUMOylation activates a metaphase checkpoint via Haspin and Aurora B kinases. *J Cell Biol* **219**. doi:10.1083/jcb.201807189

Papapetrou EP, Schambach A. 2016. Gene Insertion Into Genomic Safe Harbors for Human Gene Therapy. *Mol Ther J Am Soc Gene Ther* **24**:678–684. doi:10.1038/mt.2016.38

Patel S, Jazrawi E, Creighton AM, Austin CA, Fisher LM. 2000. Probing the interaction of the cytotoxic bisdioxopiperazine ICRF-193 with the closed enzyme clamp of human topoisomerase IIalpha. *Mol Pharmacol* **58**:560–568. doi:10.1124/mol.58.3.560

Pelisch F, Sonneville R, Pourkarimi E, Agostinho A, Blow JJ, Gartner A, Hay RT. 2014. Dynamic SUMO modification regulates mitotic chromosome assembly and cell cycle progression in Caenorhabditis elegans. *Nat Commun* **5**:5485. doi:10.1038/ncomms6485

Pelisch F, Tammsalu T, Wang B, Jaffray EG, Gartner A, Hay RT. 2017. A SUMO-Dependent Protein Network Regulates Chromosome Congression during Oocyte Meiosis. *Mol Cell* **65**:66–77. doi:10.1016/j.molcel.2016.11.001

Powers M, Evans EK, Yang J, Kornbluth S. 2001. Preparation and use of interphase Xenopus egg extracts. *Curr Protoc Cell Biol* **Chapter 11**:Unit 11.10. doi:10.1002/0471143030.cb1110s09

Reverter D, Lima CD. 2006. Structural basis for SENP2 protease interactions with SUMO precursors and conjugated substrates. *Nat Struct Mol Biol* **13**:1060–1068. doi:10.1038/nsmb1168

Reverter, David LC. 2004. A Basis for SUMO Protease Specificity Provided by Analysis of Human Senp2 and a Senp2-SUMO Complex - ScienceDirect. *Structure*. doi:10.1016/j.str.2004.05.023

Roca J, Ishida R, Berger JM, Andoh T, Wang JC. 1994. Antitumor bisdioxopiperazines inhibit yeast DNA topoisomerase II by trapping the enzyme in the form of a closed protein clamp. *Proc Natl Acad Sci U S A* **91**:1781–1785.

Ruan J, Li H, Xu K, Wu T, Wei J, Zhou R, Liu Z, Mu Y, Yang S, Ouyang H, Chen-Tsai RY, Li K. 2015. Highly efficient CRISPR/Cas9-mediated transgene knockin at the H11 locus in pigs. *Sci Rep* **5**:14253. doi:10.1038/srep14253

Ryu H, Azuma Y. 2010. Rod/Zw10 complex is required for PIASy-dependent centromeric SUMOylation. *J Biol Chem* **285**:32576–32585. doi:10.1074/jbc.M110.153817

Ryu H, Furuta M, Kirkpatrick D, Gygi SP, Azuma Y. 2010. PIASy-dependent SUMOylation regulates DNA topoisomerase IIalpha activity. *J Cell Biol* **191**:783–794. doi:10.1083/jcb.201004033

Schimmel J, Eifler K, Sigurðsson JO, Cuijpers SAG, Hendriks IA, Verlaan-de Vries M, Kelstrup CD, Francavilla C, Medema RH, Olsen JV, Vertegaal ACO. 2014. Uncovering SUMOylation dynamics during cell-cycle progression reveals FoxM1 as a key mitotic SUMO target protein. *Mol Cell* **53**:1053–1066. doi:10.1016/j.molcel.2014.02.001

Shamu CE, Murray AW. 1992. Sister chromatid separation in frog egg extracts requires DNA topoisomerase II activity during anaphase. *J Cell Biol* **117**:921–934. doi:10.1083/jcb.117.5.921

Spence JM, Phua HH, Mills W, Carpenter AJ, Porter ACG, Farr CJ. 2007. Depletion of topoisomerase IIalpha leads to shortening of the metaphase interkinetochore distance and abnormal persistence of PICH-coated anaphase threads. *J Cell Sci* **120**:3952–3964. doi:10.1242/jcs.013730

Sridharan V, Azuma Y. 2016. SUMO-interacting motifs (SIMs) in Polo-like kinase 1-interacting checkpoint helicase (PICH) ensure proper chromosome segregation during mitosis. *Cell Cycle Georget Tex* **15**:2135–2144. doi:10.1080/15384101.2016.1191713

Sridharan V, Park H, Ryu H, Azuma Y. 2015. SUMOylation regulates polo-like kinase 1-interacting checkpoint helicase (PICH) during mitosis. *J Biol Chem* **290**:3269–3276. doi:10.1074/jbc.C114.601906

Wang LH-C, Mayer B, Stemmann O, Nigg EA. 2010. Centromere DNA decatenation depends on cohesin removal and is required for mammalian cell division. *J Cell Sci* **123**:806–813. doi:10.1242/jcs.058255

Wang LH-C, Schwarzbraun T, Speicher MR, Nigg EA. 2008. Persistence of DNA threads in human anaphase cells suggests late completion of sister chromatid decatenation. *Chromosoma* **117**:123–135. doi:10.1007/s00412-007-0131-7

Whitehouse I, Stockdale C, Flaus A, Szczelkun MD, Owen-Hughes T. 2003. Evidence for DNA translocation by the ISWI chromatin-remodeling enzyme. *Mol Cell Biol* **23**:1935–1945. doi:10.1128/mcb.23.6.1935-1945.2003

Yoshida MM, Ting L, Gygi SP, Azuma Y. 2016. SUMOylation of DNA topoisomerase IIα regulates histone H3 kinase Haspin and H3 phosphorylation in mitosis. *J Cell Biol* **213**:665–678. doi:10.1083/jcb.201511079

Zhang X-D, Goeres J, Zhang H, Yen TJ, Porter ACG, Matunis MJ. 2008. SUMO-2/3 modification and binding regulate the association of CENP-E with kinetochores and progression through mitosis. *Mol Cell* **29**:729–741. doi:10.1016/j.molcel.2008.01.013

Zhu F, Gamboa M, Farruggio AP, Hippenmeyer S, Tasic B, Schüle B, Chen-Tsai Y, Calos MP. 2014. DICE, an efficient system for iterative genomic editing in human pluripotent stem cells. *Nucleic Acids Res* **42**:e34. doi:10.1093/nar/gkt1290

Primers used for amplification of homology arms

TopoIIα Left HA Forward	ggctgcctgtccagaaagc
TopoIIα Left HA Reverse	ctcaagaaccctgaaagcgactaaacagg
TopoIIα Right HA Forward	accATGGAAGTGTCACCATTGCAGG
TopoIIα Right HA Reverse	CCTGCATACATTATTTACCGAGTGCCTA
hH11 Left HA Forward	gattaaaattgcatatgctaagtgtg
hH11 Left HA Reverse	tgacctgttggggtc
hH11 Right HA Forward	catagccttgtggctaataccagtatatc
hH11 Right HA Reverse	gaagctgaggaatcacatgg

gRNA sequences used for Cas9 targeting of RCC1 locus or PICH locus

gRNA TopoIIα-1	ttccatggtgacggtcgtga
gRNA TopoIIα-2	cccgcgagccgtacctgcaa
gRNA TopoIIα-3	aaccctgaaagcgactaaac
gRNA hH11-1	ATAGCCTTGTGGCTAATACC
gRNA hH11-2	CCCAACAGGTCAGTTTATAC

Primers used for genomic PCR

hH11 F	cctgtgtcaacagtttgg
Pause Site R	gttttgatggagagcgtatgttagtac
Sv40 F	ccgAGATCTctctagaggatctttgtgaag
hH11 R	gtaaacatgatttgtttgagag
Hygro Rev	TCAGCGAGAGCCTGACCTAT
T2A F	CAATGTGCTGCGAATACAGACTC
T2A R	cagacacatattatctcaccaagtgg

Supporting Information Table 3.1

Chapter 4 Depletion of PICH slows mitotic progression

Introduction

PICH is an SNF2 family DNA translocase that binds SUMOylated proteins and is important for chromosome bridge resolution during mitosis (Baumann et al., 2007; Sridharan and Azuma, 2016). Although, discovered in 2007, the role of PICH during mitosis still remains elusive (Baumann et al., 2007). Initially, PICH was found and proposed to be a checkpoint protein important for SAC checkpoint activation, but that finding was found to be due to an siRNA off-target effect (Hübner et al., 2010). A recent discovery has shown that PICH and TopoIIα coordinate during mitosis to ensure proper chromosome segregation (Nielsen et al., 2015). TopoIIα is an ATP-dependent decatenase, that functions during mitosis to decatenate tangled centromeric DNA at the onset of anaphase to ensure proper sister chromatid disjunction (Fortune and Osheroff, 1998). TopoIIα does this using its Strand Passage Reaction (SPR), this activity can be inhibited by TopoIIα inhibitors such as ICRF-193 which blocks TopoIIα in the last stage of its SPR in which two decatenated DNA molecules are held within the enzyme (Morris et al., 2000; Roca et al., 1994). I also discussed the relationship between SUMOylated TopoIIα and PICH in Chapter three, where we found that PICH interacts with SUMOylated TopoIIα during mitosis. TopoIIα SUMOylation has been shown to be a physiologically relevant form for a TopoII-dependent metaphase checkpoint that occurs upon catalytic inhibition/SUMOylation of TopoIIα and subsequent maintenance of DNA entanglement between sister chromatids (Pandey et al., 2020).

This chapter discusses the potential role of PICH in the metaphase/catenated DNA checkpoint (TopoII-dependent checkpoint) which signals through Aurora B (AurB) activation and Haspin 3 kinases (Pandey et al., 2020). This checkpoint was recently uncovered using a combination of *Xenopus laevis* egg extract and HeLa cell studies. These studies found that when TopoII activity is inhibited by ICRF-193 the checkpoint becomes activated leading to TopoII C-terminal domain (CTD) SUMOylation which promotes binding of SUMOylated TopoIIα with Haspin, a kinase for Histone H3 at threonine 3 (H3T3P) (Edgerton et al., 2016; Yoshida et al., 2016). The increase of TopoIIα SUMOylation causes mobilization of AurB from inner centromeres to proximal centromeres and the core of chromosome arms. This Aurora B mobilization is caused by Haspin-dependent (H3T3P). We confirmed this pathway to be TopoIIα-CTD SUMOylation dependent by using siRNA-mediated knockdown of TopoIIα combined with Tet-inducible expression of exogenous TopoIIα. By mutating the SUMOylation sites on TopoIIα CTD Pandey et. al. discovered that the cells could bypass this checkpoint, and this perturbs AurB recruitment. Thus, stalled SUMOylated TopoIIα on mitotic chromosomes is critical to induce this novel TopoII-dependent mitotic checkpoint (Pandey et al., 2020).

The unanswered question is how this TopoII-dependent checkpoint can be resolved in cells. My finding that PICH functions in remodeling SUMOylated chromosomal proteins provides a hint in this undetermined regulatory mechanism in the TopoII-dependent checkpoint. Because PICH could control binding of SUMOylated TopoIIα to chromosomes as described in Chapter three, this led to a hypothesis that PICH plays a role in this checkpoint activity by regulating chromosomal binding of

SUMOylated TopoIIα. If the checkpoint is activated by trapped TopoIIα on DNA and this causes TopoIIα SUMOylation, PICH could be recruited and resolve the stalled SUMOylated TopoIIα from catenated DNA thus resolving the checkpoint and enabling mitotic progression. In this chapter, I examined this hypothesis by using conditional PICH-replaced cell lines.

Results

Depletion of PICH causes Aurora B mislocalization

Using the mAID-PICH cell line PICH was depleted for 10 hours and then mitotic cells were isolated by mitotic shake off and cytospun to induce chromosome spreading. Chromosome spreads were then fixed and stained for Aurora B (AurB) and CENP-C (centromere marker) while DNA was labeled with DAPI. In control cells AurB localizes at the centromere between the two sister centromeres marked by CENP-C. Intriguingly, when PICH is depleted AurB localization to the centromere is lost and signal can be observed along the chromosome arms (Figure 4.1). This AurB localization phenocopies the Pandey et. al. observations which showed upon inhibition of TopoII activity AurB is mobilized from inner centromeres to kinetochore proximal centromeres in both XEE and HeLa cells.

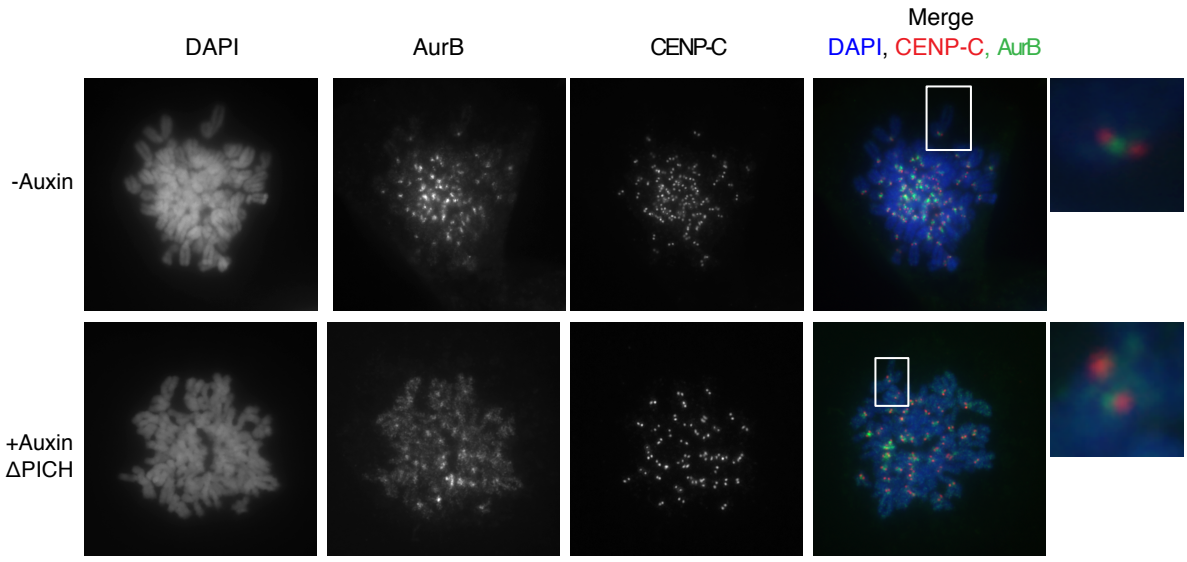

Figure 4.1 PICH depletion causes Aurora B mislocalization.
mAID-PICH DLD-1 cells were treated with or without auxin, synchronized in mitosis, and isolated for cytospin to spread chromosomes. Chromosomes were then stained with indicated antibodies: Aurora B (green), CENP-C (red), and DNA was stained with DAPI. White rectangles indicate enlarged regions.

PICH depletion causes mitotic delay rescued by PICH WT replacement

Since PICH depleted cells recapitulate the AurB phenotype seen with the activated TopoII-dependent checkpoint, I sought to examine whether PICH depletion affects the progression of mitosis. To analyze that, PICH-depleted cells were imaged using live cell microscopy to time mitotic progression. To do this ΔPICH cells were synchronized by Thymidine block for 17 hours, released, and 8 hours later imaged every ten minutes for 12 hours to observe mitotic progression. DLD-1 cells typically divide quickly with one mitosis taking 30-40 minutes from nuclear envelope breakdown

to cytokinesis. But, ΔPICH cells took longer to divide averaging 70-121 minutes from nuclear envelope breakdown to cytokinesis, and many of them arrested in prometaphase never performing anaphase (Figure 4.2A bottom panel, 4.2B, mitotic duration found in Table 4.2).

In order to determine if depleting PICH was the cause of the mitotic delay/arrest cells with mAID-PICH and a Tet-inducible promoter driving expression of a wild type PICH-mCherry were synchronized in mitosis using a thymidine block and then treated with auxin and doxycycline for 14 hours to enable depletion of endogenous PICH and replacement with WT PICH-mCherry. After performing mitotic shake off and chromosome spread cells were fixed and stained with AurB, mCherry, and DNA was labeled with DAPI. In WT PICH replacement cells AurB does not localize to the chromosome arms, and forms foci as it did in control cells, presumably at the centromere (Figure 4.2C).

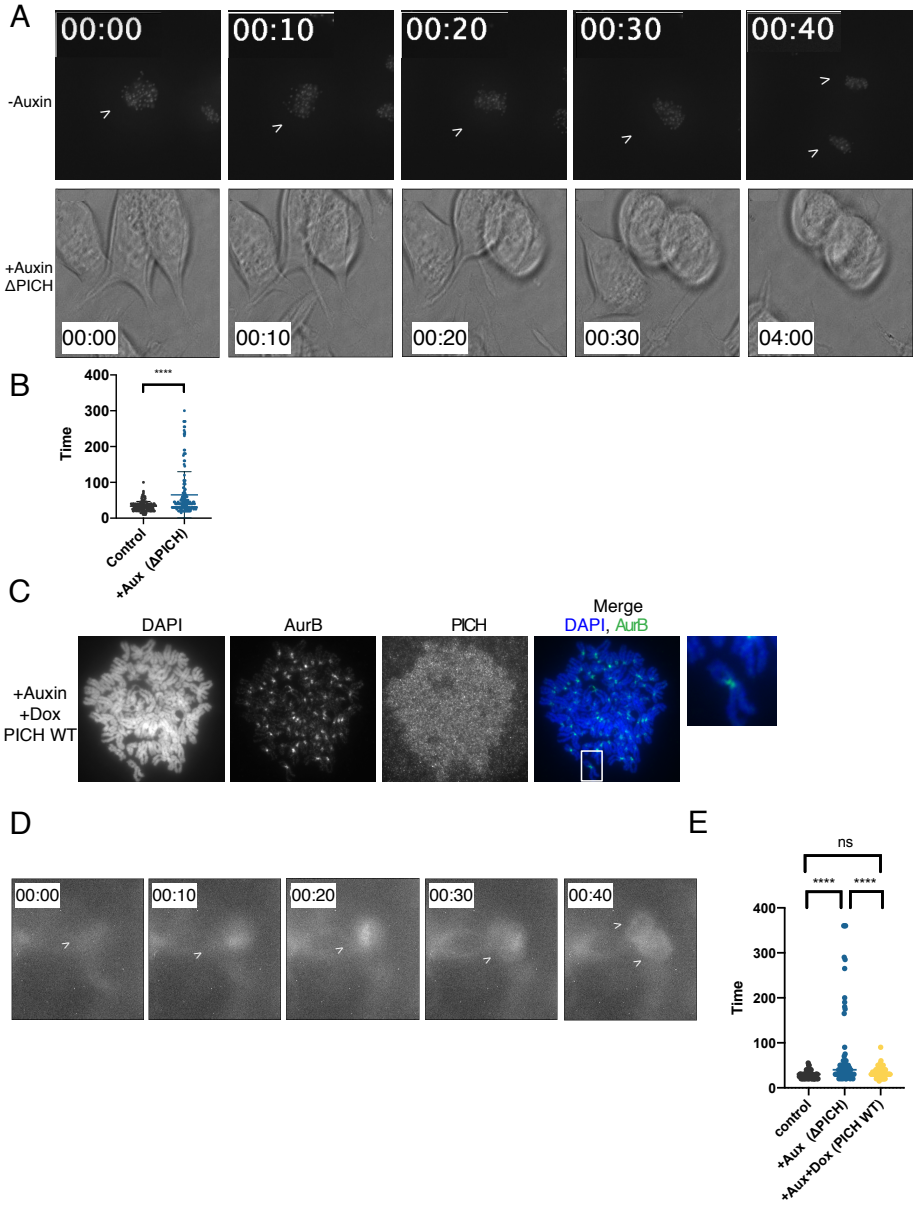

Figure 4.2 PICH depletion causes mitotic arrest.

A) mAID-PICH DLD-1 cells were treated with or without auxin, synchronized in mitosis, and subjected to live cell imaging. The top panel shows a mAID-PICH cell with CENP-A mCherry tag. The bottom panel shows bright field images of mAID-PICH cells arresting in metaphase.

B) 20 mitoses were counted among 8 different experiments with or without auxin treatment. p values for comparison among 8 experiments were calculated using a one-way ANOVA analysis of variance and Tukey multi-comparison correction; ****: p< 0.0001.

C) mAID-PICH with inducible WT PICH mCherry were treated with auxin and doxycycline and synchronized in mitosis and chromosomes were spread using cytospin. Chromsomes were then stained with indicated antibodies: Aurora B (green), mCherry (not merged), and DNA was stained with DAPI. White rectangle indicates enlarged region.

D) mAID-PICH with inducible WT PICH mCherry were treated with auxin and doxycycline and synchronized in mitosis and subjected to live cell imaging.

E) 20 mitoses in three separate experiments were counted from **(D)** p values for comparison among 3 experiments were calculated using a one-way ANOVA analysis of variance and Tukey multi-comparison correction; ns: not significant; ****: p< 0.0001.

To identify if WT PICH could rescue the mitotic progression phenotype these cells were then treated with thymidine, auxin, and doxycycline to synchronize and 8 hours after thymidine release were imaged every ten minutes over the course of 12 hours. Again, cells treated with auxin alone showed a significant delay and many cells arrested completely (Figure 4.2E, blue). But, when WT PICH mCherry was expressed the cells were seen to enter and exit mitosis within the control 30-40-minute window, showing no significant difference to non-treated cells (Figure 4.2D, E, yellow).

PICH SUMO-binding and translocase activity required for proper progression of mitosis

To determine which function of PICH was necessary to rescue the delay phenotype a cell line with mAID-PICH and Tet-inducible SUMO-binding deficient PICH mutant (d3SIM-mCherry) or translocase deficient (K128A-mCherry) mutant were timed during mitosis. d3SIM-mCherry cells were synchronized, treated, and imaged as stated in the previous section. Only cells expressing mCherry were counted. Cells expressing d3SIM-mCherry are seen to loosely localize to chromosomes upon nuclear envelope breakdown, where they are observed to maintain localization, but fail to perform anaphase (Figure 4.3A, B). In contrast, K128A-mCherry cells show strong chromosome binding, but similarly fail to perform anaphase (Figure 4.4A, B). Both mutants show this lack of anaphase phenotype but d3SIM indicate a strong necessity for SUMO-binding ability, where 51% of cells timed did not progress through anaphase. Whereas the translocase deficient K128A mutant showed this phenotype in 36% of cells timed. This could simply be due to not having a third K128A experiment but could also indicate a

stronger role of SUMO binding ability of PICH over translocase activity in cells transitioning into and performing anaphase (Table 4.1).

	Completed Anaphase	No Anaphase	Percentage No Anaphase
ΔPICH	130	26	17
WT	56	0	0
K128A	18	10	36*
d3SIM	30	31	51

Table 4.1. Percentage of anaphase completion. The average number of cells that failed to divide was calculated by dividing the number of cells that completed anaphase by the number of cells that did not in each treatment. *indicates that only 28 cells were counted (n=2)

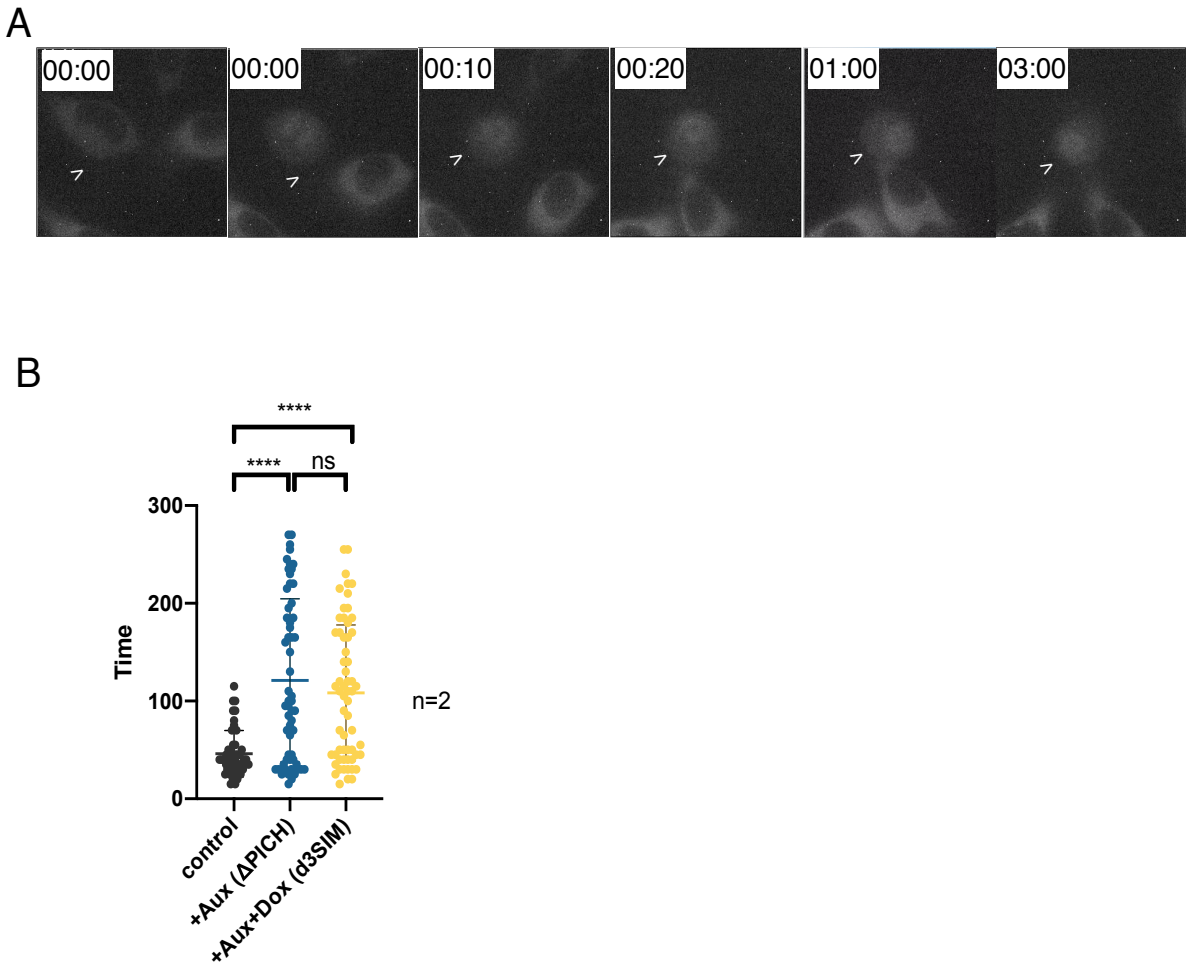

Figure 4.3 Non-SUMO interacting PICH mutant does not rescue mitotic arrest.

A) mAID-PICH with inducible PICH d3SIM mCherry were treated with auxin and doxycycline and synchronized in mitosis and subjected to live cell imaging.

B) 20 mitoses were counted among 3 different experiments with or without auxin/doxycycline treatment. p values for comparison among 3 experiments were calculated using a one-way ANOVA analysis of variance and Tukey multi-comparison correction; ns: not significant; ****: p< 0.0001.

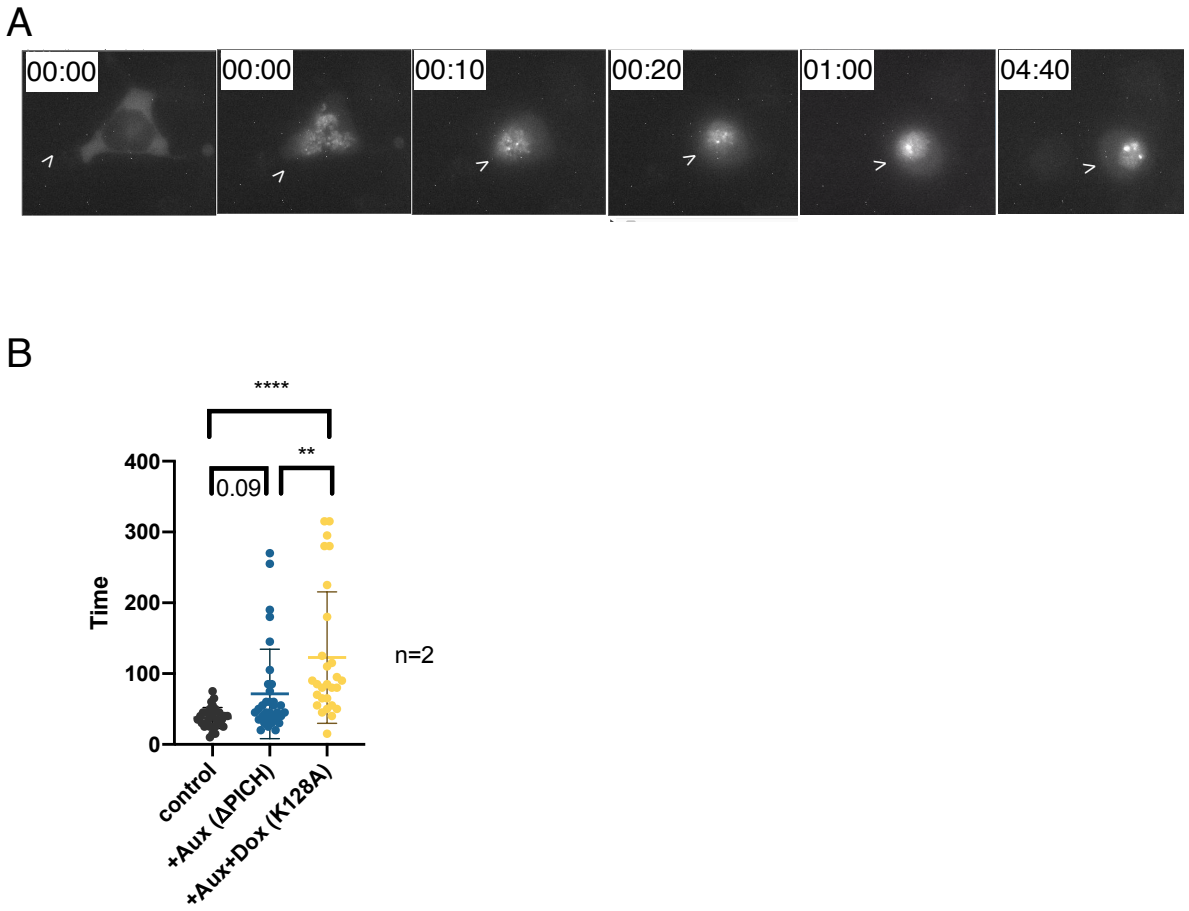

Figure 4.4 Translocase deficient PICH mutant does not rescue mitotic arrest.
A) mAID-PICH with inducible PICH K128A mCherry were treated with auxin and doxycycline and synchronized in mitosis and subjected to live cell imaging.
B) 20 mitoses were counted among 2 different experiments with or without auxin/doxycycline treatment. p values for comparison among 2 experiments were calculated using a one-way ANOVA analysis of variance and Tukey multi-comparison correction; **: p< 0.001; ****: p< 0.0001.

The d3SIM control cells took 46-minutes to go through mitosis, on average, while ΔPICH cells took 121-minutes. When ΔPICH cells were replaced with non-SUMO-binding mutant d3SIM the average time to go through mitosis is 108-minutes (Table 4.2, yellow rows). The K128A control cells showed an average mitotic timing of 37.3-minutes, while ΔPICH cells took 71.4-minutes on average. Cells with translocase

deficient replaced PICH showed an average timing of 122.6-minutes (Table 4.2 blue rows). This increase in mitotic timing is intriguing because this cell line only has an n of two. Further experimentation would likely reveal a dominant negative affect with K128A replacement indicating a necessity of translocase activity on the duration of mitosis.

	Average mitotic duration (min)
- Auxin	46
+ Auxin	121
d3SIM	108.3
- Auxin	37.3*
+ Auxin	71.4*
K128A	122.6*

Table 4.2. Average mitotic duration in PICH replacement cells. The average time it took d3SIM or K128A cells to go through mitosis after no treatment, depletion of PICH, or depletion of PICH/mutant expression. 60 cells were counted in all except *indicates that ~40 cells were counted (n=2)

Discussion

The complex process of assembling proteins at the centromere to promote chromosome segregation and proper mitotic timing is under investigation. Despite years of research, many holes in our understanding of how chromosome segregation is regulated still exist. These holes include how tangled DNA is sensed and resolved by

TopoIIα in a time-sensitive manner (Clarke and Azuma, 2017). PICH, a SUMO-interacting protein with translocase activity has shed light on a potential mechanism for regulation of mitotic timing through its interaction with decatenase TopoIIα. To identify the potential role of PICH on mitotic timing we utilized live cell imaging of PICH depleted as well as PICH replaced cell lines. This enabled us to elucidate a novel role of PICH on the progression of mitosis. This was shown by depleting PICH and observing a significant increase in mitosis timing, as well as complete prometaphase arrest. These findings suggest that PICH plays a role in the regulation of transition from prometaphase to anaphase. We could postulate that this role is based on its interaction with TopoIIα which has recently been shown to be necessary for mitotic progression (Pandey et al., 2020). In this manuscript Pandey et. al. show that SUMOylated TopoIIα is necessary to regulate a metaphase checkpoint which functions through recruitment of Haspin kinase followed by activation of AurB kinase. Activation of AurB kinase was shown to be through TopoIIα CTD SUMOylation which was shown to be important in the TopoIIα/PICH interaction discussed in Chapter three of this dissertation. This finding is significant because it suggests a role for PICH in chromosome segregation which has been hypothesized, but the direct molecular mechanism has not been elucidated (Biebricher et al., 2013; Ke et al., 2011; Nielsen and Hickson, 2016). Taking into account the Pandey et. al. data, my data suggest that when TopoIIα becomes trapped on mitotic chromosomes, even in normal conditions without its inhibitor, this initiates the metaphase checkpoint which halts mitotic progression and induces TopoIIα SUMOylation. Because of PICH's activity to remodel SUMOylated trapped TopoIIα, cells can progress through mitosis without causing detectable mitotic arrest. In the

presence of high concentrations of ICRF-193, which Pandy et.al reported, increased SUMOylated TopoIIα might exceed the capability of PICH in resolving trapped TopoIIα thus it causes mitotic arrest and/or delay. It would be intriguing to examine whether simply overproducing PICH can reduce the ICRF-193 dependent mitotic arrest under ICRF-193 treatment.

To further elucidate whether PICH is indeed removing stalled SUMOylated TopoIIα and resolving the TopoII-dependent checkpoint, the following assays are necessary; ICRF-193 treatment in ΔPICH cells and Aurora B inhibitor treatment in ΔPICH cells (Pandey et al., 2020). The first experiment would enable the measurement of mitotic timing when there is an increase of stalled TopoIIα by inhibitor treatment. If my hypothesis is correct, more stalled TopoIIα would lead to a more severe delay in cells that lack PICH. The second experiment would enable me to test whether these cells can bypass the arrest by inactivating a major signaler in the arrest cascade (Petsalaki et al., 2011). By inactivating Aurora B, I could test whether cells lacking PICH are able to go through mitosis without any delay. This would indicate that PICH is the necessary protein needed to resolve the TopoII-dependent checkpoint. Another useful experiment would be to perform the above experiments in the PICH mutant replacement cell lines to elucidate which function of PICH is necessary in this checkpoint resolution. I would hypothesize that both SUMO-binding ability and translocase activity are necessary for checkpoint resolution, but the translocase function of PICH would show a more severe phenotype. This is due to the idea that PICH K128A would still be able to bind SUMOylated TopoIIα but, without translocase ability, would remain trapped on the chromosomes.

Although it is tempting to interpret the preliminary results as I have hypothesized, it is possible that there are alternative explanations for these observations. One being that when PICH is depleted in cells, centromere regions are disrupted causing chromosomal abnormalities that might induce tension checkpoint activation. This is supported by Nielson et. al. which showed chromosomal defects in PICH knockout cells. This publication also indicated that loss of PICH can reduce TopoIIα activity. This would support our model that PICH depletion is causing TopoII-dependent checkpoint activation but by way of reduction of TopoIIα activity. Both theories are intriguing and lead to the point that further PICH research is important and necessary to elucidate its role in mitotic progression. This will be the focus of a section discussed in Chapter five.

Materials and Methods

Plasmids, constructs, and site-directed mutagenesis

All plasmid, constructs and site-directed mutagenesis was described in Chapters two and three.

Cell culture, Transfection, and Colony Isolation

mAID-PICH and PICH mutant replacement cell line creation was described in Chapter two.

Preparation of mitotic cells and chromosome spreads

DLD-1 cells were grown in McCoy's 5A 1x L-glutamine 10% FBS media for no more than 10 passages. To analyze mitotic chromosomes, cells were synchronized by Thymidine/Nocodazole cell cycle arrest protocol discussed in Chapter three. After shake-off, the mitotic cells were treated for 5 min with 1 ml of water to hypotonic shock the cells for better chromosome spreading. 500 µl of the hypotonic mixture was added to a cytology funnel attached to a glass slide with a Cytospin (Thermo Fisher Scientific) clip. The assembly was spun for 5 min at 2,000 rpm with maximum acceleration. Working quickly so that the cells did not fully dry out, glass slides were removed from the clip, and a circle was drawn around the deposited cells with a Super-PAP pen to form a hydrophobic barrier to help keep the fixing and staining reagents on the cells. When the Super-PAP dried sufficiently, the cells were fixed with 3.8% PFA for 5 min. Cells were permeated with 0.05% Triton X-100 in PBS for 5 min. Cells were then treated with 50 mM ammonium chloride in PBS for 2 min to quench PFA. Cells were washed with PBS-0.01% Triton X-100 and then blocked with 5% casein in PBS-0.01% Triton X-100. Cells were stained

overnight at 4°C with primary antibodies. The following primary antibody staining, cells were washed three times with PBS-0.01% Triton X-100 and stained with secondary antibody for 1 h. Following secondary antibody staining, chromosomes were washed three times with PBS-0.01% Triton X-100 and VECTASHIELD® Antifade Mounting Medium with DAPI (#H-1200, Vector laboratory) and sealed with nail polish. The following primary antibodies were used for staining: Rabbit anti-PICH 1:800, Mouse anti-Aurora B (AIM-1) 1:500, (BD Biosciences # 611082), Guinea Pig anti-CENP-C (1:500), (#PD030). The following secondary antibodies were used for staining: Goat anti-rabbit IgG Alexa Fluor 568 (#A11036, 1:500, Thermo/Fisher), Goat anti-mouse IgG Alexa Fluor 488 (#A32723, 1:500, Thermo/Fisher), goat anti-guinea pig IgG Alexa Fluor 568 (#A21450, 1:500, Thermo/Fisher). Images were acquired at 20°C using the Plan Apo 100×/1.4 objective lens on a Nikon TE2000-U microscope with a Retiga SRV charge-coupled device camera (QImaging) operated by Volocity imaging software (PerkinElmer).

Live cell imaging

DLD-1 mAID-PICH or mAID-PICH mutant replacement cells were plated in a 4-chamber, 3-cm glass-bottom plate treated with Thymidine for 24 hours then cells were released by 3 washes with tet-free medium. For PICH depletion or mutant expression auxin or doxycycline was added for 14 hours. Medium was replaced with CO2-independent medium. Cells were then quickly transferred to the heated Delta Vision microscope chamber (for Figure 4.5 cells were treated with ICRF-193 drugs then moved to microscope). Cells were imaged for 12 h, and cells that were seen to enter prometaphase during the time course were scored for time to anaphase and chromosome decondensation. Cells were imaged using a DeltaVision microscope system (Applied

Precision) based on an Olympus IX-71 inverted microscope and either an Olympus UPLSAPO 100×, 1.40-NA, oil objective for stained images (mounted with ProLong Gold, Invitrogen). No other adjustments were made to the images. Figures were prepared from exported images in Adobe illustrator.

Statistical analysis

All statistical analyses were performed with either 1- or 2-way ANOVA, followed by the appropriate post-hoc analyses using GraphPad Prism 8 software. Graphs are presented as mean with standard deviation.

Collaborations and workload allocations

For all experiments designed in this chapter Victoria Hassebroek designed, conducted, and analyzed data.

References

Biebricher, A., Hirano, S., Enzlin, J.H., Wiechens, N., Streicher, W.W., Huttner, D., Wang, L.H.-C., Nigg, E.A., Owen-Hughes, T., Liu, Y., et al. (2013). PICH: a DNA translocase specially adapted for processing anaphase bridge DNA. Mol. Cell *51*, 691–701.

Clarke, D.J., and Azuma, Y. (2017). Non-Catalytic Roles of the Topoisomerase IIα C-Terminal Domain. Int. J. Mol. Sci. *18*.

Edgerton, H., Johansson, M., Keifenheim, D., Mukherjee, S., Chacón, J.M., Bachant, J., Gardner, M.K., and Clarke, D.J. (2016). A noncatalytic function of the topoisomerase II CTD in Aurora B recruitment to inner centromeres during mitosis. J. Cell Biol. *213*, 651–664.

Ke, Y., Huh, J.-W., Warrington, R., Li, B., Wu, N., Leng, M., Zhang, J., Ball, H.L., Li, B., and Yu, H. (2011). PICH and BLM limit histone association with anaphase centromeric DNA threads and promote their resolution. EMBO J. *30*, 3309–3321.

Morris, S.K., Baird, C.L., and Lindsley, J.E. (2000). Steady-state and rapid kinetic analysis of topoisomerase II trapped as the closed-clamp intermediate by ICRF-193. J. Biol. Chem. *275*, 2613–2618.

Nielsen, C.F., and Hickson, I.D. (2016). PICH promotes mitotic chromosome segregation: Identification of a novel role in rDNA disjunction. Cell Cycle Georget. Tex *15*, 2704–2711.

Pandey, N., Keifenheim, D., Yoshida, M.M., Hassebroek, V.A., Soroka, C., Azuma, Y., and Clarke, D.J. (2020). Topoisomerase II SUMOylation activates a metaphase checkpoint via Haspin and Aurora B kinases. J. Cell Biol. *219*.

Petsalaki, E., Akoumianaki, T., Black, E.J., Gillespie, D.A.F., and Zachos, G. (2011). Phosphorylation at serine 331 is required for Aurora B activation. J. Cell Biol. *195*, 449–466.

Roca, J., Ishida, R., Berger, J.M., Andoh, T., and Wang, J.C. (1994). Antitumor bisdioxopiperazines inhibit yeast DNA topoisomerase II by trapping the enzyme in the form of a closed protein clamp. Proc. Natl. Acad. Sci. U. S. A. *91*, 1781–1785.

Yoshida, M.M., Ting, L., Gygi, S.P., and Azuma, Y. (2016). SUMOylation of DNA topoisomerase IIα regulates histone H3 kinase Haspin and H3 phosphorylation in mitosis. J. Cell Biol. *213*, 665–678.

Chapter 5 PICH interaction with SUMOylated proteins current understanding and future directions

General Summary of Dissertation Chapters

Understanding how faithful chromosome segregation occurs and is regulated in cells, is a complex question. Chapter one of this dissertation discusses the known mechanisms for timing and chromosome structure. In which post translational modifications play a crucial role. The modification which my work focuses on is SUMOylation. In the past decade many SUMOylated substrates have been identified, one SUMO substrate that our lab identified, Topoisomerase IIα (TopoIIα), functions during mitosis (Azuma et al., 2003). The work in this dissertation elucidated a role for Polo-like kinase interacting checkpoint helicase (PICH), in conjunction with TopoIIα, on faithful chromosome segregation and efficient mitotic timing.

The role of PICH was revealed after implementation and creation of a novel PICH depletion and mutant add-back cell line discussed in Chapter two of this dissertation. I created this cell line using the auxin inducible degron system (Natsume et al., 2016), which enabled rapid depletion of PICH within one cell cycle, and by combining with the Tet-inducible expression system I was able to rapidly replace endogenous PICH with exogenous PICH mutants. This enabled me to examine the TopoIIα/PICH relationship in the context of TopoIIα SUMOylation. This system also enables us to examine the function of PICH utilizing molecular genetic approaches not previously available. In Chapter three I explain my findings that when cells are treated with ICRF-193 TopoIIα SUMOylation increases and recruits PICH to mitotic

chromosomes. If PICH is depleted SUMOylated TopoIIα levels on the chromosomes increase. Finally, if PICH is depleted and replaced with a translocase deficient mutant SUMO signals on the chromosomes increase significantly. The translocase mutant form of PICH showing strong SUMO2/3 foci indicates PICH as a SUMOylated protein remodeler. This finding led to a hypothesis that PICH is recruited to chromosomes when TopoIIα activity is perturbed. From previous work by Pandey et. al. we know that TopoIIα plays a critical role in a TopoII-dependent checkpoint (Pandey et al., 2020). This checkpoint functions through TopoIIα SUMOylation and therefore I asked if PICH plays a role in resolution of this checkpoint. In Chapter four of this dissertation I discussed how depletion of PICH causes a significant mitotic delay related to TopoII-dependent checkpoint. My hypothesis of "PICH as a remodeler of stalled SUMOylated TopoIIα" is further supported by the fact that neither non-SUMO interacting, or translocase deficient PICH mutant can rescue this delay. This indicates a role of PICH on the resolution of ICRF-193 induced stalled SUMOylated TopoIIα. Because PICH is a promiscuous SUMO binding protein it is intriguing to hypothesize that it does not only function to resolve stalled SUMOylated TopoIIα but also plays a role in binding and remodeling other SUMOylated proteins, which I will discuss in the following sections.

TopoIIα a target of PICH

Identifying new PICH interacting proteins would help to elucidate its function during mitosis, but it is also important to continue teasing out the mechanism of interaction between PICH and SUMOylated TopoIIα. To do this it is necessary to create an assay to test PICH remodeling activity on SUMOylated TopoIIα *in vitro.* Before

designing and implementing a new assay I began to ask this question about PICH remodeling using the DLD-1 PICH replacement cell lines. I synchronized cells in mitosis incubated with or without auxin to deplete PICH for 8 hours and then isolated mitotic cells and incubated them in a hypotonic solution, then cells were transferred to a cytology funnel where they were spun for 5 minutes to induce chromosome spreading. Chromosomes spreads were then fixed and stained. Figure 5.1 indicates that when PICH is depleted TopoIIα localization on chromosome arms is affected. This was an intriguing, yet difficult to understand phenotype as we previously saw increased SUMOylated TopoIIα in Chapter three of this dissertation. This could be indicating a different role of PICH on non-modified TopoIIα, which previous groups have shown.

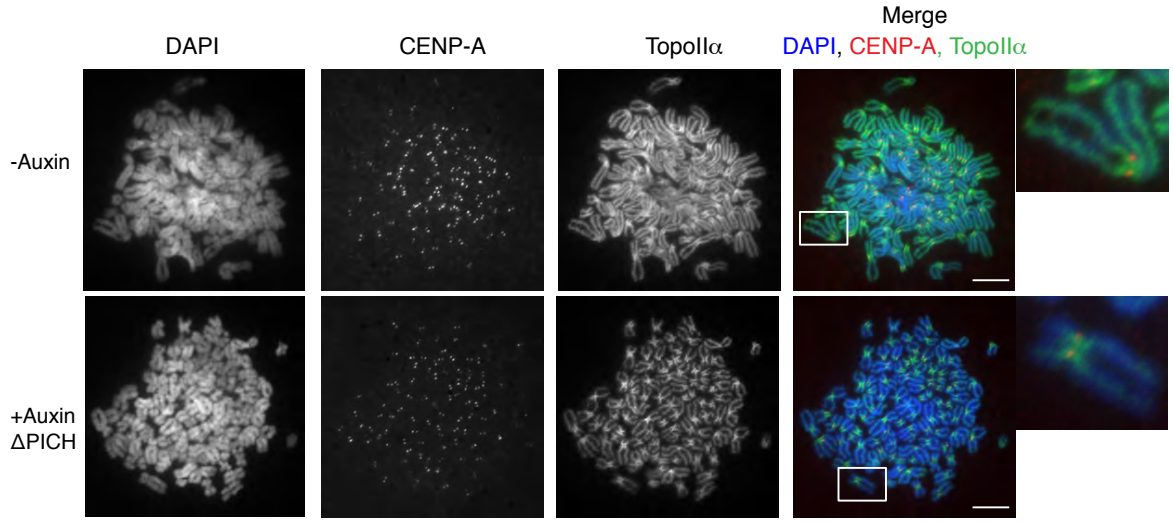

Figure 5.1 ΔPICH chromosome spreads indicate a role in the relocation of TopoIIα to chromosome arms. Cells were synchronized in mitosis and treated with or without auxin to deplete PICH. Mitotic cells were then isolated, placed in a hypotonic solution, and cytospun to spread chromosomes. Fixed chromosomes were then stained with the following antibodies: CENP-A (red), TopoIIα (green), and DNA was stained with DAPI. The white rectangles indicate enlarged regions.

To identify which function of PICH was necessary for the redistribution of TopoIIα on chromosomes, PICH mutant replacement cells were synchronized and treated as above with plus or minus doxycycline to induce expression of mutant PICH. When PICH WT mCherry was expressed TopoIIα localized to chromosome arms and centromeric regions as in -auxin control cells (Figure 5.2A). But when PICH d3SIM mCherry was expressed TopoIIα localization seemed to be more enriched at chromosome centromeres (Figure 5.2B). Lastly, when the translocase deficient PICH K128A mCherry was expressed, arm region TopoIIα was lost (Figure 5.2C). This indicates that the translocase activity of PICH is required for redistribution of TopoIIα from centromere regions to chromosome arms. Interestingly, PICH was observed to have different localizations in cytospun samples as well, which support observations in Chapter three of this dissertation. In Figure 5.2B the d3SIM PICH mutant is seen to lose strong association with chromosomes. This is also supported by Sridharan et. al. which showed that PICH SIMs are required for centromeric localization (Sridharan and Azuma, 2016). Intriguingly, the translocase deficient K128A PICH mutant seems to form strong foci on cytospun chromosomes, this was observed in all chromosome spread samples over three experiments. This could indicate PICH retention at rDNA regions which is supported by Nielsen et. al (Nielsen and Hickson, 2016). These data indicate that PICH is using its SIMs and translocase activity to remodel TopoIIα on chromosomes during mitosis, but to further define its remodeling activity a critical remodeling assay must be incorporated.

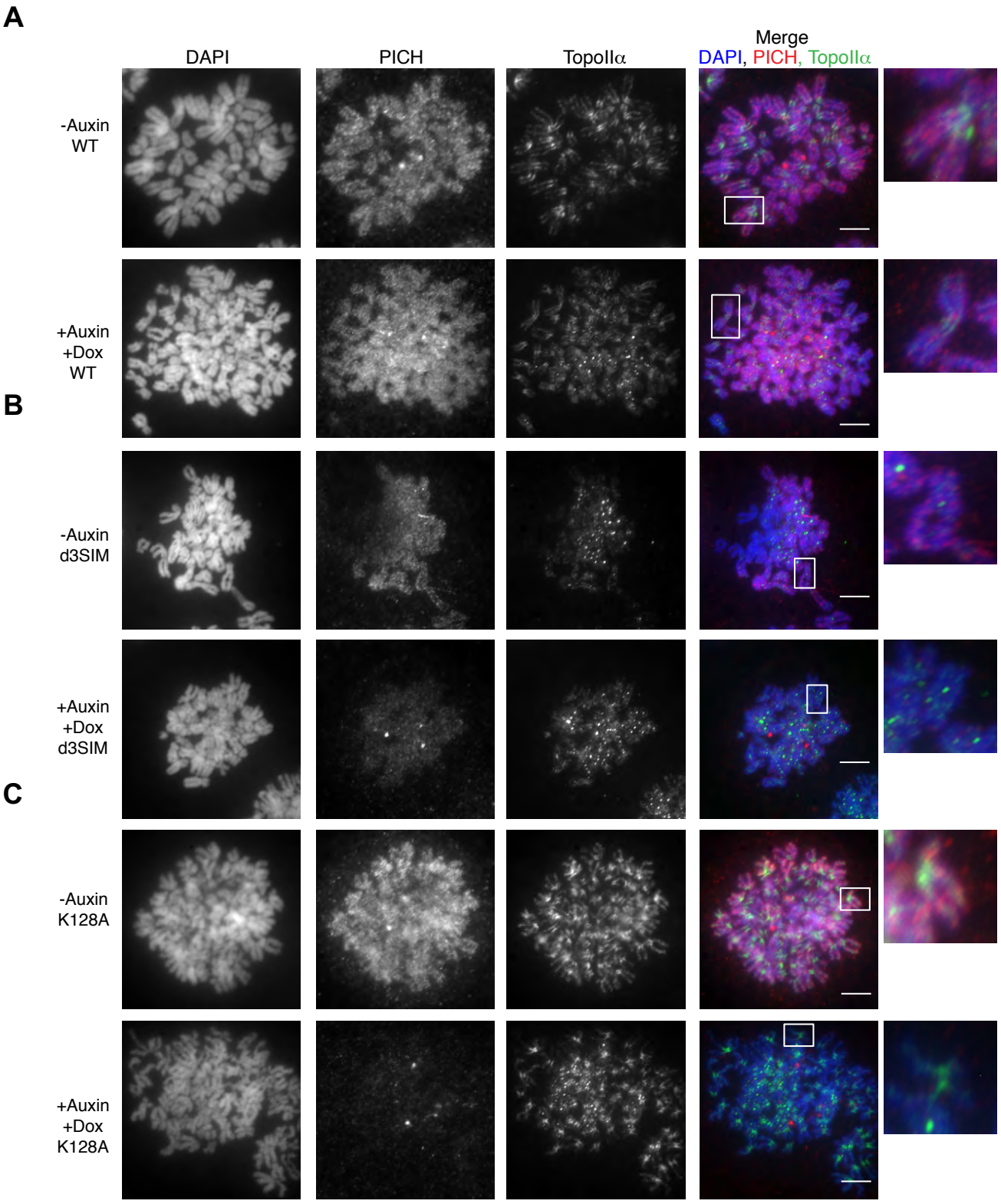

Figure 5.2 PICH SUMO-interacting and translocase ability are necessary in TopoIIα distribution to chromosome arms.

A) PICH WT replacement cells were synchronized in mitosis and treated with or without auxin to deplete PICH. Mitotic cells were then isolated, placed in a hypotonic solution, and cytospun to spread chromosomes. Fixed chromosomes were then stained with the following antibodies: PICH (red), TopoIIα (green), and DNA was stained with DAPI. The white rectangles indicate enlarged regions.
B) PICH d3SIM replacement fixed chromosomes were stained with the following antibodies: PICH (red), TopoIIα (green), and DNA was stained with DAPI. The white rectangles indicate enlarged regions.
C) PICH K128A replacement fixed chromosomes were stained with the following antibodies: PICH (red), TopoIIα (green), and DNA was stained with DAPI. The white rectangles indicate enlarged regions.

PICH as a general SUMOylated protein remodeler

Due to the fact that PICH depletion causes chromosome abnormalities, which include both condensation and cohesion defects, it is intriguing to hypothesize that it plays a role in the regulation of higher order chromatin structure (Biebricher et al., 2013; Nielsen et al., 2015). As I discussed in Chapter one of this dissertation, cohesins play a crucial role in holding sister chromatids together (Wang et al., 2010). Interestingly, cohesins are known to be SUMOylated in budding yeast (Bermúdez-López and Aragón, 2017). If this cohesin SUMOylation is maintained in higher order species and is a target of PICH SUMO-interacting motifs (SIMs), this could be the mechanism for how PICH and cohesin interact. Another chromatin structure in which PICH has been indicated to be important in maintaining is the centromere regions.

Both centromeric protein A (CENP-A) and E (CENP-E) are found at the centromere and proximal centromere regions, as their name implies (Zhang et al., 2008). Indication for CENP-E SUMOylation is summarized in a review by Zhang et. al. which shows that CENP-E localizes to the fibrous corona on the outer edge of the centromere and is modified by SUMO2/3 in human cells (Zhang et al., 2008). This microtubule motor

protein requires SUMOylation to be targeted to the kinetochore region, where it functions (Wan et al., 2012; Zhang et al., 2008). We know from previous work that PICH localizes to the centromere and when its SUMO-interacting motifs are mutated, loses its centromeric localization (Sridharan and Azuma, 2016). This indicates that PICH recognizes and binds SUMOylated proteins in this region. So far, no CENP-A defects have been observed when PICH function is perturbed in cells, but CENP-E has not yet been tested. CENP-E is an intriguing candidate for PICH interaction because of its function at the kinetochore region where microtubules attach. This interaction could account for the fact that fewer ΔPICH cells seem to be capable of anaphase.

Due to the numerous chromosome structure and segregation defects observed in PICH knockout cells it is intriguing to hypothesize which other binding partners PICH has (Nielsen et al., 2015). Although there is evidence of PICH and TopoIIα cooperation during mitosis many other groups have also indicated a role of PICH with BLM (Bloom's syndrome helicase) (Ke et al., 2011). Ian Hickson's group identified BLM decorating ultra-fine bridges around the same time that Erich Nigg's group discovered PICH on those unique DNA threads. After investigation it was found that BLM recruitment to UFBs was dependent on PICH (Ke et al., 2011). BLM is known to function during replication where it is important in the repair of damaged replication forks (Ouyang et al., 2009). Previous work has also demonstrated that preventing BLM modification by SUMO causes increased H2AX foci, which indicates DNA damage (Eladad et al., 2005). If SUMO is important in regulating BLM function during replication it is possible BLM SUMOylation plays a role in its interaction with PICH as well.

Although TopoIIα localization can be directly regulated by PICH, defects in the structural organization of chromosomes by loss of PICH could also affect TopoIIα localization. To elucidate the role PICH plays during mitosis would require direct identification of which SUMOylated proteins with which PICH is interacting. To do this it would be necessary to first identify binding proteins bound by PICH during mitosis. Then after identity validation, the protein's SUMOylation status could be revealed. Utilizing the PICH replacement cell lines would enable identification of binding partners whose interaction is based on SUMOylation (i.e. do not bind d3SIM PICH) or whose interaction was strengthened by the translocase deficient K128A mutant. Once the list of binding partners was generated, the most intriguing (based on known PICH functions) would be first validated by antibody testing of pulldown samples and then characterized. This experimentation is a streamlined protocol with which our lab has previous experience, but there are caveats to this protocol. The first challenge is that chromosome proteins do not solubilize well. To overcome this potential hurdle a new system for identifying binding partners could be used. This system is called APEX proximity biotinylation created by Burke et. al. in 2012 (Roux et al., 2012). This system enables proximity-dependent biotin identification by fusion of E. coli biotin protein ligase to a targeting protein. The E. coli biotin protein ligase (BirA) is a promiscuous ligase which enables nearby proteins to become biotinylated for subsequent affinity capture and identified by mass spectrometry. This would be relatively easy to implement in our lab as we already have a PICH targeting donor and guide RNAs for CRISPR/Cas9 mediated editing. In this experiment, once a PICH-BirA cell line has been generated, biotinylated proteins could be captured by streptavidin beads and bound proteins analyzed by mass

spectrometry. This form of pulldown would resolve the insolubility problem with the previously proposed method because the biotinylation step occurs before the solubilization step and will enable detection of both weak and transient interactions. Again, it would be useful to utilize PICH mutant replacement cell lines to validate binding partners that are SUMOylation dependent, which would show PICH WT binding, strong PICH K128A binding, and which would not bind PICH d3SIM.

Implication of PICH as a cancer chemotherapeutic target

During my initial studies utilizing different colon cancer cell lines I found that PICH and SUMO signal differ between cell lines in response to TopoII inhibitors (Figure 3A, B). This indicated that different cancer cell lines control SUMOylation differentially, in that some upregulate SUMOylation more strongly in response to TopoII inhibitors. This interested me because many groups have shown that different cancer types hijack different pathways to achieve immortality. This could indicate a role of PICH in some cancer types versus others. Intriguingly, a recent paper by Zhou et. al. indicated PICH as a potential target of chemotherapeutics in triple negative breast cancer (TNBC). TNBC is defined by the lack of expression of estrogen, progesterone, and ERBB2 receptors and has the worst prognosis of all breast cancer types. This paper reported that TNBC cells were exceptionally dependent on PICH, and when it was knocked out, TNBC cells died (Huang et al., 2019). So far, this is the first indication for a clinically relevant role of PICH. It would be interesting to follow up with this paper in the Azuma lab by measuring the levels of SUMOylation in the different TNBC cell lines used in this study. I would hypothesize that the cells are more dependent on PICH due to an

increased level of SUMOylation, and SUMOylation of TopoIIα. This would require higher PICH expression levels (as observed) to regulate SUMOylated proteins like TopoIIα. In all, I hypothesize that PICH would be a good chemotherapeutic target in TNBC cells which show higher than control levels of SUMOylation. By performing a simple screen of cancer cell SUMOylation profiles it would be useful to identify which cells would benefit from a PICH inhibitor.

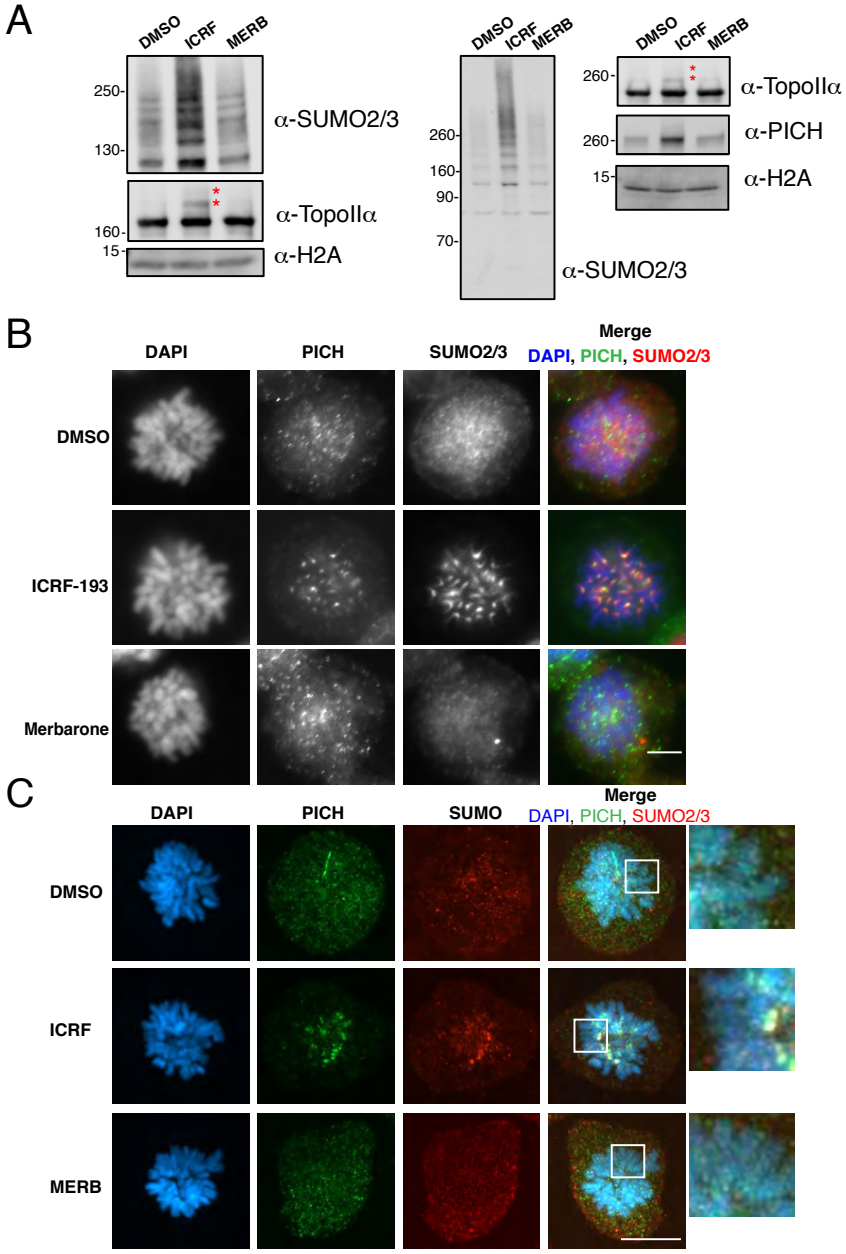

Figure 5.3 PICH and SUMO2/3 patterns in two colon cancer cell lines.
A) HCT116 (Left) or DLD1 (Right) cells were synchronized in mitosis and chromosomes were isolated and run on an 8-16% SDS-PAGE gel. Antibodies were used against: SUMO2/3, TopoIIα, and H2A was used as a loading control. * indicate SUMOylated TopoIIα
B) HCT116 mitotic cells were treated with DMSO (control), 7μM ICRF-193, or 40μM Merbarone and plated on fibronectin coverslips, fixed, and stained with the following antibodies, α-PICH (green), α-SUMO2/3 (red), and DNA was labeled with DAPI.
C) DLD-1 mitotic cells were treated with DMSO (control), 7μM ICRF-193, or 40μM Merbarone and plated on fibronectin coverslips, fixed, and stained with the following antibodies, α-PICH (green), α-SUMO2/3 (red), and DNA was labeled with DAPI. White rectangles indicate enlarged regions.

Conclusion

Overall, to uncover how chromosome structure, mitotic timing, and SUMOylation during mitosis are regulated and where PICH comes into play more studies are required. In summary, this dissertation describes a new method for studying essential proteins during mitosis, this system of rapid depletion and add back of conditional expression mutants enables a level of genetic molecular approaches which were not previously available in the field. This dissertation also describes a role of PICH on SUMOylated TopoIIα which is both SIM-and translocase-dependent. We currently do not know if this is by direct interaction to remodel SUMOylated TopoIIα and future studies would need to include an assay to describe the nature of this interaction and show direct evidence of PICH remodeling activity. I also describe a role for PICH on resolving the TopoII-dependent checkpoint, which helps to elucidate why the SUMOylated TopoIIα/PICH interaction is important for mitotic progression. But further studies are needed to test if this ΔPICH mitotic delay is the TopoII-dependent checkpoint or the tension checkpoint. Both the studies conducted, and future studies proposed would help to elucidate the role of PICH on SUMOylated proteins and lend insight to cancer researchers actively working to target PICH as a chemotherapeutic target.

Materials and Methods

Cell culture and staining

mAID-PICH and PICH mutant replacement cell culture and staining was described in Chapter two.

Preparation of mitotic cells and chromosome spreads

mAID-PICH and PICH mutant replacement cell lines creation was described in Chapter four.

References

Agostinho M, Santos V, Ferreira F, Costa R, Cardoso J, Pinheiro I, Rino J, Jaffray E, Hay RT, Ferreira J. 2008. Conjugation of human topoisomerase 2 alpha with small ubiquitin-like modifiers 2/3 in response to topoisomerase inhibitors: cell cycle stage and chromosome domain specificity. *Cancer Res* **68**:2409–2418. doi:10.1158/0008-5472.CAN-07-2092

Azuma Y, Arnaoutov A, Dasso M. 2003. SUMO-2/3 regulates topoisomerase II in mitosis. *J Cell Biol* **163**:477–487. doi:10.1083/jcb.200304088

Bachant J, Alcasabas A, Blat Y, Kleckner N, Elledge SJ. 2002. The SUMO-1 isopeptidase Smt4 is linked to centromeric cohesion through SUMO-1 modification of DNA topoisomerase II. *Mol Cell* **9**:1169–1182.

Bermúdez-López M, Aragón L. 2017. Detection of Cohesin SUMOylation In Vivo. *Methods Mol Biol Clifton NJ* **1515**:55–64. doi:10.1007/978-1-4939-6545-8_4

Biebricher A, Hirano S, Enzlin JH, Wiechens N, Streicher WW, Huttner D, Wang LH-C, Nigg EA, Owen-Hughes T, Liu Y, Peterman E, Wuite GJL, Hickson ID. 2013. PICH: a DNA translocase specially adapted for processing anaphase bridge DNA. *Mol Cell* **51**:691–701. doi:10.1016/j.molcel.2013.07.016

Clarke DJ, Azuma Y. 2017. Non-Catalytic Roles of the Topoisomerase IIα C-Terminal Domain. *Int J Mol Sci* **18**. doi:10.3390/ijms18112438

Edgerton H, Johansson M, Keifenheim D, Mukherjee S, Chacón JM, Bachant J, Gardner MK, Clarke DJ. 2016. A noncatalytic function of the topoisomerase II CTD in Aurora B recruitment to inner centromeres during mitosis. *J Cell Biol* **213**:651–664. doi:10.1083/jcb.201511080

Eladad S, Ye T-Z, Hu P, Leversha M, Beresten S, Matunis MJ, Ellis NA. 2005. Intra-nuclear trafficking of the BLM helicase to DNA damage-induced foci is regulated by SUMO modification. *Hum Mol Genet* **14**:1351–1365. doi:10.1093/hmg/ddi145

Huang Y, Li W, Yan W, Wu J, Chen L, Yao X, Gu F, Lv L, Zhao J, Zhao M, Xia T, Han Q, Li Teng, Ying X, Li Tao, Xia Q, Li A, Zhang X, Chen Y, Zhou T. 2019. Loss of PICH promotes chromosome instability and cell death in triple-negative breast cancer. *Cell Death Dis* **10**:428. doi:10.1038/s41419-019-1662-6

Ke Y, Huh J-W, Warrington R, Li B, Wu N, Leng M, Zhang J, Ball HL, Li B, Yu H. 2011. PICH and BLM limit histone association with anaphase centromeric DNA threads and promote their resolution. *EMBO J* **30**:3309–3321. doi:10.1038/emboj.2011.226

Morris SK, Baird CL, Lindsley JE. 2000. Steady-state and rapid kinetic analysis of topoisomerase II trapped as the closed-clamp intermediate by ICRF-193. *J Biol Chem* **275**:2613–2618.

Natsume T, Kiyomitsu T, Saga Y, Kanemaki MT. 2016. Rapid Protein Depletion in Human Cells by Auxin-Inducible Degron Tagging with Short Homology Donors. *Cell Rep* **15**:210–218. doi:10.1016/j.celrep.2016.03.001

Nielsen CF, Hickson ID. 2016. PICH promotes mitotic chromosome segregation: Identification of a novel role in rDNA disjunction. *Cell Cycle Georget Tex* **15**:2704–2711. doi:10.1080/15384101.2016.1222336

Nielsen CF, Huttner D, Bizard AH, Hirano S, Li T-N, Palmai-Pallag T, Bjerregaard VA, Liu Y, Nigg EA, Wang LH-C, Hickson ID. 2015. PICH promotes sister chromatid disjunction and co-operates with topoisomerase II in mitosis. *Nat Commun* **6**:8962. doi:10.1038/ncomms9962

Ouyang KJ, Woo LL, Zhu J, Huo D, Matunis MJ, Ellis NA. 2009. SUMO modification regulates BLM and RAD51 interaction at damaged replication forks. *PLoS Biol* **7**:e1000252. doi:10.1371/journal.pbio.1000252

Pandey N, Keifenheim D, Yoshida MM, Hassebroek VA, Soroka C, Azuma Y, Clarke DJ. 2020. Topoisomerase II SUMOylation activates a metaphase checkpoint via Haspin and Aurora B kinases. *J Cell Biol* **219**. doi:10.1083/jcb.201807189

Petsalaki E, Akoumianaki T, Black EJ, Gillespie DAF, Zachos G. 2011. Phosphorylation at serine 331 is required for Aurora B activation. *J Cell Biol* **195**:449–466. doi:10.1083/jcb.201104023

Roca J, Ishida R, Berger JM, Andoh T, Wang JC. 1994. Antitumor bisdioxopiperazines inhibit yeast DNA topoisomerase II by trapping the enzyme in the form of a closed protein clamp. *Proc Natl Acad Sci U S A* **91**:1781–1785.

Roux KJ, Kim DI, Raida M, Burke B. 2012. A promiscuous biotin ligase fusion protein identifies proximal and interacting proteins in mammalian cells. *J Cell Biol* **196**:801–810. doi:10.1083/jcb.201112098

Sridharan V, Azuma Y. 2016. SUMO-interacting motifs (SIMs) in Polo-like kinase 1-interacting checkpoint helicase (PICH) ensure proper chromosome segregation during mitosis. *Cell Cycle Georget Tex* **15**:2135–2144. doi:10.1080/15384101.2016.1191713

Wan J, Subramonian D, Zhang X-D. 2012. SUMOylation in control of accurate chromosome segregation during mitosis. *Curr Protein Pept Sci* **13**:467–481. doi:10.2174/138920312802430563

Wang LH-C, Mayer B, Stemmann O, Nigg EA. 2010. Centromere DNA decatenation depends on cohesin removal and is required for mammalian cell division. *J Cell Sci* **123**:806–813. doi:10.1242/jcs.058255

Yoshida MM, Ting L, Gygi SP, Azuma Y. 2016. SUMOylation of DNA topoisomerase IIα regulates histone H3 kinase Haspin and H3 phosphorylation in mitosis. *J Cell Biol* **213**:665–678. doi:10.1083/jcb.201511079

Zhang X-D, Goeres J, Zhang H, Yen TJ, Porter ACG, Matunis MJ. 2008. SUMO-2/3 modification and binding regulate the association of CENP-E with kinetochores and progression through mitosis. *Mol Cell* **29**:729–741. doi:10.1016/j.molcel.2008.01.013